Adaptive Precoding and Resource Allocation in Cognitive Radio Networks

Dissertation

zur Erlangung des akademischen Grades

Doktor der Ingenieurwissenschaften

(Dr.-Ing.)

der Technischen Fakultät

der Christian-Albrechts-Universität zu Kiel

vorgelegt von

Abdullah Yaqot

Kiel 2017

Tag der Einreichung: 29.11.2016
Tag der Disputation: 07.04.2017

Berichterstatter: Prof. Dr.-Ing. Peter Adam Höher
Prof. Dr.-Ing. Wolfgang Gerstacker

To my wife, my daughters.

Acknowledgments

This thesis was conducted during the time of working as a research assistant at the Chair of Information and Coding Theory, Faculty of Engineering, University of Kiel, Germany. The investigations have been performed under the supervision of Prof. Dr.-Ing. Adam Höher.

I would like to praise the almighty God for the good health and the wellbeing that were necessary to complete the research and the dissertation work.

I would like to express my sincere thanks to Prof. Höher for his generous support and guidance throughout my study. His constant encouragement, valuable suggestions, constructive comments, and warm feelings have contributed significantly toward accomplishing this work.

I would like to express deep gratitude to the German Academic Exchange Service (DAAD) for their financial support granted to me as a Ph.D. scholarship.

I would like to thank the disputation committee: Prof. Dr.-Ing. Wolfgang Gerstacker, Prof. Dr.-Ing. Ludger Klinkenbusch, and Prof. Dr.-Ing. Michael Höft for serving as examiners as well as for their helpful discussion and technical notes during and after thesis defense. Deep gratitude goes to Prof. Klinkenbusch for his precious recommendations which were necessary for extending the financial support of my Ph.D. program.

Last but not the least, I am greatly indebted to my parents for their encouragement, support, and love throughout my life. Great indebtedness goes to my wife for her love and patience which without them the completion of this work would never have been possible.

Kiel, April 2017 Abdullah Yaqot

Abstract

The use of cognitive radio (CR) is anticipated to enable a couple of significant enhancements in wireless communications. The major enhancements include better configuration and dynamic adaptation of radio access technologies in tone with localized conditions and more independent localized options of spectrum usage and networking configuration. Consequently, improvements in spectrum efficiency, controllable mutual interference among users, and flexible coexistence with various radio access technologies are prominent benefits. These benefits have caused involvement of cognitive networking as an integral component of next generation mobile networks. The greatly increased complexity in next generation mobile networks (due to the localized variations, the heterogeneous networking, and the availability of various access methods) will not be optimally managed with human input, or with those conventional algorithms which lack adaptability to the environmental variations. Therefore, cognitive networking will enable next generation networks to be more adaptable and successfully able to manage these conditions with greatly reduced human intervention.

Among the operational networking paradigms, the underlay cognitive radio mode suffers from short communication range. This impact results from limiting the interference at the primary users which necessitates imposing constraints on the transmit power of the cognitive transmitter. Such power limitation in turn reduces the spectral efficiency of cognitive radio compared to conventional non-cognitive radios. The use of multiple antennas is an effective technique to manage the interference at the primary radio via multiuser transmit precoding. Furthermore, by means of multiuser multiple-input multiple-output (multiuser MIMO), the spectral efficiency of the cognitive radio network can be enhanced due to enabling the management of mutual interference among the cognitive users.

In this thesis, we develop efficient resource allocation and adaptive precoding schemes for two scenarios: multiuser MIMO-OFDM and multiuser MIMO based CR networks. The aim of the adaptive precoding is to squeeze more efficiency in the low SNR regime. In the context of

the multiuser MIMO-OFDM CR network, we have developed resource allocation and adaptive precoding schemes for both the downlink (DL) and uplink (UL). The proposed schemes are characterized by both computational and spectral efficiencies. The adaptive precoder operates based on generating countable degrees of freedom (DoF) by combining the spaces of the block interference channel. The resource allocation has been formulated as a sum-rate maximization problem subject to the upper-limit of total power and interference at primary user constraints. The variables of the problem were matrix of the precoding and integer indicator of the subcarrier mapping. The formulated optimization problem is a mixed integer programming having a combinatorial complexity which is hard to solve, and therefore we separated it into a two-phase procedure to elaborate computational efficiency: Adaptive precoding (DoF assignment) and subcarrier mapping.

From the implementation perspective, the resource allocation of the DL is central based processing, but the UL is semi-distributed based. Central resource allocation task is solved to maintain central adaptive precoding and subcarrier mapping for both the DL and UL. The subcarrier mapping is performed by optimal and efficient method for the DL as the problem is modeled as convex. But, it is characterized by near-optimality for the UL despite the convexity due to the per-user resource constraints of the UL problem. The DL problem is sorted out using the Lagrange multiplier theory which is regarded as an efficient alternative methodology compared to the convex optimization theory. The solution is not only characterized by low-complexity, but also by optimality. Concerning the UL, the distributive resource allocation task is necessary to resolve the power allocation of the UL. The prominent advantages of the semi-distributed scheme in the UL are the provided computational and spectral efficiencies. Moreover, such scheme also leads to a small data overhead and helps simplify the terminal structure. Numerical simulations illustrate remarkable spectral and SNR gains provided by the proposed scheme. In addition, robustness is demonstrated against the tight and relaxed transmission conditions, i.e. interference constraints. Therefore, the proposed schemes enable larger communication range for underlay CR networks.

Concerning the multiuser MIMO CR based network, we develop an adaptive non-iterative linear precoder, namely Adaptive Minimum mean square error Block diagonalization (AMB). The proposed AMB precoder employs the proposed DoF concept which we call it here *precoding diversity*. In this context, DoFs of the proposed precoder are generated by space combining and channel path combining methods. We have also developed adaptive Zero-Forcing Block diagonalization (AZB) engaging the precoding diversity concept. The proposed AMB precoder illustrate a notable spectral and SNR gains over the conventional MMSE as well as the AZB

precoders in the SNR region of interest: The low SNR region. Unlike non-linear iterative precoders, the proposed precoders are linear non-iterative and therefore provide low-complexity along with a gainful spectral efficiency.

The complexity provided by the proposed precoders is an indispensable price for the acquired spectral efficiency compared to the state-of-the-art linear precoders. More specifically, the antenna configuration affects the complexity of both AMB and AZB precoders, which is designed according to the capacity-complexity trade-off. The growth in complexity of the proposed AMB and AZB precoders is exponential. However, possible complexity reduction aspects include parallel computing which is facilitated by the independence of the DoFs in the adaptive precoding. The other aspect relaxes the exponential complexity by working off those DoFs which don't take the entire set of cognitive users into account.

Keywords: Cognitive radio, next generation networks, adaptive precoding, precoding diversity, multiuser MIMO, OFDMA, resource allocation, convex optimization theory, Lagrange multiplier theory.

Kurzfassung

In dieser Dissertation werden effiziente Ressourcenallokation und adaptive Vorkodierungsverfahren für zwei Szenarios entwickelt: Mehrbenutzer-MIMO-OFDM und Mehrbenutzer-MIMO jeweils basierend auf CR-Netzwerken.

Im Bereich der Mehrbenutzer-MIMO-OFDM CR-Netzwerke wurden Verfahren zur Ressourcenallokation und zur adaptiven Vorkodierung jeweils für den Downlink (DL) und den Uplink (UL) entwickelt. Die Ressourcenallokation wurde als Optimierungsproblem formuliert, bei dem die Summenrate maximiert wird, wobei die Gesamtsendeleistung und die Interferenz an den Primärnutzern begrenzt ist. Das formulierte Optimierungsproblem ist ein sogenanntes Mixed-Integer-Programm, dessen kombinatorische Komplexität nur extrem aufwendig lösbar ist. Auf Grund dessen wurde es zur Komplexitätsreduktion in zwei Phasen aufgeteilt: Adaptive Vorkodierung (DoF-Zuordnung) und Subkanalzuordnung. Während die Ressourcenallokation für den DL aus Implementierungssicht ein zentralistischer Prozess ist, kann sie für den UL als semiverteilt eingeordnet werden. Die Aufgabe der zentralen Ressourcenallokation wird gelöst, um die zentrale adaptive Vorkodierung und die Subkanalzuordnung für UL und DL zu verwalten. Die Subkanalzuordnung ist für den DL optimal und effizient gelöst, indem das Problem als konvexes Problem modelliert ist. Für den UL wiederum ist das Problem trotz der Konvexität quasi-optimal gelöst, da in der Problemformulierung eine Begrenzung der Ressourcen pro Benutzer existiert.

Im Falle der Mehrbenutzer-MIMO CR-Netzwerke wurde ein adaptiver, nichtiterativer, linearer Vorkodierer entwickelt, genannt "Adaptive Minimum mean square error Block diagonalization" (AMB). Die AMB Vorkodierung generiert Freiheitsgrade und wird hier als *Vorkodierungsdiversität* bezeichnet. Der vorgestellte AMB Vorkodierer zeigt im wichtigen Bereich des niedrigen SNR bemerkbare Gewinne im SNR und der spektralen Effizient gegenüber dem konventionellen MMSE Vorkodierer. Der vorgestellte Kodierer ist linear und nichtiterativ und kann so eine geringe Komplexität zusammen mit einer Steigerung der spektralen Effizienz bieten.

Contents

1 Introduction

1.1 Overview

Since their introduction and spread, mobile communications have been smoothing people's lives through providing new services and applications. Mobile radio communications have been evolving since 1980s in form of generations each containing its own progression as illustrated in Figure 1.1. The first generation (1G) employed analog transmission for voice call services. The first cellular system in the world was launched by Nippon Telephone and Telegraph (NTT) in Tokyo, Japan. Then, popular analog cellular systems appeared in Europe in 1980s: Nordic Mobile Telephones (NMT), Total Access Communication Systems (TACS), and A/B/C-Netz. In the United States, the Advanced Mobile Phone System (AMPS) occurred in 1982. Both AMPS and TACS employ analog techniques such as frequency modulation for radio transmission and frequency division multiple access (FDMA) for traffic multiplexing [Che03, Toh02].

The second generation (2G) systems compared to 1G offered higher spectrum efficiency, low data rate services, and more advanced roaming. Global System for Mobile Communications (GSM) was deployed in Europe in the end of 1980s enabling seamless international

roaming throughout Europe. In the United States, three tracks of development were followed in 2G. The first was developed in 1991 for which a new version of services (IS-136) was added in 1996. Meanwhile, CDMA-One (IS-95) was established in 1993. Japanese Personal Digital Cellular originally recognized as Japanese Digital Cellular was released in 1990 [Che03]. The aforementioned 2G systems consider digital protocols for providing voice call and short text message services. In particular, 2G are characterized by various digital modulation schemes in radio transmission as well as time division multiple access (TDMA) technique for traffic multiplexing except the IS-95 which employs code division multiple access (CDMA). Moreover, 2G systems has exhibited improvement in capacity and coverage with data rates up to 64 kbps in a circuit switched fashion. This is followed by further improvement with a quest for high-speed data rates. General Packet Radio Service (GPRS), which is categorized as 2.5 generation (2.5G), has upgraded the data rates up to 160 kbps employing packet switching protocol rather than the circuit switching. A further advancement to GPRS, defined as 2.75 generation (2.75G) dubbed as Enhanced Data Rates for GSM Evolution (EDGE), uses higher order modulation and coding schemes to provide high data rates up to 473.6 kbps.

Standardization bodies has decided to design network standards whose services are independent of the technology platform and characterized by universality. Hence, the third generation (3G) was developed [Mis04]. The International Telecommunication Union (ITU) has termed "IMT-2000" for the 3G standard requirements. This was followed by a mobile system definition fulfilling the IMT-2000 standard by the 3rd Generation Partnership Project (3GPP). Generally speaking, 3G has been developed to open the gates for broadband mobile communications supporting multimedia and Internet services beside voice calls and text messages for speeds up to 2 Mbps in indoor environments. Europe has implemented UMTS (Universal Mobile Telecommunication System), which was driven by European Telecommunication Standards Institute (ETSI). The 3G American variant is called CDMA2000, but the Japanese variant is branded FOMA (Freedom of Mobile Multimedia Access). It is worth to point out that Wideband CDMA (WCDMA) technique characterizes the air interface technology of UMTS. Both CDMA2000 and UMTS have been evolved into 1xEV-DO (1x Evolution Data-Optimized) and HSD/UPA (High Speed Downlink/Uplink Packet Access), respectively, which have been standardized as (3.5G).

The standardization body 3GPP has developed a long-term evolution of radio access technology called as 3GPP-Long Term Evolution (LTE) [3GP], which is referred to as the fourth generation (4G). 4G is characterized by all-IP (Internet Protocol) feature, which simplifies internetworking with all fixed and wireless communication networks that have been developed so

far [Wu10, KLSD10]. Based on Release 6 [3GP06], LTE technology supports peak data rates up to 100 Mbps in downlink and 50 Mbps in uplink in a bandwidth of 20 MHz. It also improves spectral efficiency 3 to 4 times the UMTS downlink and 2 to 3 times the uplink. Concerning latency, the control plane latency is reduced to 100 ms and the user plane latency should be less than 10 ms. However, Advanced LTE termed as (LTE-A) should support enhanced peak data rate of up to 1 Gbps in downlink and 500 Mbps in uplink for low mobility scenarios [AY12]. Such 4G features facilitate mobile video conferencing and high-quality 3-dimensional graphics. The demand of high-rate mobile communication systems increases exponentially [Eri13]. In just the past 10 years, it has been seen an astonishing evolution of wireless service with exponential growth along with a stunning data usage around the globe exceeds 1 billion Gbyte in a month. In 2020, the amount of traffic in wireless networks is estimated to be 1000 times higher than that in 2010 [HHI+12].

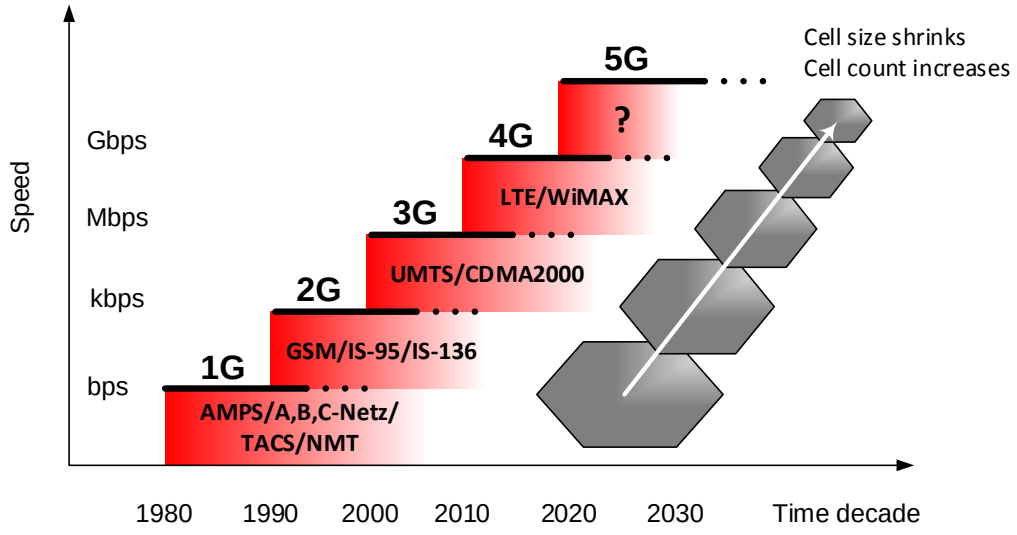

Figure 1.1: Evolutions of wireless mobile communication networks

1.2 Motivation

The emergence of new techniques and technologies in the wireless communication field as well as the increasing demands for services and applications have triggered researchers to investigate the next generation mobile networks (NGMN) categorized as the fifth generation (5G). Initial specifications of 5G have been launched by NGMN alliance in their white report [5G 15]. The

key requirements of 5G include supporting number of devices/services, spectral efficiency, peak data rate, and low latency at limits beyond what 4G and its enhancements can support. The use of cognitive radio (CR) is anticipated to enable a couple of significant enhancements in NGMN. The major enhancement includes dynamic adaptation of radio access technologies in harmony with localized conditions and spectrum usage. Consequently, improvements in spectrum efficiency, controllable mutual interference among users, and flexible co-existence with various radio access technologies are gainful benefits. Such benefits have caused a consideration of cognitive networking as integral component of NGMN [5G 15, 4G 14]. The greatly increased complexity in 5G (due to the localized variations, the heterogeneous networking, and the availability of various access methods) will not be optimally managed with human input, or with those conventional algorithms which lack adaptability to the environmental changes. Therefore, cognitive radio involvement in 5G will address adaptability and management to those localized conditions with greatly reduced human intervention.

CR has been originally proposed by Mitola [Mit00] to opportunistically use the underutilized spectrum bands of a "licensed" primary radio (PR) system by an "unlicensed" CR system. This would allow new market entrants, enterprise, public safety, and even existing wireless operators to offer higher capacity and new services without requiring a purchase for expensive and scarce spectrum. For example, a wireless network operator can provide new services by installing CR access points where the PR access points are located. This improves the area throughput of a cell via serving more users opportunistically by the CR units. In this context, users that cannot gain access in the PR network will have a chance to access the CR network. Such a goal requires wise methods to manage the multiuser interference and improve the spectral performance as well. Thus, the research work of this thesis will investigate and focus on developing new multiuser communication techniques for enhancing the performance of CR mobile networks. The emphasis of this work covers transmit preprocessing and resource allocation algorithms that can provide efficient spectrum sharing for the CR users considering the performance of the PR network as a priority.

Another viable application that motivates this thesis framework includes dense deployment scenario of overlapping WLANs in the context of future high-efficiency WLANs (HEW), so-called IEEE 802.11ax-2019 [IEE15]. This new generation of WLAN is intended to establish high-definition audio and video content exchange between users in very dense scenarios like stadiums, trains, etc. The exchange of high-definition multimedia certainly needs groundbreaking heterogeneous infrastructure which is capable of accommodating a large number of users meanwhile providing qualitative services.

Deep in the cutting-edge technologies, there are shortcomings which motivate this work. In this context, the multiantenna technology so-called multiple-input multiple-output (MIMO) is a key component in the future 5G. MIMO system can achieve capacity gain and reliable communications by means of the spatial multiplexing and spatial diversity [Tel99]. Regarding to multiantenna processing, transmit preprocessing so-called *precoding* can be regarded as a generalization of beamforming in which multiple spatial streams are supported in multiantenna wireless communications. In single-stream beamforming, the same signal is multiplied by appropriate complex weight at each transmit antenna before transmission. Such complex weights are supposed to provide optimal level of the signal power at the receiver output. However, considering single-stream beamforming for multiantenna receiver hinders concurrent signal level maximization at all the receive antennas [FG98]. Therefore, precoding is generally required in systems of multiple receive antennas.

Recently, advanced MIMO has been extended to a multiuser MIMO, which can add multiple access capabilities to MIMO. Multiuser MIMO provides high data rate as well as reliable communications and is considered a key enabler for advanced multiuser transmit and/or receive processing techniques. The MIMO broadcast channel (BC) and multiple access channel (MAC) are examples for multiuser MIMO systems. The multiuser MIMO systems have been investigated and integrated with interference cancellation and interference management processing techniques producing a significant improvement in the spectral efficiency of communication systems. Several advanced processing techniques have been intensively studied in the context of both non-CR systems as in [WSS06, JUN05, SSH04, SLL09b, ZL05, SLL09a] and CR scenarios as in [ZXL09, HZL07, LL11] taking into account the unique constraints of CR. Generally speaking, although non-linear schemes, i.e. dirty paper coding (DPC) based, provide high spectral efficiency and characterized as capacity-achieving, they remarkably require high complexity (i.e. iterative processing). Furthermore, they require efficient dirty paper codes to approach the theoretical capacity limit such as Tomlinson-Harashima precoding [Tom71, HM72]. On the other hand, despite linear processing methods provide sub-optimal spectral efficiency, nevertheless they are preferred for their tractable computational complexity. In CR networks, the computational complexity is a critical issue due to the fact that CR networks have to devote as much time as possible for spectrum sensing to avoid disturbing the PR network. Meanwhile CR has to devote as much time as possible for data transmission to provide high spectral efficiency. Therefore, such time restrictions in a CR network require efficient processing for data. In addition, one of the operational modes of the CR networks suffers from power restriction to avoid interfering the PR network. Such limitation on transmit power has the consequence

of low throughput. Therefore, the throughput-complexity trade-off in CR networks is a crucial issue and needs to be addressed by research. Such a trade-off motivates the work of this thesis.

The classic results of precoding assume flat fading channel which does not change fast. However, in practice channel suffers frequency selectivity especially at high data rates and therefore flat fading channel can be obtained by employing the multicarrier technology. Orthogonal frequency division multiplexing (OFDM) [Skl97] has been defined as an efficient multicarrier technique to mitigate inter-symbol interference (ISI) caused at the receiver by the multipath frequency selective fading [Cha66, WE71, Cim85, ZW95, JH07]. Thereby, OFDM technology provides outstanding communication reliability at high data rates. Furthermore, it is characterized by easy equalization at the receiver at large transmission bandwidth where the single carrier equalization produces intractable computational complexity. Given the above mentioned properties of OFDM, its applications have been recently extended to a multiple access scheme (OFDMA) referred to as multiuser OFDM [Law99]. OFDMA is meant for accommodating multiple users in a communication system. Perhaps the dominant advantage of OFDMA is the flexible subcarrier assignment for gaining spectral efficiency via the multiuser diversity. Due to its potential advantages, OFDMA has been involved in the recent generations of wireless networking standards which have been issued by 3GPP and Institute of Electrical and Electronics Engineers (IEEE), i.e. LTE as well as LTE-A and Wireless Local Area Network (WLAN) termed as 802.11ax [IEE15].

Yet, OFDM is well-established but considerations regarding its integration with various technologies such as MIMO, multiple access, resource allocation, etc. need to be addressed in the upcoming 5G networks to fulfill the key requirements [5G 15]. The bottleneck in OFDMA technique is how to perform optimal subcarrier assignment at low-complexity cost. The exhaustive search to assign subcarriers to users is known as a time consuming solution with exponential complexity. This motivates many researchers to find efficient subcarrier allocation paradigms which also require as little feedback as possible between base stations and users especially for the uplink case. Generally, minimize the feedback refers to either one of the following possibilities: Central scheme with little feedback or completely distributive scheme with no feedback at all. This aspect is also one of the motivations of this thesis.

1.3 Thesis Scope and Aim

This dissertation aims to develop efficient platforms for future multiuser CR networks. We assumed single cell scenarios. The proposed frameworks sort out issues related to spectrum

efficiency enhancement at acceptable computational complexity. In particular, this thesis aims to develop a couple of linear transmit precoders, which can provide remarkable spectral efficiency in the signal-to-noise ratio (SNR) region of interest, i.e. low SNR region. The precoder design utilizes the multiantenna structure efficiently to provide multiple countable independent degrees of freedom (DoFs). These DoFs can be seen as a precoding set among which one candidate DoF provides the best spectral performance. The fundamental precoding expressions are derived under two criteria: Zero-forcing (ZF) and minimum mean square error (MMSE). The corresponding precoders are termed adaptive since the design mechanism facilitates precoding adaptation according to the operating transmit power. The adaptive precoding achieves better SINR for the CR users whilst fulfilling the network constraints. The best DoF selection is similar to selection diversity, therefore the precoder is said to benefit from *precoding diversity*. The precoding diversity produces multiuser (inter-user) interference (MUI) diversity among CR users which improves the SINR of the CR users providing considerable spectral performance in the low SNR regime. The computational complexity of the adaptive precoders comes from calculating the candidate DoFs. It depends on the antenna configuration (i.e. overall number of antennas) of CR and PR systems. Generally, the complexity increases as the aggregate number of antennas and antennas per CR user increase. Since the adaptive precoders have independent DoFs, parallel computing can provide a complexity reduction by means of multiple processing cores and threads.

Concerning multicarrier CR systems, we develop an efficient two-phase scheme for efficient resource allocation (RA) task. The first phase treats DoF selection for the adaptive precoding, but the second phase elaborates subcarrier mapping. The proposed scheme is characterized by spectral and computational efficiencies if compared to the exhaustive search. In our solution, the downlink is solved by a central RA task. Important to note that the DoFs are computed and selected when the CR network is interference-limited. Then, optimal subcarrier mapping is built upon optimal power allocation that comes off the central RA task. Regarding the uplink, the problem is solved by a semi-distributed scheme: A central task to get subcarrier mapping, then per-user task to perform distributive adaptive precoding and optimal power allocation. Due to the per-user resource constraints of the uplink, the semi-distributed RA scheme provides near-optimal spectral performance which is characterized by computational efficiency.

1.4 Main Contributions

In this thesis, we assume full and perfect channel knowledge at the base station. The processing is restricted to linear precoding schemes since they are computationally efficient. The major contributions of the thesis can be summarized as follows.

- *Adaptive precoding for multiuser MIMO-OFDM CR networks*: As mentioned, the adaptive precoding produces multiple DoFs that directly improve the SNR of users and the spectral performance accordingly. The adaptive precoding in such a system takes two forms: Central and distributive. The central precoding conducts a common DoF selection on the entire set of OFDM tones. It takes place at the CR base station. However, the distributive performs DoF selection on the subset of OFDM tones assigned to the CR user and takes place at the terminal of the user. In addition to the spectral efficiency of the adaptive precoder, the best DoF selection is implemented with computational efficiency. That is by accommodating the transmit power in one of decision regions each mapped to an optimum DoF.

- *Subcarrier mapping for multiuser MIMO-OFDM CR networks*: In this procedure, we assumed the following mapping policy: Each subcarrier can not be shared by multiple CR users. We perform such procedure as a part of the central RA scheme. For the downlink, the resource constraints are central based by nature, and therefore the obtained subcarrier mapping is optimal based on the above policy. Furthermore, the computational complexity is reduced by using the Lagrange dual decomposition method. However, the optimality conditions of the uplink differ due to the per-user resource constraints for which the above mentioned method is inapplicable. The exhaustive search provides optimality, but at an exponential complexity. Hence, a relaxation is necessary to enable the use of the Lagrange decomposition. Toward this goal, the per-user power constraints of the uplink optimization problem are replaced by a single constraint which is the sum of users' power. This enables the use of the central RA scheme and produces a near-optimal solution.

- *Adaptive precoding for multiuser MIMO broadcasting CR network*: In this system, CR users interfere each other. We can use such MUI to improve the spectral performance of the system. We focused on the ZF and MMSE optimization criteria to design the corresponding adaptive precoders. By using the antenna structure of both CR and PR systems, adaptive precoding can provide many DoFs which we call it precoding diversity.

Such diversity improves the SINR of CR users and the sum-rate accordingly. The DoFs are produced by two ways: Channel path combining (CPC) and subspace combining (SC). In the CPC based method, rows of the block channel that collects channels of all CR users are combined. However, in the SC based method, spaces of the complementary block channel are combined. CPC is computationally more expensive than SC. However, two complexity reduction aspects are possible mainly for the CPC based method: Parallel computing and search space confinement. In the search space confinement, only those DoFs which consider all CR users are taken into account.

Part of thesis contributions was published as conference and journal papers in [YH14, YH16a, YH16b, YH17].

1.5 Thesis Outline

The thesis is structured as follows. **Chapter 2** presents a detailed information about CR networks such as operational transmission modes and corresponding functionalities. It also exhibits the spectrum sharing classes and the use of MIMO technology in CR networks. Also, considerations for realizing practical channel model are covered and formulated mathematically.

Chapter 3 introduces the basics and general trends of resource allocation in multiuser MIMO/OFDM CR networks. Since radio resources are allocated through optimizing a system utility function, the possible optimization objectives and constraints of CR networks are covered. Furthermore, state-of-the-art linear precoding techniques such as ZF and MMSE are derived through optimization.

Chapter 4 describes the details and efficiency of our proposed two-phase scheme for multiuser MIMO-OFDM CR networks. The first phase elaborates the design of the proposed adaptive precoding and DoF assignment. The second phase resolves fast and optimal/near-optimal subcarrier mapping for the downlink/uplink according to an optimization performed by Lagrange multiplier theory. First, system modeling and assumptions are introduced. Then, the proposed adaptive precoding is studied. Next, the mathematical steps of the proposed two-phase solution are derived in details for both the downlink and uplink.

Chapter 5 discusses a couple of adaptive precoding designs meant for a scheme in which the CR users access the radio resource non-orthogonally causing MUI among each other. The proposed adaptive precoding schemes are developed upon ZF and MMSE criteria. The system model and assumptions cover a MIMO CR broadcasting system. The degrees of freedom of the

adaptive precoder lead to further improvement in spectral performance. Since the MUI causes non-convex problem structure, that motivates new designs of power allocation.

Chapter 6 summarizes the conclusions and future work.

2

Multiantenna Cognitive Radio Systems

2.1 Cognitive Radio (CR)

The radio spectrum is considered the most valuable natural resource for wireless communications. In the last decades, the tremendous spread of wireless applications, services, and users depleted the frequency bands in general and those bands which are devoted for future mobile communication systems in particular. International bodies such as Federal Communications Commission (FCC) regulated a policy for spectrum management in the United States [FCC02a]. It emphasized that spectrum utilization is more significant than its scarcity problem. Some spectrum usage measurements indicate that some spectrum bands are fully and periodically used whereas some other bands are partially occupied for most of the time. Precisely speaking, the space-time-frequency voids, which belong to a licensed/primary radio but not utilized at a particular time are called *spectrum holes* [SW04]. Such underutilization initiated the idea of cognitive radio (CR): An unlicensed/cognitive user can access a spectrum hole which is unoccupied by the primary user at the right time and geographical location [Mit00]. Cognitive radio is identified as an intelligent wireless communication system that is aware of its surrounding

environment and can change its operational parameters accordingly. International regulatory agencies such as FCC and ITU have diverse definitions for cognitive radio as follows

- FCC definition: "A radio that can change its transmitter parameters based on interaction with the environment in which it operates. This interaction may involve active negotiation or communications with other spectrum users and/or passive sensing and decision making within the radio" [FCC03a].

- ITU definition: "A radio system employing technology that allows the system to obtain knowledge of its operational and geographical environment, established policies and its internal state; to dynamically and autonomously adjust its operational parameters and protocols according to its obtained knowledge in order to achieve predefined objectives; and to learn from the results obtained" [ITU09].

Behind these diverse definitions, CR is mainly characterized by awareness capability and reconfigurability. The reconfigurability is provided by software-defined radio (SDR) [MM99] on which CR is built. SDR is recognized as a transceiver system which can be reconfigured with the parameters of the desired standard. Such configuration guarantees that the transmission can be changed instantaneously if necessary [Spe95, Tut02, DMA03]. SDR came to reality due to the advances and convergence of digital radio and computer software technologies [Spe95].

Since a decade, CR technique has been investigated in networking. Investigations include the basic spectrum management functions that CR networks have to consider. The following list states the main required functions that CR networks have to handle [ALVM08]

- Interference avoidance with primary networks.

- Quality-of-Service (QoS) assurance via proper spectrum band selection.

- Seamless communications during movements from spectrum band to another.

Such challenges can be carried out by four major functionalities, which are described as follows [Nek06, ALVM08]

1. Spectrum sensing: CR network must detect and periodically collect information about the available spectrum holes and partially used bands in order to take suitable reactions and reconfigurations. Sensing techniques include three main categories: Primary receiver detection, primary transmitter detection, and interference temperature management. In primary transmitter detection, CR users (CUs) observe the weak signals from the primary

transmitter. This kind of detection could be achieved by various techniques like energy detection, matched filter detection, feature detection, and cooperative detection. Although cooperative detection decreases the interference probability, the primary receiver detection is more effective within the communication range of CUs. As long as CUs do not exceed a predefined tolerable interference limit at primary users (defined by FCC as *interference temperature* [FCC03b]), this model perfectly fits the spectrum sensing objective.

2. Spectrum decision: CR networks should decide which of the available spectrum bands fits which of the users according to QoS requirements. This concept in networks is known as *spectrum decision*. In CR networks particularly, spectrum decision is based not only on internal policy regarding channel conditions, fairness, opportunistic scheduling, QoS provision, interference avoidance at the PR users (PUs), etc., but also on external policy concerning primary user occurrence and activity. The channel in CR networks more likely encounters several impairments including: Interference due to the primary networks, path loss due to the distance, link errors due to the modulation scheme and interference level, and link delay due to the various protocols of different spectrum bands.

3. Spectrum sharing: Since the wireless channel in communication networks is open for all users, there should be a coordination for transmission attempts. Thus, spectrum sharing is relevant to medium access control protocol. Generally speaking, CR networks have to coordinate the access of CUs in such a way that destructive MUI effect on spectral inefficiency is avoided as possible. Spectrum sharing frameworks can be divided to four aspects: Spectrum allocation behavior, architecture, access/operational mode, and scope. Since spectrum sharing is the focus of this thesis, more details will be introduced in the next section.

4. Spectrum mobility: Since CUs are regarded as unlicensed users, they have low priority compared to PUs that appear on a specific spectrum band. Consequently, the communication of the CUs must be seamless during the transfer to another vacant or partially used portion of the spectrum. Such process imposes a new conception of handoff in CR networking dubbed *spectrum handoff*. Once a CR user changes its operating frequency, the network may require to modify the communication parameters (like modulation, power, coding, etc.) accordingly such that a fast and smooth transition can lead to minor performance degradation due to spectrum handoff.

2.2 Spectrum Sharing in CR Networks

The architecture based classification of spectrum sharing can be categorized into *centralized* and *distributed*.

- Centralized spectrum sharing: In this method, the spectrum allocation is controllable by means of a central unit.
- Distributed spectrum sharing: In this approach, the policies of spectrum allocation are distributed over local nodes [ZTSC07].

The second classification covers two classes of spectrum allocation behavior: *Cooperative* and *non-cooperative*.

- Cooperative spectrum sharing: In this class, clusters are established to share interference information.
- Non-cooperative spectrum sharing: In this type, a single node is counted [ZC05] such that interference disturbing other nodes is not counted.

The third classification includes two categories regarding sharing scope: *Intranetwork* and *internetwork* as illustrated in Figure 2.1.

- Intranetwork spectrum sharing: In this paradigm, the policy of spectrum allocation considers only the entities of a single CR network.
- Internetwork spectrum sharing: In this framework, multiple CR networks/operators are considered in spectrum sharing policies.

The fourth classification is related to three operational/access modes [MBR05, GJMS09, Wan09, BGG$^+$13]: *Interweave*, *overlay*, and *underlay*. Detailed information regarding these paradigms follows in the next section.

2.3 Cognitive Radio Network Operational Modes

The operational modes in CR differentiate according to the available network side information (i.e. activity, codebooks, channel conditions, or messages of other nodes which share the spectrum) and the regulatory constraints (i.e. the interference caused by CUs at the PUs, so-called

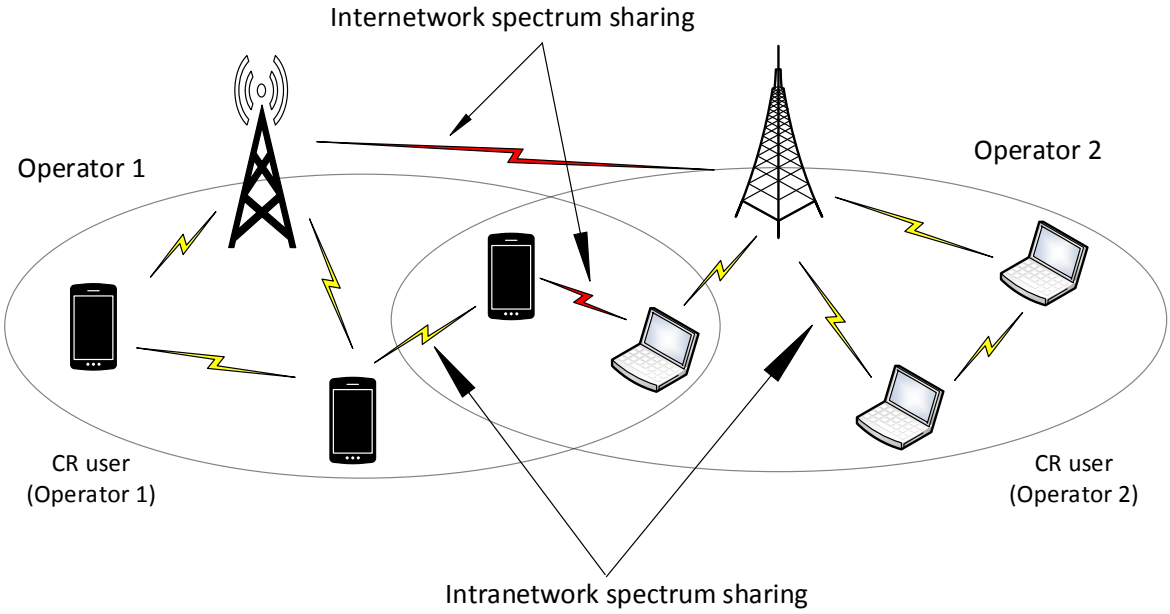

Figure 2.1: Intranetwork and internetwork spectrum sharing in CR networks

PU interference (PUI)) into the three aforementioned schemes [Kol05]. These approaches have different procedures and considerations to be taken into account for the corresponding networking and circuitry designs. It is worth to know that hybrid platforms combining the above mentioned methods [WN07] can have potentiality to achieve remarkable spectral efficiency gains.

1. **Interweave Mode**: This mode was the original motivation of CR, and counts on *opportunistic communication* idea [Mit00]. This idea has been studied afterwards by FCC [FCC02b] exhibiting that the spectrum holes change with geographic location and time, and can be utilized by CUs. Thus, the interweave technique imposes knowledge of PUs activity in the spectrum. In other words, interweave CR requirements are: (a) Periodic spectrum monitoring, (b) accurate detection to spectrum occupancy, (c) opportunistic communication over spectrum holes, and (d) seamless communication during spectrum handoff. Interweave CR paradigm faces signal processing challenges, perhaps the major one is the accuracy of PUs detection in the radio spectrum in which the PUI is minimal preserved as demonstrated in Figure 2.2. As a technology, interweave CR networks occurred about a decade ago within the context of Wireless Regional Area Networks

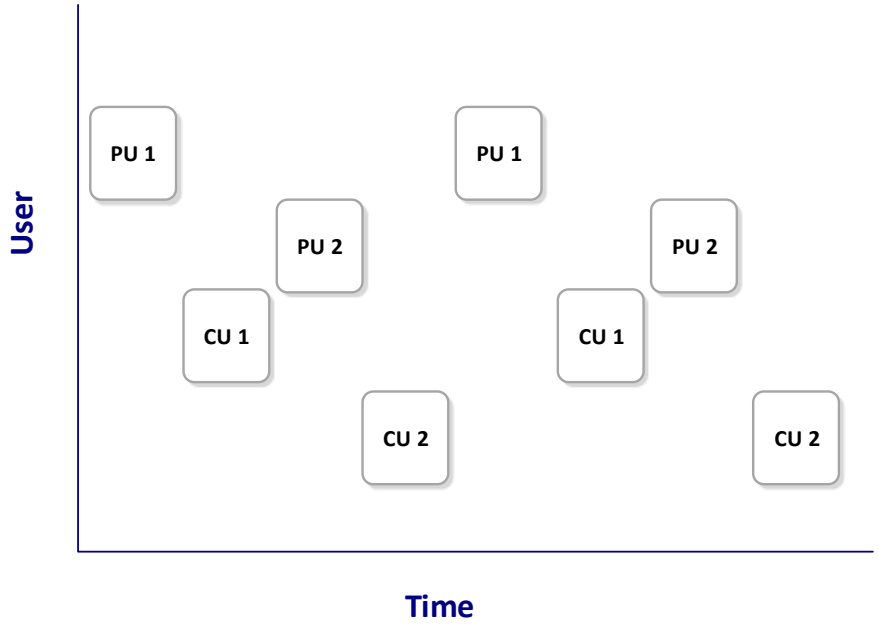

Figure 2.2: The interweave scheme of cognitive radio using time sharing

(WRAN) which is the first standard released by IEEE 802.22 working group [IEE08]. WRAN employs the CR techniques for utilizing television unused white spectrum bands opportunistically. The key specifications of WRAN include: Rural area coverage range between 17 to 100 km, spectrum bands between 54 and 862 MHz, user mobility of up to 114 km/h, and peak data rates of up to 1.5 Mbps for downlink and 384 kbps for the uplink.

2. **Underlay Mode**: In this mode, the cognitive radio constrains its transmit power to ensure that the interference power caused at the PUs by the CUs (i.e. PUI) does not exceed a predefined threshold. In other words, this paradigm allows concurrent cognitive and primary radio communications as long as the PUI insignificantly degrades the performance of the PR receivers. Candidate techniques to conduct the underlay mode include beamforming by means of the multiantenna technology and spread spectrum. In the spread spectrum technique, the CR signal is spread over a wide bandwidth to reach the noise floor level as illustrated in Figure 2.3. In beamforming, the multiantenna structure en-

ables the interference control at the PUs as illustrated in Figure 2.4. The interference constraint in underlay scenarios is typically tight, thus it limits the CUs transmit power and consequently restricts the communication range to short distances. Since the short communication range is the major limiting factor of the underlay paradigm, it will be addressed in this thesis.

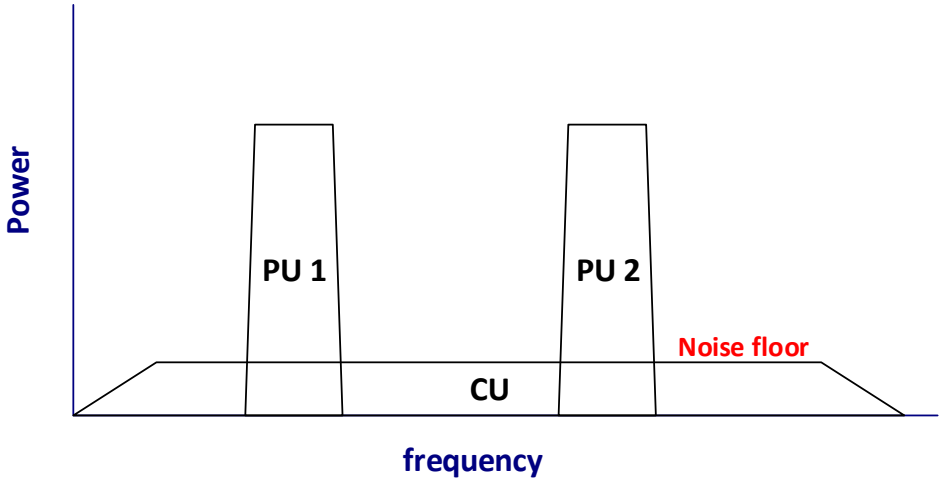

Figure 2.3: The underlay scheme of cognitive radio using spread spectrum

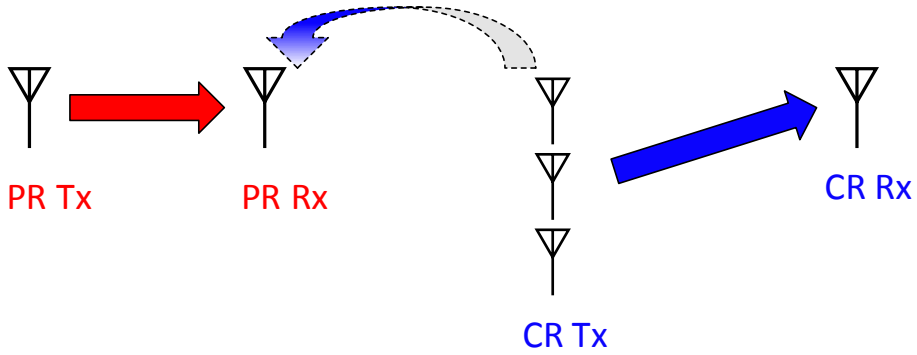

Figure 2.4: The underlay scheme of cognitive radio using multiantenna techniques

3. **Overlay Mode**: In this scheme, the CR transmitter knows the PR users' broadcasted messages and codebooks. A possible form for the overlay model follows. The PR transmitter

sends its message to the CR user before establishing the data communication. Knowledge of the PR users' information can be employed for canceling or mitigating the induced interference at the receiver of the CR user. From another perspective, the CR user benefits from this information in power allocation for establishing its own communications and assisting the PR users' communications as illustrated in Figure 2.5. In more details, the CR user assigns part of the power to its own communications and the other part to assist PR user by serving as a relay. The CR transmitter has no restrictions on power such that no matter how much PUI is induced. Because the decrease in the SNR of the PR link due to the PUI is compensated by an improvement due to the CR relaying.

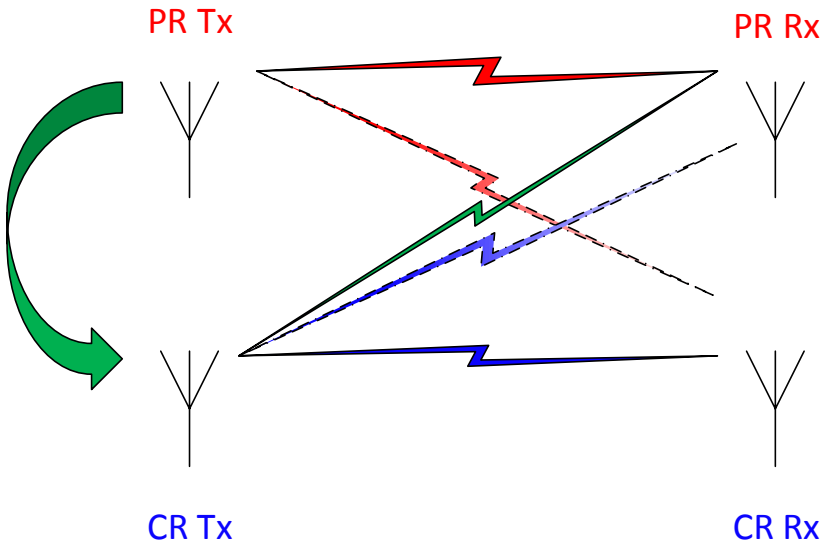

Figure 2.5: The overlay scheme of cognitive radio

2.4 Multiantenna Technology in Underlay CR

Since the radio spectrum is a precious natural resource involved for many applications, such as radio/TV broadcasting, cellular networks, satellite links, etc., the licenses are expensive. In particular, those bands which are suitable for long-distance applications. Thus, it is necessity to design wireless systems characterized by spectral efficiency. The available transmit power is the only limiting factor of the spectrum efficiency of a single path transmission (single-input

single-output) [Sha48]. However, the spectral efficiency can be increased via frequency reuse mechanism by parallel spatially-separated devices, that is by dividing the area into cells and sectors as in mobile radio networks. Such near-orthogonal resource allocation greatly avoids the MUI, but it suffers spectral inefficiency if compared to non-orthogonal controlled-interference approaches [SB05].

The engagement of multiple antenna in communications increases the spectral efficiency linearly in terms of the number of antennas if the channel is known [FG98, MF70, Tel99]. The advantages obtained from the multiple antenna structure include spatial multiplexing, spatial diversity, and beamforming as illustrated in Figure 2.6.

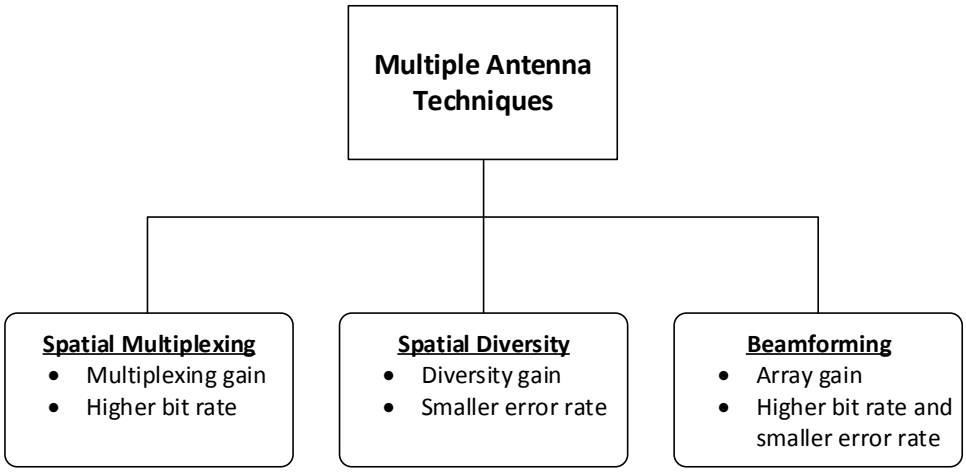

Figure 2.6: Possible benefits of using multiple antennas

CR networks which incorporate multiantenna structure and advanced signal processing techniques can withstand higher levels of noise and interference than the conventional non-CR systems. Precoding technique is sort of generalized beamforming as it provides multiple spatial streams in MIMO systems. In point-to-point systems, precoding support multistream beamforming such that each data stream has independent and proper complex weights to maximize the link data rate at the receiver output. In multiuser MIMO, the data streams are directed to different users such that certain quality measure is optimized (e.g. sum-rate, energy efficiency, fairness, etc.). The channel state information is required in multiuser MIMO systems to handle the MUI [GKHJ$^+$07]. In particular, the users of CR and PR networks have to have multiple antennas to facilitate the MUI and PUI management among CR users and toward the PR users, respectively.

2.5 Wireless Channel Modeling

To provide reliable and high-speed communications, wireless channel poses a big challenge. It suffers not only noise, interference, and other impairments, but also their random variations over time due to transmitter and/or receiver mobility. Those variations in the received signal are driven by path loss, shadowing, and multipath effects. Path loss describes the attenuation in the transmit power when it radiates away from transmitter. Influence of the path loss variation happens over large distances (100-1000 m), thus it is referred to as large-scale fading effect. Shadowing defines the attenuation in signal power rendered by obstructions between transmitter and receiver, in particular, because of absorption, scattering, and diffraction. Such variation occurs over distances proportional to the object length (10-100 m), hence it is regarded as medium-scale fading effect. Multipath variation happens when multiple variants of the transmitted signal follow different paths during propagation toward receiver arriving at different time delays. Multipath is resulted from signal reflections and occurs over short distances on the order of the signal wavelength and is, therefore, dubbed small-scale fading effect. Figure 2.7 illustrates the combined effects of path loss, shadowing, and multipath.

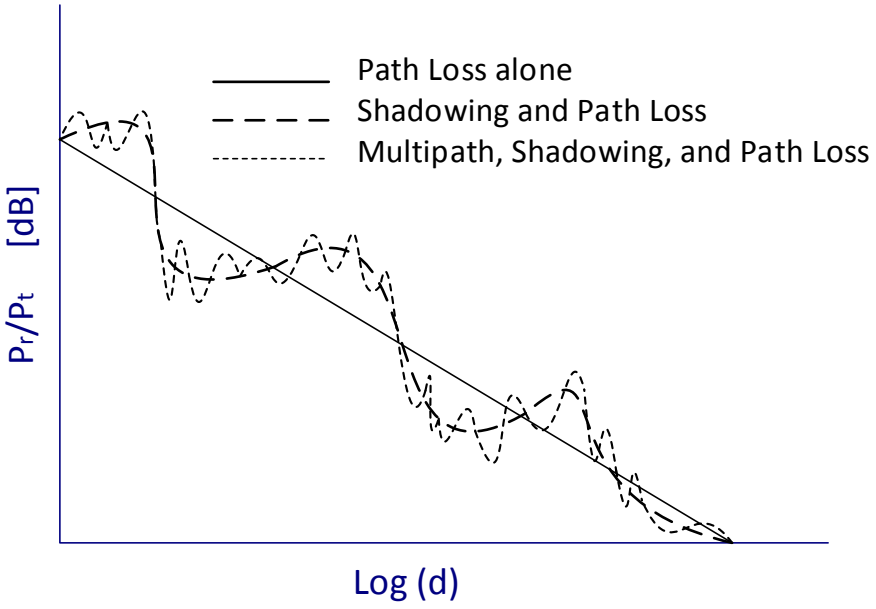

Figure 2.7: Fading effect on signals due to the wireless channel

2.5.1 Path Loss Modeling

To obtain precise path loss modeling, empirical measurements with tight specifications or complex models have to be determined. But, for general system designs, it is convenient to use a simple model approximating real channel due to the fact that channel modeling is not the main focus in this thesis. Since the path loss varies with distance, it is non-trivial to consider the following model

$$\begin{aligned} \frac{\mathrm{P}_r}{\mathrm{P}_t} &= \mathrm{Z}_{\mathrm{PL}} \\ &= \mathrm{Z}_0 \left(\frac{d_0}{distance} \right)^{\gamma} \\ &= \left(\frac{\lambda}{4\pi d_0} \right)^2 \left(\frac{d_0}{distance} \right)^{\gamma} \end{aligned} \tag{2.1}$$

The dB path loss is expressed as

$$\mathrm{Z}_{\mathrm{PL(dB)}} = \mathrm{Z}_{\mathrm{0(dB)}} - 10\gamma \log_{10} \left(\frac{d_0}{distance} \right) \tag{2.2}$$

where Z_0 is a unitless constant which relies on the average channel attenuation and the antenna characteristics, d_0 points to a reference distance in the antenna far-field, and γ is the path loss exponent. For approximating either an empirical or analytical model, the parameters Z_0, d_0, and γ can be obtained. The model (2.1) is only valid for $distance > d_0$, where d_0 is assumed to be 10-100 m outdoors. For empirical measurements, Z_0 is set to free-space path gain with normalized antenna gains as formed in (2.1) assuming omnidirectional antennas. Empirical data backs such assumption at 100 m distance for free-space path loss [EGT+99]. Alternately, Z_0 can be measured at d_0 or optimized by means of MMSE between model and measurements [EGT+99]. The value of γ can be obtained for complex environments via MMSE to fit measurements or alternatively from empirically based model which considers frequency and antenna height [EGT+99]. On the other hand, γ is simply set to 2 or 4 according to the propagation model either free-space or two-ray, respectively. In general, path loss tends to increase for higher frequencies [TT92, DMW95, TTP98, DRX98], but it rather decreases for higher antenna heights [EGT+99].

2.5.2 Shadowing Modeling

The signal while propagation experiences random variations due to obstructing objects in its path which gives rise to random variations in the received power. Since such variations are

caused by phenomena such as absorption, scattering, and diffraction with unknown locations, sizes, and dielectric properties, statistical models are able to identify this attenuation. A common model which has been recognized empirically as an accurate model to represent these variations is the log-normal shadowing [EGT+99, GGK+03]. In log-normal shadowing model, the quantity $\mathrm{Z_{S(dB)}} = 10\log_{10}\left(\frac{\mathrm{P}_r}{\mathrm{P}_t}\right)$ is modeled as a log-normal distributed random variable for which the probability density function is given as

$$p(\mathrm{Z_{S(dB)}}) = \frac{1}{\sqrt{2\pi}\sigma_{\mathrm{S(dB)}}} \exp\left(-\frac{(\mathrm{Z_{S(dB)}} - \psi_{\mathrm{S(dB)}})^2}{2\sigma^2_{\mathrm{S(dB)}}}\right) \tag{2.3}$$

The log mean $\psi_{\mathrm{S(dB)}}$ and the standard deviation $\sigma_{\mathrm{S(dB)}}$ characterize shadowing performance. Note that the probability in (2.3) decreases when $\psi_{\mathrm{S(dB)}}$ is large and positive indicating to the mean power variations with distance due to the path loss. In other words, the average attenuation is directly proportional with distance as a result of the potential larger number of disturbing objects. The standard deviation $\sigma_{\mathrm{S(dB)}}$ values between four and thirteen are supported for outdoors channels by many empirical studies [Jak74, Gud91, BBL92, GG93, Stu01].

2.5.3 Multipath Modeling

The received signal experiences small variations on the scale of the signal wavelength due to several replicas (pulse train) reaching the receiving antenna from multiple paths as a consequence of pulse reflections. The harmful influence of multipath on the received signal are the destructive interference and the signal phase shift. Such effects cause fading. In particular, the time delay spread caused by signal reflections is a characteristic of a multipath channel. The delay spread represents the time delay between the first and last arrivals of the received signal components resulted from a single transmitted pulse. If the channel delay spread happens to be small compared to the inverse of signal bandwidth, it causes non-resolvable narrow band fading which spreads the received signal a little. However, delay spread larger than the signal pulse duration causes resolvable wide band fading as well as gives rise to time spreading. Thus a significant distortion in the received signal is caused and known as ISI. The multipath channel is also characterized as time-variant, which arises because of transmitter and/or receiver mobility. Therefore, for repeatedly transmission of pulses from moving transmitter it is natural to observe different variations in the delays, amplitudes, and the number of multipath components corresponding to each pulse. Statistically, the magnitude of the multipath received signal has Rayleigh distribution when it has no line of sight component. Other than that, fading follows the Ricean distribution. For any two Gaussian random variables $\mathrm{Z_{m,I}}$ (in-phase component) and $\mathrm{Z_{m,Q}}$ (quadrature component) both have zero mean and equal variance σ_m^2, i.e.

$Z_{m,I}$ and $Z_{m,Q} \sim \mathcal{N}(0, \sigma_m^2)$, then signal envelope

$$Z_m = \left| Z_{m,I} + j\, Z_{m,Q} \right| = \sqrt{Z_{m,I}^2 + Z_{m,Q}^2} \tag{2.4}$$

is Rayleigh distributed whereas signal power Z_m^2 has exponential distribution [PP02].

2.5.4 Combined Channel Model

The aforementioned models of path loss, shadowing, and multipath can be combined for tracing the power decay in terms of the distance. In this model, the average path loss in dB characterizes the log mean of shadowing fading, and they both characterize the mean parameter of Rayleigh fading. Thus the models (2.1), (2.3), and (2.4) can be combined [Gol05] as

$$\frac{P_r}{P_t} = Z_{PL}\, Z_S\, Z_m^2 = Z_0 \left(\frac{d_0}{distance} \right)^{\gamma} Z_S\, Z_m^2 = |\text{gain}|^2 \tag{2.5}$$

where $Z_S = 10^{Z_{S(dB)}/10}$; $Z_{S(dB)} \sim \mathcal{N}(0, \sigma_{S(dB)}^2)$.

2.6 Chapter Summary

Since the radio spectrum resource is precious for wireless communications, temporal and spatial reuse of spectrum is one of the recent interesting solutions for the scarcity issue. The space-time-frequency voids, which belong to a licensed/primary radio, can be reused by unlicensed/cognitive radio with high priority to the primary radio. Cognitive radio is an intelligent communication system that is aware of the surrounding environment and able to adapt transmission parameters accordingly. In this chapter, we covered the major issues related cognitive radio and the aspects of realizing such kind of a radio system. The cognitive radio operates on sensing, deciding, sharing, and switching the spectrum bands in an interactive manner. The main paradigms of cognitive radio include interweave, underlay, and overlay. The realization of underlay cognitive radio is possible by means of spread spectrum, ultra wide band, and multiuser MIMO techniques. Spectrum sharing in underlay cognitive radio is one of the major challenges that need to be addressed by research. Beamforming is a potential candidate for solving cognitive radio related issues such as spectrum efficiency. Realistic channel modeling taking small-, medium-, and large-scale fading under consideration is important for realizing feasible and transparent solutions.

3

Resource Allocation and Transmit Precoding

3.1 Radio Resource Management

Radio resource management (RRM) covers the control of system level parameters such as interference, transmission characteristics, and radio resources in wireless communication systems like mobile radio networks. RRM employs functions and strategies for managing parameters such as transmit power, user scheduling, subcarrier allocation, admission control, beamforming, data rates, modulation scheme, coding scheme, handover criteria, macro diversity, etc. [TRV01] as illustrated in Figure 3.1. In addition, RRM takes multiuser and multicell network capacity issues into account such that the limited radio spectrum and network infrastructure are utilized as efficiently as possible. Particularly, the spectral efficiency of interference-limited systems can be enhanced by efficient dynamic RRM schemes, for example cellular and broadcast networks. Resource allocation schemes usually deals with spectral/energy efficiency as a cost function under some regulatory constraints depending on the system requirements. As the conventional

RRM considers the allocation of time and frequency with fixed spatial reuse patterns, the recent multiuser MIMO techniques facilitate adaptive resource allocation in spatial domain. This actually replaces the need to fractional frequency reuse by universal frequency reuse as in LTE standard [BJ13].

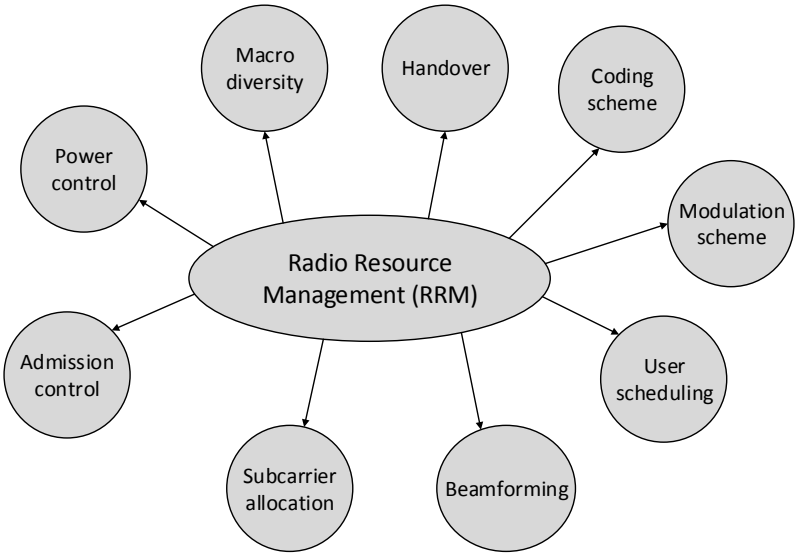

Figure 3.1: Some radio resource management (RRM) functions

RRM can be classified into static and dynamic. The static RRM is based on fixed radio network planning, however the dynamic RRM changes the network parameters adaptively according to some factors such as quality of service requirements, base station density, user mobility, etc. The dynamic scheme aims to minimize the expensive cost of manual cell planning and to achieve better spectral efficiency via small-scale frequency reuse patterns. Table 3.1 exhibits some examples for the static and dynamic RRM.

3.2 Resource Allocation (RA) for Multiuser Systems

The multiantenna technology enables modern resource allocation techniques which benefit from the space dimension for steering data toward the intended users. This signal steering is called beamforming as illustrated in Figure 3.2. By means of beamforming, some advantages are obtained: limited interference at non-intended users, increased received power at intended users (array gain), enabled global utilization of spectral resources, and relinquished cell sectorization and fixed frequency reuse patterns.

Table 3.1: Examples for some static and dynamic RRM

Static functions	Dynamic functions
- Deployment of base station sites	- Power control
- Antenna heights	- Precoding algorithms
- Sector antenna directions	- Channel dependent scheduling
- Selection of modulation and coding schemes	- Link adaptation schemes
- Fixed channel allocation	- Dynamic channel allocation
- Static handover criteria	- Adaptive handover criteria
- Static base station diversity (micro & macro)	- Dynamic diversity, e.g. space-time coding

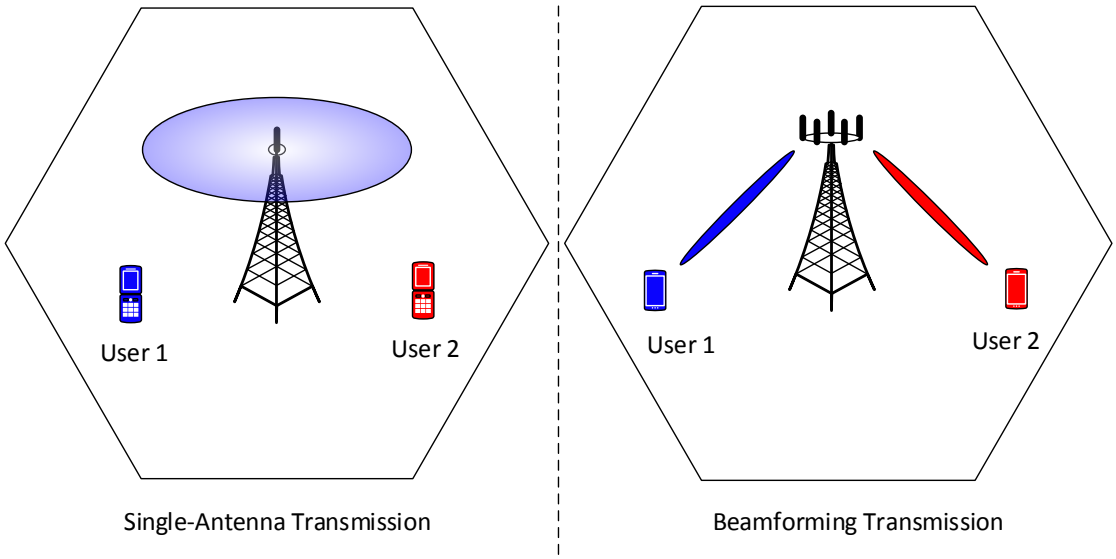

Figure 3.2: Single-antenna versus multiantenna transmissions

In a multiuser downlink systems with K users, designing transmits covariance matrices in compliance with the constraints on power is dubbed *resource allocation*. Such covariance matrices determine the transmission strategy and what is received at the users. For instance, let's consider the design of transmission covariance matrices $\{\mathbf{S}_1, \ldots, \mathbf{S}_K\}$ of the underlay CR network serving K CUs as described in Figure 3.3. Assuming the objective of resource allocation problem is channel capacity maximization with two conditions: Total power and PUI constraints, then the optimization problem takes the following form

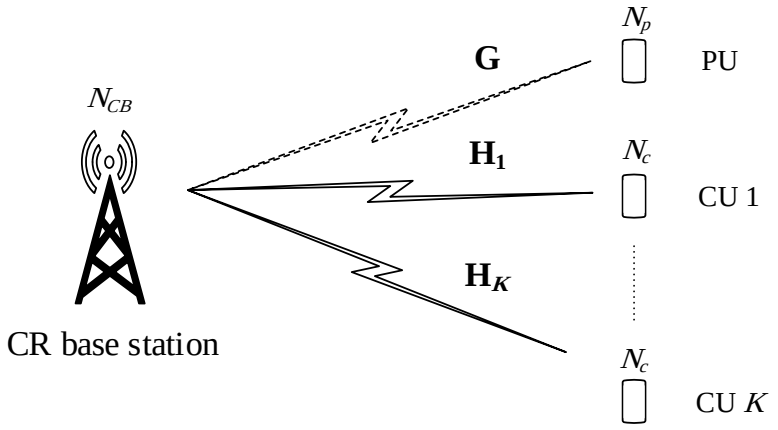

Figure 3.3: Multiuser MIMO CR based broadcast channel model

$$\begin{aligned} \max_{\{\mathbf{S}_1,\ldots,\mathbf{S}_K\}} \quad & \sum_{k=1}^{K} \log_2 \left|\mathbf{I}_{N_c} + \text{SINR}_k\right| \\ \text{subject to} \quad & \sum_{k=1}^{K} \text{Tr}\left(\mathbf{S}_k\right) \leq P_T \\ & \sum_{k=1}^{K} \text{Tr}\left(\mathbf{G}\mathbf{S}_k\mathbf{G}^H\right) \leq I_{th} \end{aligned} \tag{3.1}$$

where

$$\text{SINR}_k = \left(\sigma_n^2\mathbf{I}_{N_c} + \mathbf{H}_k\left(\sum_{j\neq k}^{K}\mathbf{S}_j\right)\mathbf{H}_k^H\right)^{-1}\mathbf{H}_k\mathbf{S}_k\mathbf{H}_k^H$$

The first constraint regulates the total radiated power toward the K CR users preventing power overshot above the budget P_T. The second constraint controls the interference caused at the PR users up to an upper limit I_{th}. The rank of $\mathbf{S}_k$ refers to the number of supported data streams to be multiplexed at the kth CU. Tr$(\mathbf{S}_k)$ quantifies the assigned power for transmission to CU k, such that the eigenvalues and eigenvectors of $\mathbf{S}_k$ describe the spatial distribution of power over the eigenmodes. In multiuser MIMO networks, users can simultaneously access the channel in *spatial division multiple access* (SDMA) manner [RO91], which gives rise to MUI and harms spectral efficiency when channel state information (CSI) is uncertain. OFDMA scheme [Law99] is another attractive technique to serve multiple users simultaneously with multiuser interference avoidance. OFDMA leads to improvement in channel capacity added

to the advantages of easy equalization and frequency selective fading mitigation. In multiuser MIMO CR based networks, managing the interference among CUs (i.e. MUI) and at PUs (i.e. PUI) can be performed by means of transmit precoding. The general structure of the transmit precoder synthesizes mainly two elements: The multiuser space matrix coming off the interfering channel and the spatial power distribution matrix. Design criteria of precoders and examples are described in the following sections.

3.3 Precoding for Multiuser MIMO Systems

In multiuser MIMO, a multiantanna transmitter transmits concurrently with multiple receivers (with one or multiple antennas per each). From the implementation point of view, precoding algorithms can be categorized into linear and nonlinear classes. Nonlinear precoding schemes are known as capacity-achieving [WSS04], but linear schemes achieve relatively lower complexity with reasonable spectral performance.

Linear precoding strategies include maximum ratio transmission (MRT) [Lo99], zero-forcing (ZF) precoding [SSH04, SLL09b], and regularized zero-forcing formulated based on minimum mean square error (MMSE) precoding [SLL09b, SLL09a]. The optimal linear precoding is computed by monotonic optimization which costs high complexity exponentially in terms of the number of users [UB12]. Nonlinear precoding design is based on dirty paper coding (DPC) concept. In DPC, the interference subtraction or cancelation takes place without penalty of radio resources if the optimal precoding order on the transmit signal is followed [WSS06]. In addition to the high computational complexity, DPC requires efficient dirty paper codes to approach the theoretical capacity limit which is another disadvantage of such scheme. Tomlinson-Harashima precoding [Tom71, HM72] is an example.

3.4 State-of-the-Art Linear Precoding

This section presents the precoding design of the conventional approaches: CR based ZF block diagonalization (ZF-BD) and CR based MMSE block diagonalization (MMSE-BD) subject to two particular constraints: PUI and transmit power. For a multiuser MIMO CR based broadcast channel model as in Figure 3.3, the details of ZF-BD and MMSE-BD follow.

3.4.1 Zero Forcing Block Diagonalization

In the conventional ZF-BD precoder, PUI and MUI are suppressed thoroughly at the kth CU receiver since the precoding matrix $\mathbf{F}_k \in \mathbb{C}^{N_{CB} \times N_c}$ lies in the null space of the interference channel $\bar{\mathbf{H}}_k \in \mathbb{C}^{\mathcal{R}_k \times N_{CB}}$ defined as

$$\bar{\mathbf{H}}_k = [\mathbf{G}^T \mathbf{H}_1^T \dots \mathbf{H}_{k-1}^T \mathbf{H}_{k+1}^T \dots \mathbf{H}_K^T]^T$$

where $\mathcal{R}_k = (K-1)N_c + N_p$. Denote $\bar{\mathbf{H}}_k^{(0)}$ as a matrix contains the null space orthonormal bases of $\bar{\mathbf{H}}_k$. Therefore, $\mathbf{F}_k$ satisfies zero PUI and MUI conditions:

$$\mathbf{G}\mathbf{F}_k = \mathbf{0}_{N_p \times N_c} \tag{3.2}$$

$$\mathbf{H}_j \mathbf{F}_k = \mathbf{0}_{N_c \times N_c} \forall j \neq k \tag{3.3}$$

Towards achieving this approach, the number of transmit and receive antennas should fulfill $N_{CB} \geq KN_c + N_p$ to provide a null space to each CU. The kth CU power $\mathbf{P}_k$ (i.e. diagonal of $\mathbf{S}_k$) is allocated by waterfilling approach as described in [SSH04] after diagonalizing the kth CU effective channel by using singular value decomposition (SVD) as

$$\mathbf{H}_k \bar{\mathbf{H}}_k^{(0)} = \check{\mathbf{U}}_k \check{\mathbf{\Lambda}}_k \check{\mathbf{V}}_k^H$$

Ultimately, the precoder of the kth CU can be expressed as

$$\mathbf{F}_k^{\text{ZB}} = \bar{\mathbf{H}}_k^{(0)} \check{\mathbf{V}}_k \mathbf{P}_k^{\frac{1}{2}} \tag{3.4}$$

3.4.2 Minimum Mean Square Error Block Diagonalization

The MMSE-BD precoder improves the performance as it regularizes the channel inverse via including the transmit power and noise covariance. The precoder addresses the transmit power boost issue found in ZF-BD through employing the MMSE criterion. The optimization design suppresses MUI subject to a transmit power and a constrained PUI threshold I_{th}. Given that $\underline{\hat{\mathbf{F}}} = [\hat{\mathbf{F}}_1 \dots \hat{\mathbf{F}}_K]$ and $\underline{\mathbf{H}} = [\mathbf{H}_1^T \dots \mathbf{H}_K^T]^T$, then the regularized channel inversion is written as [LL11]

$$\begin{aligned} \underline{\hat{\mathbf{F}}} &= \gamma \, \underline{\bar{\mathbf{F}}}(\mu) \\ &= \gamma \left(\underline{\mathbf{H}}^H \underline{\mathbf{H}} + \mu \mathbf{G}^H \mathbf{G} + \frac{N_r - \mu I_{th}}{P_T} \mathbf{I}_{N_{CB}} \right)^{-1} \underline{\mathbf{H}}^H \end{aligned} \tag{3.5}$$

where $\gamma = \sqrt{P_T / \text{Tr}\left(\underline{\bar{\mathbf{F}}}(\mu) \underline{\bar{\mathbf{F}}}(\mu)^H\right)}$ and μ is a positive parameter lies in the interval $0 \leq \mu \leq N_r / I_{th}$ aiming to fulfill the problem constraints at the upper-limit. In other words, the optimum

value of μ ensures dissipating the transmit power P_T in whole while fulfilling the PUI constraint as described in [LL11], and it can be found numerically by the bisection method [BV04]. However, for zero PUI constraint ($I_{th} = 0$), the regularized channel inversion (3.5) takes another form given by

$$\underline{\hat{\mathbf{F}}} = \gamma\, \mathbf{G}^{\perp}\underline{\mathbf{H}}^{H}\left(\underline{\mathbf{H}}\mathbf{G}^{\perp}\underline{\mathbf{H}}^{H} + \frac{N_r}{P_T}\mathbf{I}_{N_r}\right)^{-1} \tag{3.6}$$

The null space of $\mathbf{G}$ is defined as

$$\mathbf{G}^{\perp} = \mathbf{I}_{N_{CB}} - \mathbf{G}^{H}(\mathbf{G}\mathbf{G}^{H})^{-1}\mathbf{G} \tag{3.7}$$

Then, the QR decomposition can be used to compute the orthonormal bases spanned by the corresponding projection matrix $\hat{\mathbf{F}}_k$ of CU k as

$$\hat{\mathbf{F}}_k = \mathbf{Q}_k\mathbf{R}_k, \forall k \tag{3.8}$$

where $\mathbf{Q}_k \in \mathbb{C}^{N_{CB}\times N_c}$ contains the N_c columns of the orthonormal bases. As a counterpart to waterfilling power allocation, the MMSE combining matrix $\mathbf{P}_k^{\text{MB}}$ for the kth CU minimizes the sum MSE subject to transmit power constraint as shown in [SLL09b]. It is given as

$$\mathbf{P}_k^{\text{MB}} = \beta\bar{\mathbf{P}}_k^{\text{MB}} \tag{3.9}$$

where

$$\bar{\mathbf{P}}_k^{\text{MB}} = \left(\mathbf{Q}_k^{H}\Sigma_{j=1}^{K}\mathbf{H}_j^{H}\mathbf{H}_j\mathbf{Q}_k + \frac{N_r}{P_T}\mathbf{I}_{N_c}\right)^{-1}\mathbf{Q}_k^{H}\mathbf{H}_k^{H}\mathbf{H}_k\mathbf{Q}_k$$

and β normalizes the sum power and defined as

$$\beta = \sqrt{P_T/\Sigma_{k=1}^{K}\text{Tr}\left(\bar{\mathbf{P}}_k^{\text{MB}\,H}\bar{\mathbf{P}}_k^{\text{MB}}\right)}$$

To this end, the SVD is then applied to diagonalize the effective channel as

$$\mathbf{H}_k\mathbf{Q}_k\mathbf{P}_k^{\text{MB}} = \check{\mathbf{U}}_k\check{\mathbf{\Lambda}}_k\check{\mathbf{V}}_k^{H}$$

Ultimately, the precoder of MMSE-BD is expressed as

$$\mathbf{F}_k^{\text{MB}} = \mathbf{Q}_k\mathbf{P}_k^{\text{MB}}\check{\mathbf{V}}_k \tag{3.10}$$

It is worth to know that MMSE-BD outperforms ZF-BD in low SNR regime, but in high SNR regime (when $I_{th} = 0$) they converge and consequently have equivalent performance.

3.5 Chapter Summary

Radio resource management covers and employs functions and strategies for managing system level parameters such as interference, transmission characteristics, and radio resources in wireless communication systems like mobile radio networks. In addition, RRM takes multiuser MIMO and multicell network capacity issues into account such that the limited radio spectrum, the spatial domain, and the network infrastructure are utilized as efficiently as possible. Particularly, the recent multiuser MIMO techniques facilitate adaptive resource allocation in spatial domain and replace the need to fractional frequency reuse by universal frequency reuse as in LTE standard. General resource allocation schemes usually deal with spectral/energy efficiency as a cost function under some regulatory constraints depending on the system requirements. Designing the transmit strategy, i.e. covariance matrices, of a multiuser MIMO system in compliance with the power constraints is dubbed resource allocation. The design of interference management within resource allocation schemes is the technical description of transmit precoding. Precoding can also be considered as a generalization of beamforming that support multiple data streams for the same user. Despite their sub-optimal spectral efficiency, linear precoders are preferred over non-linear due to the low complexity they provide. The criteria of conventional linear precoder design include zero-forcing and minimum mean square error, which demonstrate tractable computational complexity compared to others such as maximum ratio and monotonic precoding schemes.

4

MIMO-OFDM Cognitive Radio Networks

Currently the radio spectrum is not efficiently used: Some frequency bins are overloaded, while others are sparsely used for most of the time. This situation can be improved by CR [Mit00]. A powerful application of CR is to adaptively allocate frequency bins used by PUs to unlicensed users, so-called CUs. The underlay CR network can concurrently operate with the PR network but, however, has to restrict its transmit power to induce interference at the PUs below a predefined limit called interference temperature [Hay05]. Consequently, this limits the communication range of underlay CR networks. By means of a multicarrier structure, frequency selective fading is mitigated, moreover more degrees of freedom in subcarriers assignment for performance enhancement can be provided. The multiantenna structure and transmitter-side channel knowledge are the key enabling techniques with respect to (w.r.t) preprocessing methods for handling interference management. Generally speaking, precoding boosts spectral efficiency of multiuser applications such as broadcast channels and multiple access channels, whether non-CR systems as in [JUN05, SLL09a, ZL05, SLL09b, SAR09], or CR systems as in [HZL07, YH16a, LL11, ZLC10].

The underlay CR based networks have more restrictions w.r.t transmit power and interfer-

ence. Moreover, they have to devote time slots for kernel functionalities such as spectrum sensing. Thus, it is not convenient to involve non-linear preprocessing during data transmission since it requires expensive computations. From this perspective, CR systems benefit from employing efficient linear processing techniques in terms of performance optimization as they have acceptable performance in the practical (low) SNR regimes. Nevertheless, the fixed linear processing (preprocessing/post-processing) techniques addressed for MIMO-OFDM based CR networks in major part of the literature so far (e.g. [ZLC10, AA14, ZL08a, AAN14, SMpV11, RCL10, LHCT11]) are not sufficient to handle the multiuser and primary user interferences (spectrally) efficiently.

Roughly speaking, involving frequency domain equalization procedure for the OFDM system, also known as single carrier FDMA (SC-FDMA), improves power efficiency and substantially maintains the same spectral performance [FABSE02]. Therefore, it has been agreed on employing such scheme as multiple access method in the uplink (UL) of LTE for improving the power efficiency of the terminals [Eri05]. Thus, the RA schemes in [ZJL16, YEHD14, HSAB09, NS08, GC08, KHK07], which count on OFDM in the UL even in non-CR context, are characterized by high power consumption due to the high peak to average power ratio [HL05]. Although the works in [WH08a, WH08b] have focused on the UL of a multiuser OFDM system using SC-FDMA, they did not take underlay CR requirements into account. In addition, most initial work joining OFDM, CR, and RA has considered the downlink (DL) case (as in [ZL08a, XL14, SMpV11, RCL10, LHCT11, ZL08b, BHB11, PWLW07, Wan10, WZGW12]) for which the optimality conditions can not be straightforward adopted for the UL due to differences in the resource constraints.

In this chapter, we propose an efficient RA scheme treating both the DL and UL of multiuser MIMO-OFDM/SC-FDMA based underlay CR networks. The benefit of the proposed scheme is two-fold: Relaxing underlay CR networks to be power-limited systems allowing more transmit power and hence larger communication range. Furthermore, it preserves optimality at low computational complexity with linear order in terms of M, i.e. number of OFDM tones, instead of the exponential order of the exhaustive search as will be discussed in the analysis. From the implementation perspective, the proposed scheme is carried out by a *central* RA task for the DL and a *semi-distributed* (central plus distributive) RA task for the UL. The proposed RA scheme is a two-phase procedure: Adaptive precoding and subcarrier mapping for assigning OFDM/SC-FDMA tones to the CUs. In particular, the central RA task is solved in two phases: The first phase performs the proposed central adaptive precoding which improves the SNR of CUs due to the degrees of freedom it can provide. The second phase derives optimal/near-

optimal subcarrier mapping for the DL/UL. The distributive RA allocates power and conducts per-user adaptive precoding for a given subcarrier assignment obtained from the central RA. It is necessary for the UL but optional for the DL. Such semi-distributed RA scheme in the UL replaces the optimal exhaustive search by a near-optimal yet computationally efficient scheme. Furthermore, it distributes processing between CR central unit and user equipment leading to small data overhead and low-complexity architecture for the terminals.

4.1 System Model and Problem Formulation

We consider a MIMO underlay CR network coexisting and sharing the spectrum of a PR network. The CR base station (CR-BS) with N_{CB} antennas communicates with a set of K CUs, denoted as $\mathcal{K} = \{1, 2, \ldots, K\}$. The kth CU has N_c antennas and occupies $\mathcal{S}_k$ subcarrier subset from the overall set of OFDM tones denoted as $\mathcal{M} = \{1, 2, \ldots, M\}$. The different CUs occupy orthogonal subcarrier sets. It is not condition for the the PR network to employ OFDM, but for the ease of presentation, let us assume L PUs each equipped with N_p antennas. The different PUs occupy orthogonal subsets of subcarriers given that the set of subcarriers allocated to the PU l is denoted as $\mathcal{S}_l$. System model is described in Figure 4.1. By means of active signal

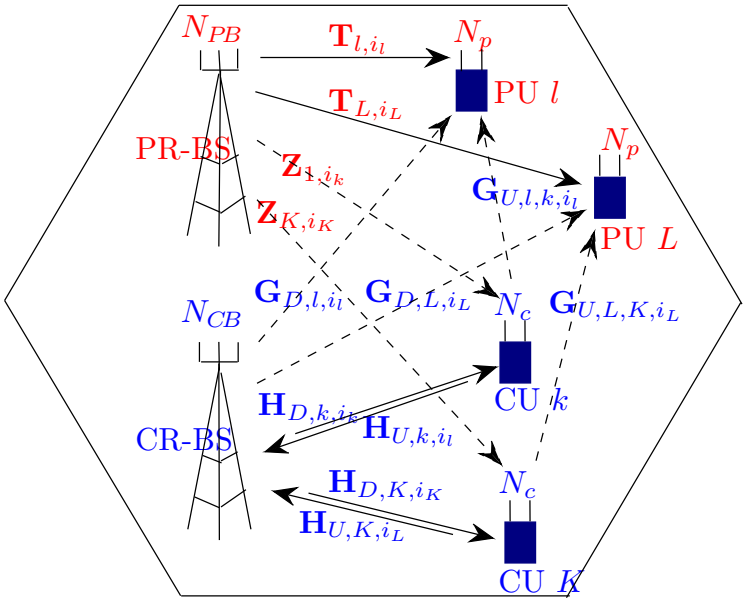

Figure 4.1: Multiuser MIMO-OFDM CR based network model

shaping or superposition modulation [HW11], the CR transmit signals can be fairly assumed

Gaussian distributed. Since CUs do not know the codebooks of the PUs and vice versa, the disturbing interference introduced from one another can be fairly modeled as additive white Gaussian noise (AWGN) as well. To soften the effect of interference plus noise, whitening filters are used at both receiver sides of the CR links. The CR-BS is assumed to have full channel state information of both cognitive UL and DL, denoted as $\{\mathbf{H}_{\cdot}\}$, and all interference links toward active PUs, denoted as $\{\mathbf{G}_{\cdot}\}$, while the kth CU only knows its own link and the interference link from the PR base station (PR-BS), denoted as $\mathbf{Z}_{\cdot}$. The CR system is assumed to operate in time-division duplex (TDD) mode and can, therefore, use the reciprocity argument for estimating the channels of the direct CR and interference links. In the DL, the transmit signals are directly mapped to the desired OFDM subcarriers. However, they are precoded by M-point discrete Fourier transform (DFT)-precoder) in the UL before being mapped to the OFDM tones to produce SC-FDMA scheme [WH08a]. To avoid interfering the UL of the PR network by the CR transmissions (since PUs' transmitters have limited power to boost the UL SNR_{PR}), it is convenient to assume both UL and DL transmissions of the CR network within the time interval of the DL of the PR network. For convenience, functionalities other than data transmission, such as spectrum sensing and estimating the channels $\{\mathbf{G}_{\cdot}\}$, can take place whilst the PR network in a UL state. In non-cooperative legacy PR networks, no information is expected from the PR network to the CR network about the interference temperature. Thus, the CR network can fix the interference temperature to noise floor or to some value causing a desired PU rate loss as will be shown in the sequel.

CR Downlink Notation: Denote the DL channel from the CR-BS to CU k (to PU l) on subcarrier i by $\mathbf{H}_{D,k,i} \in \mathbb{C}^{N_c \times N_{CB}} (\mathbf{G}_{D,l,i} \in \mathbb{C}^{N_p \times N_{CB}})$, $\forall k, i, l$.

For the DL, denote the data vector, precoding matrix, diagonal power matrix, noise vector and post-coding matrix on subcarrier i for CU k as $\mathbf{s}_{D,k,i} \in \mathbb{C}^{N_c \times 1}$, $\mathbf{F}_{D,k,i} \in \mathbb{C}^{N_{CB} \times N_c}$, $\mathbf{P}_{D,k,i} \in \mathbb{R}^{N_c \times N_c}$, $\mathbf{n}_{k,i} \in \mathbb{C}^{N_c \times 1}$ and $\mathbf{W}_{D,k,i} \in \mathbb{C}^{N_c \times N_c}$, respectively.

CR Uplink Notation: Similarly for the UL, denote the UL channel from CU k to the CR-BS (to the PU l) on subcarrier i as $\mathbf{H}_{U,k,i} = \mathbf{H}_{D,k,i}^H \in \mathbb{C}^{N_{CB} \times N_c}$ (and $\mathbf{G}_{U,l,k,i} \in \mathbb{C}^{N_p \times N_c}$), $\forall k, i, l$. Note that reciprocity is inapplicable for estimating $\mathbf{G}_{U,l,k,i}$ from $\mathbf{G}_{D,k,i}$ since they are uncorrelated (i.e. due to the spatial separation between CR-BS and CUs) and differ in dimensions as well. The DFT-precoded data vector, precoding matrix, diagonal power matrix, noise vector and post-coding matrix on subcarrier i for CU k are denoted by $\mathbf{s}_{U,k,i} \in \mathbb{C}^{N_c \times 1}$, $\mathbf{F}_{U,k,i} \in \mathbb{C}^{N_c \times N_c}$, $\mathbf{P}_{U,k,i} \in \mathbb{R}^{N_c \times N_c}$, $\mathbf{n}_{k,i} \in \mathbb{C}^{N_{CB} \times 1}$ and $\mathbf{W}_{U,k,i} \in \mathbb{C}^{N_{CB} \times N_{CB}}$, respectively.

PR Link Notation: Denote the channel from the PR-BS to CU k (to PU l) on subcarrier i by $\mathbf{Z}_{k,i} \in \mathbb{C}^{N_c \times N_{PB}} (\mathbf{T}_{l,i} \in \mathbb{C}^{N_p \times N_{PB}})$. For the PR link, denote the data vector, noise vector,

diagonal power matrix, and SVD precoder on the ith subcarrier for the lth PU as $\mathbf{s}_{l,i} \in \mathbb{C}^{N_p \times 1}$, $\mathbf{n}_{l,i} \in \mathbb{C}^{N_p \times 1}$, $\mathbf{P}_{l,i} \in \mathbb{R}^{N_p \times N_p}$, and $\mathbf{F}_{l,i} \in \mathbb{C}^{N_{PB} \times N_p}$.

4.1.1 Cognitive Radio Downlink

The aggregate DL received signal of the CR network can be expressed as

$$\underline{\mathbf{y}}_D = \underline{\mathbf{H}}_D \underline{\mathbf{F}}_D \underline{\mathbf{s}}_D + \underline{\mathbf{Z}}\underline{\mathbf{F}}_{PR} \underline{\mathbf{s}}_{PR} + \underline{\mathbf{n}}_D \tag{4.1}$$

where $\underline{\mathbf{y}}_D = [\mathbf{y}_{D,.,1}^T \dots \mathbf{y}_{D,.,M}^T]^T$ is the $MN_c \times 1$ DL received vector, $\underline{\mathbf{H}}_D = \text{blkd}(\mathbf{H}_{D,.,1} \dots \mathbf{H}_{D,.,M})$ is the $MN_c \times MN_{CB}$ DL block channel, $\underline{\mathbf{F}}_D = \text{blkd}(\mathbf{F}_{D,.,1} \dots \mathbf{F}_{D,.,M})$ is the $MN_{CB} \times MN_c$ DL block precoder, $\underline{\mathbf{s}}_D = [\mathbf{s}_{D,.,1}^T \dots \mathbf{s}_{D,.,M}^T]^T$ is the $MN_c \times 1$ DL data vector, $\underline{\mathbf{Z}} = \text{blkd}(\mathbf{Z}_{.,1} \dots \mathbf{Z}_{.,M})$ is the $MN_c \times MN_{PB}$ interference block channel from the PR-BS, $\underline{\mathbf{n}}_D = [\mathbf{n}_{.,1}^T \dots \mathbf{n}_{.,M}^T]^T$ is the $MN_c \times 1$ noise vector. The PR link parameters $\underline{\mathbf{F}}_{PR} \in \mathbb{C}^{MN_{PB} \times MN_p}$ and $\underline{\mathbf{s}}_{PR} \in \mathbb{C}^{MN_p \times 1}$ are defined in subsection 4.1.3.

The entries of the noise vector $\mathbf{n}_{k,i}$ are independent and identically distributed (i.i.d.) circular symmetric complex Gaussian (CSCG) samples characterized by $\mathbf{n}_{k,i} \sim \mathcal{CN}(\mathbf{0}, \sigma_n^2 \mathbf{I}_{N_c})$. Therefore, the inverse of the interference plus noise covariance matrix at the kth CU receiver on the ith subcarrier can be factorized as

$$(\mathbf{Z}_{k,i} \mathbf{P}_{l,i} \mathbf{Z}_{k,i}^H + \sigma_n^2 \mathbf{I}_{N_c})^{-1} = \mathbf{\Gamma}_{D,k,i} \mathbf{\Gamma}_{D,k,i}^H \tag{4.2}$$

where $\mathbf{\Gamma}_{D,k,i} \in \mathbb{C}^{N_c \times N_c}$ defines the receive whitening filter of the kth CU on the ith subcarrier and $\text{Tr}(\mathbf{P}_{l,i}) = \text{Tr}(\mathbf{F}_{l,i} \mathbf{F}_{l,i}^H)$ as stated in subsection 4.1.3. The block of whitening filters can be written as $\underline{\tilde{\mathbf{W}}}_D = \text{blkd}(\mathbf{\Gamma}_{D,.,1} \dots \mathbf{\Gamma}_{D,.,M})$. Thus, the aggregate whitened received signal is given by

$$\underline{\tilde{\mathbf{y}}}_D = \underline{\tilde{\mathbf{H}}}_D \underline{\mathbf{F}}_D \underline{\mathbf{s}}_D + \underline{\tilde{\mathbf{n}}}_D \tag{4.3}$$

where $\underline{\tilde{\mathbf{H}}}_D = \underline{\tilde{\mathbf{W}}}_D \underline{\mathbf{H}}_D$ and $\underline{\tilde{\mathbf{n}}}_D = \underline{\tilde{\mathbf{W}}}_D (\underline{\mathbf{Z}}\underline{\mathbf{F}}_{PR} \underline{\mathbf{s}}_{PR} + \underline{\mathbf{n}}_D)$. We assume unit variance for the DL data block symbol of the CR network $\mathbb{E}\left\{\underline{\mathbf{s}}_D \underline{\mathbf{s}}_D^H\right\} = \mathbf{I}_{MN_c}$. The block power matrix of the DL $\underline{\mathbf{P}}_D$ is obtained from distributing the CR-BS power P_T over the data streams of $\underline{\tilde{\mathbf{H}}}_D \underline{\mathbf{F}}_D$ via waterfilling (WF) given that $\mathbb{E}\left\{\|\underline{\mathbf{F}}_D \underline{\mathbf{s}}_D\|^2\right\} \leq P_T$. Note that $\underline{\tilde{\mathbf{n}}}_D$ is a whitened noise vector with zero-mean and identity covariance matrix. From the above, the whitened received signal of the kth CU on the ith subcarrier is expressed as

$$\tilde{\mathbf{y}}_{D,k,i} = \tilde{\mathbf{H}}_{D,k,i} \mathbf{F}_{D,k,i} \mathbf{s}_{D,k,i} + \tilde{\mathbf{n}}_{k,i} \tag{4.4}$$

where $\tilde{\mathbf{H}}_{D,k,i} = \tilde{\mathbf{W}}_{D,k,i} \mathbf{H}_{D,k,i}$ and $\tilde{\mathbf{n}}_{k,i} = \tilde{\mathbf{W}}_{D,k,i} (\mathbf{Z}_{k,i} \mathbf{F}_{l,i} \mathbf{s}_{l,i} + \mathbf{n}_{k,i})$.

4.1.2 Cognitive Radio Uplink

The aggregate whitened UL received signal can be expressed as

$$\underline{\tilde{\mathbf{y}}}_U = \underline{\tilde{\mathbf{H}}}_U \underline{\mathbf{F}}_U \underline{\mathbf{s}}_U + \underline{\tilde{\mathbf{n}}}_U \tag{4.5}$$

where $\underline{\tilde{\mathbf{y}}}_U = [\tilde{\mathbf{y}}_{U,.,1}^T \dots \tilde{\mathbf{y}}_{U,.,M}^T]^T$ is the $MN_{CB} \times 1$ UL whitened received vector, $\underline{\tilde{\mathbf{H}}}_U = \underline{\tilde{\mathbf{W}}}_U \underline{\mathbf{H}}_U =$ blkd$(\tilde{\mathbf{H}}_{U,.,1} \dots \tilde{\mathbf{H}}_{U,.,M})$ is the $MN_{CB} \times MN_c$ UL whitened block channel, $\underline{\mathbf{F}}_U =$ blkd$(\mathbf{F}_{U,.,1} \dots \mathbf{F}_{U,.,M})$ is the $MN_c \times MN_c$ UL block precoder, $\underline{\mathbf{s}}_U = [\mathbf{s}_{U,.,1}^T \dots \mathbf{s}_{U,.,M}^T]^T$ is the $MN_c \times 1$ UL data vector, and $\underline{\tilde{\mathbf{n}}}_U = [\tilde{\mathbf{n}}_{.,1}^T \dots \tilde{\mathbf{n}}_{.,M}^T]^T$ is the $MN_{CB} \times 1$ whitened noise vector. We also assume unit variance for the UL data block vector of the CR network $\mathbb{E}\left\{\underline{\mathbf{s}}_U \underline{\mathbf{s}}_U^H\right\} = \mathbf{I}_{MN_c}$. The block power matrix of the UL $\underline{\mathbf{P}}_U$ is obtained from distributing each per-user power P_k over the data streams of $\tilde{\mathbf{H}}_{U,k,i}\mathbf{F}_{U,k,i}, \forall i \in \mathcal{S}_k$ via WF given that $\sum_{i \in \mathcal{S}_k} \mathbb{E}\left\{\|\mathbf{F}_{U,k,i}\mathbf{s}_{U,k,i}\|^2\right\} \leq P_k$.

Since the CR-BS receives the kth CU signal plus noise only [1], noise component alone needs to be whitened in the UL state of the CR network. In this case, the whitening filter is defined as $(\sigma_n^2 \mathbf{I}_{N_{CB}})^{-1} = \mathbf{\Gamma}_{U,k,i} \mathbf{\Gamma}_{U,k,i}^H$, where $\mathbf{\Gamma}_{U,k,i} \in \mathbb{C}^{N_{CB} \times N_{CB}}$ and $\underline{\tilde{\mathbf{W}}}_U =$ blkd$(\mathbf{\Gamma}_{U,.,1} \dots \mathbf{\Gamma}_{U,.,M})$. Therefore, the whitened received vector for the kth CU on the ith subcarrier at the CR-BS can be written as

$$\tilde{\mathbf{y}}_{U,k,i} = \tilde{\mathbf{H}}_{U,k,i} \mathbf{F}_{U,k,i} \mathbf{s}_{U,k,i} + \tilde{\mathbf{n}}_{U,k,i} \tag{4.6}$$

where $\tilde{\mathbf{H}}_{U,k,i} = \tilde{\mathbf{W}}_{U,k,i} \mathbf{H}_{U,k,i}$, and $\tilde{\mathbf{n}}_{k,i} = \tilde{\mathbf{W}}_{U,k,i} \mathbf{n}_{k,i}$.

Toward the goal of capacity maximization, the central and distributive RA tasks should take place once within the coherence time of the channel.

4.1.3 Primary Radio Link

During the DL state of the CR network, note that the entire PUs receive interference vector from the CR-BS equals $\underline{\mathbf{G}}_D \underline{\mathbf{F}}_D \underline{\mathbf{s}}_D$. However, they receive interference vector from the entire CUs equals $\underline{\mathbf{G}}_U \underline{\mathbf{F}}_U \underline{\mathbf{s}}_U$ during the UL state of the CR network. Therefore, the aggregate received signal of the PR network on the overall subcarrier set can be written as

$$\begin{aligned} \underline{\mathbf{y}}_{PR} = \underline{\mathbf{TF}}_{PR} \underline{\mathbf{s}}_{PR} \; &+ \; \rho \underline{\mathbf{G}}_D \underline{\mathbf{F}}_D \underline{\mathbf{s}}_D \\ &+ \; (1-\rho) \underline{\mathbf{G}}_U \underline{\mathbf{F}}_U \underline{\mathbf{s}}_U + \underline{\mathbf{n}}_{PR} \end{aligned} \tag{4.7}$$

[1] Assuming that no interference is introduced from the PR-BS at CR-BS. This can be realized by installing sector antennas physically high for both stations so as they are aligned side-by-side to cover the same sector. Due to the height and narrow beamwidth, no directed nor reflected paths cause them to interfere each other.

where ρ is set to 1 when the CR network in DL state and 0 if the CR network in UL state. The multicarrier matrices and vectors of (4.7) are defined as follows. $\underline{\mathbf{y}}_{PR} = [\mathbf{y}_{.,1}^T \dots \mathbf{y}_{.,M}^T]^T$ is the $MN_p \times 1$ PR receive vector, $\underline{\mathbf{s}}_{PR} = [\mathbf{s}_{.,1}^T \dots \mathbf{s}_{.,M}^T]^T$ is the $MN_p \times 1$ PR data vector, $\underline{\mathbf{T}} = \text{blkd}(\mathbf{T}_{.,1} \dots \mathbf{T}_{.,M})$ is the $MN_p \times MN_{PB}$ block channel of the direct PR link, $\underline{\mathbf{F}}_{PR} = \text{blkd}(\mathbf{F}_{.,1} \dots \mathbf{F}_{.,M})$ is the $MN_{PB} \times MN_p$ block SVD precoder of the PR network, $\underline{\mathbf{G}}_D = \text{blkd}(\mathbf{G}_{D,.,1} \dots \mathbf{G}_{D,.,M})$ is the $MN_p \times MN_{CB}$ block interference channel from CR-BS, $\underline{\mathbf{G}}_U = \text{blkd}(\mathbf{G}_{U,.,.,1} \dots \mathbf{G}_{U,.,.,M})$ is the $MN_p \times MN_c$ block interference channel from the CUs, $\underline{\mathbf{n}}_{PR} = [\mathbf{n}_{.,1}^T \dots \mathbf{n}_{.,M}^T]^T$ is the $MN_p \times 1$ PR noise vector. The entries of the noise vector $\mathbf{n}_{l,i}$ are i.i.d. CSCG samples, i.e. $\mathbf{n}_{l,i} \sim \mathcal{CN}(\mathbf{0}, \sigma_n^2 \mathbf{I}_{N_p})$.

It is assumed that the data symbol has unit variance $\mathbb{E}\left\{\underline{\mathbf{s}}_{PR}\underline{\mathbf{s}}_{PR}^H\right\} = \mathbf{I}_{MN_p}$. The PR block power matrix $\underline{\mathbf{P}}_{PR} \in \mathbb{R}^{MN_p \times MN_p}$ is obtained by distributing the PR-BS power P_{PB} over the data streams of all PUs, i.e. the eigenmodes of each block in $\underline{\mathbf{T}}$, via WF such that $\text{Tr}\left(\underline{\mathbf{P}}_{PR}\right) = \text{Tr}\left(\underline{\mathbf{F}}_{PR}\mathbb{E}\left\{\underline{\mathbf{s}}_{PR}\underline{\mathbf{s}}_{PR}^H\right\}\underline{\mathbf{F}}_{PR}^H\right) \leq P_{PB}$.

4.1.4 Problem Formulation for the Downlink

The central RA task for the DL takes place in the CR-BS and can be expressed mathematically as follows

$$
\begin{aligned}
C_D^{opt} = & \max_{\{\theta_{k,i}^{(d)}, \mathbf{F}_{D,k,i}^{(d)} \in \mathcal{F}_D\}} \frac{\tau_D}{M} \sum_{k=1}^{K} \sum_{i=1}^{M} \theta_{k,i}^{(d)} \log_2 |\mathbf{I}_{N_c} + \mathbf{W}_{D,k,i}^{(d)} \mathbf{H}_{D,k,i} \mathbf{F}_{D,k,i}^{(d)} \mathbf{F}_{D,k,i}^{(d)H} \mathbf{H}_{D,k,i}^H \mathbf{W}_{D,k,i}^{(d)H}| \\
& \text{s.t.:} \\
& \textit{C1}: \sum_{k=1}^{K} \sum_{i=1}^{M} \theta_{k,i}^{(d)} \mathbb{E}\left\{ \|\mathbf{F}_{D,k,i}^{(d)} \mathbf{s}_{D,k,i}\|^2 \right\} \leq P_T \\
& \textit{C2}: \sum_{k=1}^{K} \sum_{i \in \mathcal{S}_l} \theta_{k,i}^{(d)} \mathbb{E}\left\{ \|\mathbf{G}_{D,l,i} \mathbf{F}_{D,k,i}^{(d)} \mathbf{s}_{D,k,i}\|^2 \right\} \leq I_l^{th}, \forall l \\
& \textit{C3}: \theta_{k,i}^{(d)} \in \{0,1\} \\
& \textit{C4}: \sum_{k=1}^{K} \theta_{k,i}^{(d)} = 1, \forall i
\end{aligned}
\tag{4.8}
$$

where P_T is the transmission power budget of the CR-BS. τ_D refers to the DL time sharing weight, which is fulfilling with the UL weight τ_U the condition $\tau_D + \tau_U = 1$. In other words, if the DL time weight is τ, the UL time weight will be $(1 - \tau)$. To utilize the radio resource efficiently, τ can be designed to turn the TDD flexibly to either half or full duplexing mode according to [5G 15] for improving the spectral efficiency. $\theta_{k,i}^{(d)}$ can be either 1 or 0 indicating whether the subcarrier i is occupied by the CU k or not. *C3* and *C4* informing that each sub-

carrier cannot be shared by multiple CUs. Note that $\theta_{k,i}^{(d)}$ highly depends on the dth degree of freedom (DoF) of the adaptive precoder $\mathbf{F}_{D,k,i}^{(d)}$ since each DoF changes the effective channel of the kth CU accordingly. In other words, the kth CU may have the best channel conditions at some DoF but not at the rest DoFs. Consequently, the subcarrier assignment procedure is dependent on the DoF of the adaptive precoder. In (4.8), we try to maximize the sum-rate of the CR system under the transmission power budget of the CR-BS, while guaranteeing tolerable PUI. I_l^{th} is the PUI threshold of the PU l, which is usually set in underlay CR systems to the noise floor.

Without loss of generality, we can adjust the PUI threshold according to *PU rate loss* (PRL) as follows

Proposition 1: To link the PUI threshold I_l^{th} to PRL, first define the lth PRL as

$$\text{PRL}_l = \frac{C_{SNR} - C_{SINR}}{C_{SNR}} = 1 - \frac{C_{SINR}}{C_{SNR}} \tag{4.9}$$

where C_{SNR} and C_{SINR} are the sum-rate of the eigenmodes $\Lambda_{j,l}$'s of the PU l *without* and *with interference* component due to the CR system, respectively, which are formed as $C_{SNR}=\sum_{j=1}^{N_p}\log_2\left(1+\frac{p_{j,l}\Lambda_{j,l}^2}{\sigma_n^2}\right)$ and $C_{SINR}=\sum_{j=1}^{N_p}\log_2\left(1+\frac{p_{j,l}\Lambda_{j,l}^2}{\sigma_n^2+\alpha_l\sigma_n^2}\right)$, where α_l is called temperature parameter and $\alpha_l\sigma_n^2$ is the interference caused by the CR transmitter at the lth PU. Then, simplify (4.9) for $\text{SNR}_{PR} \to 0$ to $\alpha_l = \frac{\text{PRL}_l}{1-\text{PRL}_l}$. Next, express the scalar PUI threshold I_l^{th} in terms of the temperature parameter α_l as follows

$$I_l^{th} = \sum_{i\in\mathcal{S}_l} \text{Tr}(\mathbf{I}_{l,i}^{th}) \tag{4.10}$$

where $\mathbf{I}_{l,i}^{th} \in \mathbb{R}^{N_c\times N_c}, \forall i \in \mathcal{S}_l$ is a PUI diagonal matrix. We need to express the contribution of CUs' eigenmodes in the PUI threshold over the set $\mathcal{S}_l$. Thus, equal contributions infer that the elements of $\mathbf{I}_{l,i}^{th}$ are equally weighted as $\frac{\text{Tr}\left(\alpha_l\sigma_n^2\mathbf{I}_{N_p}\right)}{N_c}$, where the diagonal matrix $\alpha_l\sigma_n^2\mathbf{I}_{N_p}$ refers to the interference on the eigenmodes of the lth PU for the subcarrier $i \in \mathcal{S}_l$.

Proof: See Appendix F.1.

Note that the PRL is maximum in the low SNR_{PR} regime, but decreases as SNR_{PR} increases. Obviously, (4.8) defines mixed integer programming problem, which involves integer variables $\theta_{k,i}^{(d)}$ and complex-matrix variables $\mathbf{F}_{D,k,i}^{(d)}$. It is not convex and generally hard to solve (4.8) because it is combinatorial and generates an exponential complexity[2]. We develop a two-phase

[2]Convex relaxation is possible for the OFDMA scheme if every OFDM tone can be shared by users in time so-called OFDMA-TDMA. Mathematically, the integer parameter θ would be replaced by a time-sharing factor, which is real parameter between 0 and 1. That would define convex objective and constraint set. However, when

procedure to address it. The solution carries out adaptive precoding (DoF assignment) and subcarrier mapping separately. Particularly, best DoF of the adaptive precoder is assigned first to the CR system under study for a given initial subcarrier mapping (under the assumption of interference-limited underlay CR system in which *C2* tighter than *C1*). Then, the assigned DoF enables accurate subcarrier mapping even for power-limited underlay CR system, i.e. *C1* tighter than *C2*.

4.2 Downlink Adaptive Precoding and Degree of Freedom Assignment

4.2.1 Central Adaptive Precoding

It is convenient to develop new linear precoding method since linear processing is characterized by low computational complexity. We develop an adaptive linear precoder utilizing the multiple antenna structure for boosting spectrum efficiency. In the adaptive precoder, we scan all combinations of the spaces of the interference channel $\mathbf{G}_{D,l,i}$ to get countable independent DoFs. The precoding matrix is adapted by selecting the best DoF to achieve maximum SNR. The adaptation happens according to the amount of transmit power even if the channels are time-invariant. For the CU k on the subcarrier i, unlike ZF precoder, the PUI condition to be fulfilled by the dth DoF of the adaptive precoder is formed as $\mathbf{G}_{D,l,i}\mathbf{F}_{D,k,i}^{(d)} \geq \mathbf{0}_{N_p \times N_c}, \forall k, l$. The adaptive precoder relaxes the PUI constraint converting the CR system from interference-limited to power-limited. The overall DoF set of the DL is denoted as $\mathcal{F}_D = \{\underline{\mathbf{F}}_D^{(0)}, \ldots, \underline{\mathbf{F}}_D^{(|\mathcal{D}|)}\}$, where the index set is denoted as $\mathcal{D} = \{0, 1, 2, \ldots, \text{Rank}(\mathbf{G}_{D,l,i})\}$. We need to select the best DoF in the set $\mathcal{F}_D$. Note that for each DoF we combine the similar indices for the subcarrier set $\mathcal{M}$ no matter which CUs occupy them, so-called central adaptive precoding. For instance, the DoF of index $d = 1$ collects the precoding matrices indexed as $d = 1$ from all subcarriers, i.e. $\underline{\mathbf{F}}_D^{(1)} = \text{blkd}(\mathbf{F}_{D,.,1}^{(1)}, \ldots, \mathbf{F}_{D,.,M}^{(1)})$. Per-user or distributive adaptive precoding combines the similar indices, however, for the kth CU subcarrier subset $\mathcal{S}_k$.

The design of the dth DoF of the adaptive precoder on the ith subcarrier follows. The subspaces of $\mathbf{G}_{D,l,i}$ are combined such that not only the null space is taken into account, but

the number of OFDM tones approaches infinity, the OFDMA-TDMA solution approaches the optimum OFDMA. In other words, for sufficiently large number of subcarriers, the OFDMA-TDMA solution that allocates every subcarrier to the user with the largest time-sharing factor will produce negligible performance loss compared to the optimum OFDMA solution.

also the space of smallest d non-zero singular values. Note that the cardinality of the precoding set is $|\mathcal{D}| = \mathcal{R} + 1$, where $\mathcal{R} = \text{Rank}(\mathbf{G}_{D,l,i})$. For instance, let the singular values of $\mathbf{G}_{D,l,i}$ be ordered as $\lambda_1 \geq \lambda_2 \geq \cdots \geq \lambda_{\mathcal{R}}$ and the null space is indexed as $d = 0$, therefore the DoF indexed as $d = 3$ refers to the spaces of the null as well as the smallest three non-zero singular values (i.e. $\lambda_{\mathcal{R}-2}, \lambda_{\mathcal{R}-1}, \lambda_{\mathcal{R}}$). Now, denote $\mathbf{V}_{D,l,i}^{(d)} \in \mathbb{C}^{N_{CB} \times d}$ as the spaces of dth DoF obtained from $\mathbf{G}_{D,l,i}$. Apply the SVD as $\tilde{\mathbf{H}}_{D,k,i}\mathbf{V}_{D,l,i}^{(d)} = \check{\mathbf{U}}_{D,k,i}^{(d)}\check{\mathbf{\Lambda}}_{D,k,i}^{(d)}\check{\mathbf{V}}_{D,k,i}^{(d)H}$ to diagonalize the effective channel before applying power allocation $\mathbf{P}_{D,k,i}$. Let's denote $\hat{\mathbf{F}}_{D,k,i}^{(d)} = \mathbf{V}_{D,l,i}^{(d)}\check{\mathbf{V}}_{D,k,i}^{(d)}$ as the projection matrix. The precoder and receive filter can be written as

$$\begin{aligned} \mathbf{F}_{D,k,i}^{(d)} &= \hat{\mathbf{F}}_{D,k,i}^{(d)}\mathbf{P}_{D,k,i}^{\frac{1}{2}} \\ \mathbf{W}_{D,k,i}^{(d)} &= \check{\mathbf{U}}_{D,k,i}^{(d)H}\mathbf{\Gamma}_{D,k,i} \end{aligned} \tag{4.11}$$

Consequently, the whitened baseband received signal for the CU k on the subcarrier i is given by

$$\tilde{\mathbf{y}}_{D,k,i} = \check{\mathbf{\Lambda}}_{D,k,i}^{(d)}\mathbf{P}_{D,k,i}^{\frac{1}{2}}\mathbf{s}_{D,k,i} + \check{\mathbf{U}}_{D,k,i}^{(d)H}\tilde{\mathbf{n}}_{k,i} \tag{4.12}$$

4.2.2 Efficient Degree of Freedom Assignment

This section introduces an efficient algorithm for DoF selection. The best DoF is selected based on the following maximum achievable capacity criterion

$$\underline{\mathbf{F}}_D^{(\hat{d})} = \arg\max_{d \in \mathcal{D}} \sum_{k=1}^{K} r_k\left(\underline{\mathbf{F}}_D^{(d)}\right) \tag{4.13}$$

where $r_k\left(\underline{\mathbf{F}}_D^{(d)}\right)$ is the data rate of the kth CU. This selection criterion refers to conducting WF power allocation for every CU and every candidate DoF on every subcarrier, that actually consumes a plenty of time. Therefore, it is desired to carry out a DoF selection with low computational complexity. Toward this goal, we replace (4.13) by a time efficient algorithm. First, we substitute (4.11) in (4.8) and refer to $\mathbf{\Omega}_{D,k,i}^{(d)} \in \mathbb{C}^{N_c \times N_c}$ as the effective interfering channel power toward the PU l obtained as $\mathbf{\Omega}_{D,k,i}^{(d)} = \text{diag}\left(\hat{\mathbf{F}}_{D,k,i}^{(d)H}\mathbf{G}_{D,l,i}^{H}\mathbf{G}_{D,l,i}\hat{\mathbf{F}}_{D,k,i}^{(d)}\right)$. Then,

rewrite (4.8) as

$$
\begin{aligned}
C_D^{opt} = & \max_{\{\theta_{k,i}^{(d)}, \mathbf{P}_{D,k,i}, d\in\mathcal{D}\}} \frac{\tau_D}{M}\sum_{k=1}^{K}\sum_{i=1}^{M}\theta_{k,i}^{(d)}\log_2|\mathbf{I}_{N_c}+\check{\mathbf{\Lambda}}_{D,k,i}^{(d)2}\mathbf{P}_{D,k,i}| \\
\text{s.t.} \quad & : \\
\textit{C1} \quad & : \quad \sum_{k=1}^{K}\sum_{i=1}^{M}\theta_{k,i}^{(d)}\text{Tr}\left(\hat{\mathbf{F}}_{D,k,i}^{(d)H}\hat{\mathbf{F}}_{D,k,i}^{(d)}\mathbf{P}_{D,k,i}\right) \leq P_T \\
\textit{C2} \quad & : \quad \sum_{k=1}^{K}\theta_{k,i}^{(d)}\text{Tr}\left(\mathbf{\Omega}_{D,k,i}^{(d)}\mathbf{P}_{D,k,i}\right) \leq \text{Tr}(\mathbf{I}_{l,i}^{th}), \forall l,i \\
\textit{C3} \quad & \quad \text{and } \textit{C4} \text{ as in (4.8)} \\
\textit{C5} \quad & : \quad \mathbf{P}_{D,k,i} \geq 0, \forall k,i
\end{aligned} \tag{4.14}
$$

Before going through DoF assignment algorithm, note that the DoF assignment is a prerequisite to obtain an accurate subcarrier mapping. Particularly, we depend on the achievable rates of OFDM tones to accomplish the subcarrier mapping. In an OFDM based CR network, a subcarrier with higher SNR may generate more PUI, which means the PUI threshold also set an upper bound of the maximum transmission power of a subcarrier. Thus, it is crucial to jointly consider the SNR of a subcarrier and the PUI threshold in *C2* to calculate the maximum achievable rate over that subcarrier. However, the maximum achievable rate also depends on the adaptive precoding (specifically, on the assigned DoF as it affects $\bar{\mathbf{\Lambda}}_{D,k,i}^{(d)2}$). Hence, to solve (4.14) with spectrum efficiency, we need to address the adaptive precoding (DoF assignment) procedure before executing the subcarrier mapping procedure.

For a fast DoF selection criterion, we count on analytical power computations assuming interference-limited underlay CR system. Precisely, we calculate a couple of precoding-thresholds (power values) that separate countable precoding-regions within which a breakthrough in the system sum-rate occurs. The following theorem and corollary prove our observation.

Theorem 1. *For the dth precoding DoF, as $P_T \to 0$, the sum-rate fulfills $C_D^{(d-1)} < C_D^{(d)}$, and conversely as $P_T \to \infty$, the sum-rate fulfills $C_D^{(d-1)} > C_D^{(d)}$.*

Proof: See [ZL08a] and Theorem 3 and 4 therein.

Corollary 1. *There is an intersection point equalizes the capacity of both DoFs d and $(d-1)$ such that the equality holds $C_D^{(d-1)} = C_D^{(d)}$. At this point the precoding-threshold $P_{D,th}^{(d,d-1)}$ is located.*

The following proposition exhibits the DoF assignment procedure.

Proposition 2: The precoding-thresholds are calculated for each two-consecutive DoF indices (i.e. d and $(d-1)$) to get a couple of precoding-regions. Then, the DoF selection can be efficiently handled by comparing the transmit power budget P_T with the precoding-threshold set denoted as $\{P_{D,th}^{(d,d-1)}\}_{d=1}^{\mathcal{R}}$ to accommodate P_T in the corresponding precoding-region. Then, assign the optimum DoF precoding matrix $\hat{\mathbf{F}}_{D,k,i}^{(\hat{d})}$ to the CR system under study as shown below. Mathematically, we express the DoF selection as follows

$$P_T \underset{\hat{d}=d-1}{\overset{\hat{d}=d}{\lessgtr}} P_{D,th}^{(d,d-1)}, \forall d \in \mathcal{D} \tag{4.15}$$

The set of thresholds can be calculated as follows

$$\left\{ P_{D,th}^{(d,d-1)} = \sum_{i=1}^{M} \max_{l} \text{Tr}\left({\boldsymbol{\Omega}_{D,\bar{k},i}^{(d)}}^{-1} \mathbf{I}_{l,i}^{th} \right) \right\}_{d=1}^{\mathcal{R}} \tag{4.16}$$

where $\mathcal{R} = \text{Rank}(\mathbf{G}_{D,l,i})$.

Proof: See Appendix F.2.

Given that $|\mathcal{D}| = \mathcal{R}+1$ is the number of DoFs, the defined $(\mathcal{R}+1)$ precoding-regions are separated by $(\mathcal{R})$ precoding-thresholds according to ***Proposition 2***.

4.3 Fast Subcarrier Mapping for Downlink

In this procedure, we propose computational efficient and optimal subcarrier mapping algorithm for the DL for a given DoF assignment. The subcarrier mapping scheme for the DL is characterized by optimality since it is built upon optimal power allocation no matter if the CR system under investigation is power-limited or interference-limited. The variable index d is fixed to a value within the set $\mathcal{D}$ once DoF assignment is completed, then the CR network is preprocessed by the optimum DoF $\{\hat{\mathbf{F}}_{D,k,i}^{(\hat{d})}\} \forall k, i$. Hence, the subcarrier mapping procedure can skip d from (4.14) for notation simplicity.

Problem (4.14) defines a mixed integer programming and can optimally be solved with computational efficiency by using the Lagrange dual decomposition method [BV04] that decomposes the problem into M parallel subproblems converting the exponential complexity $\mathcal{O}(K^M)$ into a linear order in terms of M. Since each subcarrier cannot be shared by multiple CUs, we can execute subcarrier mapping procedure according to the maximum achievable rate on the OFDM tones. Each subcarrier can be assigned to the CU that produces the highest achievable

rate over it. Toward this end, Lagrangian of the problem (4.14) is written as

$$\mathcal{L}_D(\{\mathbf{P}_{D,k,i},\theta_{k,i}\},\mu_D,\boldsymbol{\delta}_D,\boldsymbol{\Psi}_D,\boldsymbol{\zeta}) = C_D^{opt} - \mu_D\left(\sum_{i=1}^{M}\sum_{k=1}^{K}\theta_{k,i}\mathrm{Tr}\Big(\hat{\mathbf{F}}_{D,k,i}^H\hat{\mathbf{F}}_{D,k,i}\mathbf{P}_{D,k,i}\Big)-P_T\right)$$
$$-\sum_{i=1}^{M}\delta_{D,i}\left(\sum_{k=1}^{K}\theta_{k,i}\mathrm{Tr}\left(\boldsymbol{\Omega}_{D,k,i}\mathbf{P}_{D,k,i}\right)-\mathrm{Tr}(\mathbf{I}_{l,i}^{th})\right)-\sum_{i=1}^{M}\sum_{k=1}^{K}\psi_{D,k,i}\mathbf{P}_{D,k,i}-\sum_{i=1}^{M}\left(\sum_{k=1}^{K}\zeta_{k,i}\theta_{k,i}-\zeta_{k,i}\right) \tag{4.17}$$

where μ_D is a dual variable associated with the constraint *C1*, $\boldsymbol{\delta}_D = [\delta_{D,1},\delta_{D,2},\ldots,\delta_{D,M}]$ is a vector of dual variables each associated with one of the constraints set *C2*, $\boldsymbol{\zeta} = [\zeta_{k,1},\ldots,\zeta_{k,M}]$ is a vector of dual variables each belongs one in the set *C4*, and $\boldsymbol{\Psi}_D = [\psi_{D,1,1},\ldots,\psi_{D,K,M}]$ is a vector of dual variables each associated with one of the constraint set *C5*. The Lagrange dual function can be expressed as

$$\mathcal{G}_D(\mu_D,\boldsymbol{\delta}_D,\boldsymbol{\Psi}_D,\boldsymbol{\zeta}) = \max_{\{\mathbf{P}_{D,k,i},\theta_{k,i}\}}\mathcal{L}_D\left(\{\mathbf{P}_{D,k,i},\theta_{k,i}\},\mu_D,\boldsymbol{\delta}_D,\boldsymbol{\Psi}_D,\boldsymbol{\zeta}\right) \tag{4.18}$$

The Lagrange dual optimization problem is

$$\min_{\mu_D\geq 0,\boldsymbol{\delta}_D\geq\mathbf{0},\boldsymbol{\Psi}_D\geq\mathbf{0},\boldsymbol{\zeta}\geq\mathbf{0}}\mathcal{G}_D\left(\mu_D,\boldsymbol{\delta}_D,\boldsymbol{\Psi}_D,\boldsymbol{\zeta}\right) \tag{4.19}$$

It is observed that (4.18) can be rewritten as

$$\mathcal{G}_D\left(\mu_D,\boldsymbol{\delta}_D,\boldsymbol{\Psi}_D,\boldsymbol{\zeta}\right) = \sum_{i=1}^{M}\mathcal{G}_{D,i}(\mu_D,\delta_{D,i},\psi_{D,k,i},\zeta_{k,i}) + \mu_D P_T \tag{4.20}$$

where

$$\mathcal{G}_{D,i}(\mu_D\ ,\ \delta_{D,i},\psi_{D,k,i},\zeta_{k,i}) = \max_{\{\mathbf{P}_{D,k,i},\theta_{k,i}\}}\frac{\tau_D}{M}\sum_{k=1}^{K}\theta_{k,i}\log_2\left|\mathbf{I}_{N_c}+\check{\boldsymbol{\Lambda}}_{D,k,i}^2\mathbf{P}_{D,k,i}\right|$$
$$-\ \ \mu_D\sum_{k=1}^{K}\theta_{k,i}\mathrm{Tr}\Big(\hat{\mathbf{F}}_{D,k,i}^H\hat{\mathbf{F}}_{D,k,i}\mathbf{P}_{D,k,i}\Big)-\delta_{D,i}\left(\sum_{k=1}^{K}\theta_{k,i}\mathrm{Tr}\left(\boldsymbol{\Omega}_{D,k,i}\mathbf{P}_{D,k,i}\right)-\mathrm{Tr}(\mathbf{I}_{l,i}^{th})\right)$$
$$-\ \ \sum_{k=1}^{K}\psi_{D,k,i}\mathbf{P}_{D,k,i}-\sum_{k=1}^{K}\zeta_{k,i}\theta_{k,i}+\zeta_{k,i} \tag{4.21}$$

It is clear that (4.19) is decomposed into M independent unconstrained optimization subproblems each can be solved numerically by updating the dual variables $\mu_D,\{\delta_{D,i}\},\{\psi_{D,k,i}\}$, and $\{\zeta_{k,i}\}$ iteratively (concentric loops) using the bisection method [BV04].

Remark 1: For reduced numerical calculations, we can drop the loops of $\{\psi_{D,k,i}\}$, which guarantee semidefinite power matrix, and replace them by the operator $[a]^+ = \max(a,0)$, where a is real number.

Remark 2: Based on the subcarrier mapping policy, the last two terms of (4.21) cancel each other for the selected CU. Therefore, the drop of $\zeta_{k,i}$ is not only valid but also reduces the numerical calculations.

Based on *Remark 1* and *Remark 2*, we can skip the last two terms of (4.17) during the optimal power derivation as follows.

Theorem 2. *The optimal power can be derived* $\forall i \in \mathcal{M}, \forall k \in \mathcal{K}$ *by applying the Karush-Kuhn-Tucker (KKT) conditions of optimality. From the gradient of* $\mathcal{L}_D$*, the optimal power is expressed as*

$$\hat{\mathbf{P}}_{D,k,i} = \left[\left\{ \frac{M \ln 2}{\tau_D} \left(\mu_D \hat{\mathbf{F}}_{D,k,i}^H \hat{\mathbf{F}}_{D,k,i} + \delta_{D,i} \mathbf{\Omega}_{D,k,i} \right) \right\}^{-1} - \check{\mathbf{\Lambda}}_{D,k,i}^{-2} \right]^+ \tag{4.22}$$

Proof: See Appendix F.3.

Since both the DoF assignment and power allocation procedures are completed now, it is possible to execute the subcarrier mapping step. As mentioned above, the subcarrier mapping policy is to assign the subcarrier i to only one CU that has the highest achievable rate on it. Thus, we can carry out the subcarrier mapping procedure according to the achievable rate defined in (4.21). The procedure is over when all subcarriers are allocated.

Mathematically, we map the subcarriers by finding the values of $\theta_{k,i}$'s as follows

$$\theta_{k,i} = \left\{ \begin{array}{ll} 1 & \hat{k} = \arg\max\limits_{k} \mathcal{G}_{D,i}\left(\mu_D, \delta_{D,i}\right) \\ 0 & \text{otherwise} \end{array} \right\}, \forall i \in \mathcal{M} \tag{4.23}$$

The algorithm of the proposed scheme is summarized in Table 4.1.

4.4 Problem Formulation for the Uplink and Optimality Condition

4.4.1 Problem Formulation

The optimality condition derived for the DL can not be directly followed to the UL due to the differences in resource constraints. The challenging aspect in the SC-FDMA based UL that make the RA task intractable is the per-user power constraints. Up to the knowledge of authors, optimal and fully distributed UL subcarrier assignment can be performed by means of an exhaustive search. Furthermore, it confines all processing tasks at the terminals causing huge hardware complexity. It requires no data overhead between CR base station and CR terminals. On the other hand, fully centralized method can be efficient concerning processing time.

Table 4.1: The Downlink Algorithm of the Proposed Scheme

Analytical Procedure: *Adaptive Precoding (DoF Assignment)*

A) $\forall d \in \mathcal{D}$ **do**

1. $\forall k \in \mathcal{K}, i \in \mathcal{M}$ **do**

Calculate $\{\mathbf{I}_{l,i}^{th}\}, \forall l, i$ by (4.10) **end**.

2. Calculate $P_{D,th}^{(d,d-1)}, \forall d$ by (4.16) **end**.

B) Allocate the optimum precoding DoF $\hat{d}$ to the CR system by (4.15).

C) Return $\{\mathbf{F}_{D,k,i}^{(\hat{d})}\}, \forall k, i$.

Numerical Procedure: *Subcarrier Mapping*

A) Initialization: $\mu_D^{min} = 0$ and $\mu_D^{max} = \hat{\mu}_D$ where $\hat{\mu}_D$ is a large value.

B) Repeat until $\left(\mu_D^{max} - \mu_D^{min}\right) \leq \epsilon$

1. $\mu_D^{(\nu)} = \left(\mu_D^{min} + \mu_D^{max}\right)/2$

a) Initialization: $\forall i \in \mathcal{M}, \delta_{D,i}^{min} = 0$ and $\delta_{D,i}^{max} = \hat{\delta}_{D,i}$, where $\hat{\delta}_{D,i}$ is a large value.

b) $\forall i \in \mathcal{M}$ repeat until $\left(\delta_{D,i}^{max} - \delta_{D,i}^{min}\right) \leq \epsilon$

i) $\delta_{D,i}^{(j)} = \left(\delta_{D,i}^{min} + \delta_{D,i}^{max}\right)/2$

ii) $\forall k \in \mathcal{K}$, calculate $\hat{\mathbf{P}}_{D,k,i}^{(\nu,j)}$ by (4.22)

iii) Calculate $\mathcal{G}_{D,i}\left(\mu_D, \delta_{D,i}\right)$ by (4.21). Then, allocate the ith subcarrier to the best CU (i.e. find $\{\theta_{k,i}\}, \forall k$) by (4.23).

iv) If $\sum_{k=1}^{K} \theta_{k,i} \mathrm{Tr}\left(\mathbf{\Omega}_{D,k,i} \hat{\mathbf{P}}_{D,k,i}^{(\nu,j)}\right) \leq \mathrm{Tr}(\mathbf{I}_{l,i}^{th}), \forall l$, set $\delta_{D,i}^{max} = \delta_{D,i}^{(j)}$, otherwise $\delta_{D,i}^{min} = \delta_{D,i}^{(j)}$.

2. If $\sum_{k=1}^{K} \sum_{i=1}^{M} \theta_{k,i} \mathrm{Tr}\left(\mathbf{F}_{D,k,i}^{H} \mathbf{F}_{D,k,i} \hat{\mathbf{P}}_{D,k,i}^{(\nu,j)}\right) \leq P_T$, set $\mu_D^{max} = \mu_D^{(\nu)}$, otherwise $\mu_D^{min} = \mu_D^{(\nu)}$.

C) Return $\{\hat{\mathbf{P}}_{D,k,i}, \theta_{k,i}\}, \forall k, i$.

where ϵ is a small constant

It causes simple terminal architecture as the processing takes place at the central unit. However, it requires large preamble information to feed the parameterization back to the terminals. Therefore, we propose a semi-distributed platform for the UL which is characterized by efficient computational complexity, simple terminal architecture, and small data overhead. Toward this goal, we initially relax the optimization problem of the UL which has K per-user power constraints into a centrally solvable form according to ***Proposition 3***. This form is solved at the CR-BS.

Proposition 3: The K per-user power constraints are absorbed into a single sum-power constraint to solve the adaptive precoding and subcarrier mapping centrally for the UL problem

as follows

$$\sum_{k=1}^{K}\sum_{i=1}^{M}\theta_{k,i}\text{Tr}\left(\hat{\mathbf{F}}_{U,k,i}^{(d)H}\hat{\mathbf{F}}_{U,k,i}^{(d)}\mathbf{P}_{U,k,i}\right)\leq\sum_{k=1}^{K}P_k \tag{4.24}$$

where P_k is the transmission power budget of the kth CU. The central RA task of the UL has the same structure of (4.14) with replacement of P_T by $\sum_{k=1}^{K}P_k$.

We solve the central RA of the UL to obtain subcarrier mapping which is computationally efficient solution because of using the M parallel decomposed routines. This mapping is rigorously optimal under the sum-power constraint defined in (4.24), but near-optimal under per-user power constraints. The solution steps are identical to those of the DL described in Table 4.1. Since WF is recognized as opportunistic power distribution, the sum-power constrained RA may violate the per-user power constrained RA. In other words, the power distribution over $\mathcal{S}_k$ due to the UL central RA may likely exceed the budget P_k. Therefore, distributed RA task with per-user power constraint is necessary at each terminal to obtain optimal power distribution. Once the central RA optimization terminates, the assigned subcarriers are fed back to each terminal via signaling channels in order to enable the distributed RA.

4.4.2 Distributive RA Task and Per-User Adaptive Precoding

For the subcarrier mapping obtained from the central RA, we re-optimize the RA task distributively at the terminal of the CU with the per-user power constraint. Distributive RA assigns the DoF and the power over the allocated subcarriers set of the kth CU, i.e. $\mathcal{S}_k$, by solving the following task

$$\begin{aligned}
C_{U,k} = &\max_{\{d\in\mathcal{D},\mathbf{P}_{U,k,i}\}}\frac{\tau_U}{M}\sum_{i\in\mathcal{S}_k}\log_2\left|\mathbf{I}_{N_c}+\check{\mathbf{\Lambda}}_{U,k,i}^{(d)}\mathbf{P}_{U,k,i}\right|\\
\text{s.t.}\quad &:\\
\textit{C1}\quad &:\quad \sum_{i\in\mathcal{S}_k}\text{Tr}\left(\hat{\mathbf{F}}_{U,k,i}^{(d)H}\hat{\mathbf{F}}_{U,k,i}^{(d)}\mathbf{P}_{U,k,i}\right)\leq P_k\\
\textit{C2}\quad &:\quad \text{Tr}\left(\mathbf{\Omega}_{U,k,l,i}^{(d)}\mathbf{P}_{U,k,i}\right)\leq\text{Tr}(\mathbf{I}_{l,i}^{th}),\forall l,\forall i\in\mathcal{S}_k\\
\textit{C3}\quad &:\quad \mathbf{P}_{U,k,i}\geq 0,\forall i\in\mathcal{S}_k
\end{aligned} \tag{4.25}$$

Clearly, (4.25) can be solved by a two-phase procedure. First, efficient DoF assignment (per-user adaptive precoding) is elaborated according to (4.15) given in ***Proposition 2*** but for the subcarrier subset $\mathcal{S}_k$. Second, optimal power is allocated among the eigenmodes of $\mathcal{S}_k$ similar to (4.22) and given $\forall i\in\mathcal{S}_k$, as

$$\hat{\mathbf{P}}_{U,k,i}=\left[\left\{\frac{M\ln 2}{\tau_U}\left(\mu_U\hat{\mathbf{F}}_{U,k,i}^{H}\hat{\mathbf{F}}_{U,k,i}+\delta_{U,i}\mathbf{\Omega}_{U,k,i}\right)\right\}^{-1}-\check{\mathbf{\Lambda}}_{U,k,i}^{-2}\right]^{+} \tag{4.26}$$

Then, the sum-rate of the UL can be calculated by adding up the data rates of all CUs according to

$$C_U^{opt} = \sum_{k=1}^{K} C_{U,k} \tag{4.27}$$

Similarly, per-user adaptive precoding can be applied for the DL by solving distributive RA having a structure like (4.25) for a given subcarrier mapping and per-user power constraints obtained from solving the central RA task (4.14). Unlike UL, the DL distributive RA procedure takes place at the CR-BS.

4.4.3 Complexity Analysis

In the central RA procedure, the adaptive precoding step (DoF assignment) requires $|\mathcal{D}|$ calculations for the precoding-thresholds $\forall k, i$, and thus costs $MK|\mathcal{D}|$. Furthermore, the subcarrier mapping step needs c_c iterations per each power calculation $\forall k, i$, and hence costs $c_c MK$. Therefore, the central RA step requires complexity of $MK(c_c + |\mathcal{D}|)$. The distributive RA procedure carries out $|\mathcal{S}_k||\mathcal{D}|$ calculations for the per-user adaptive precoding and $c_d|\mathcal{S}_k|$ for the power distribution. Thus, the distributive RA procedure complexity $\forall k$ is $(c_d + |\mathcal{D}|)\Sigma_k|\mathcal{S}_k| = M(c_d + |\mathcal{D}|)$, where c_d denotes the average number of iterations per subcarrier in the distributed RA task. The overall complexity of both central and distributive RA procedures is $\mathcal{O}\left(M(K+1)(c+|\mathcal{D}|)\right)$, where c denotes the average number of iterations per subcarrier. The exhaustive search requires testing $K|\mathcal{D}|$ combinations per subcarrier and each combination requires c iterations, thus for M subcarriers that costs $\prod_{i=1}^{M} cK|\mathcal{D}| = (cK|\mathcal{D}|)^M$. The RA scheme in [YH14] costs $\mathcal{O}(cM + MK|\mathcal{D}|)$. Other RA schemes, which have lower performance than our proposal, have complexity $\mathcal{O}\left(cMK\right)$ [SMpV11, PWLW07].

4.5 Simulation Results

4.5.1 Channel Model and System Configuration

In the simulations, we consider a multiuser MIMO-OFDM/SC-FDMA based CR DL/UL with OFDM subchannels suffering from independent Rayleigh flat fading. The path loss (PL), shadowing, and Rayleigh-distributed multipath fading assumed for channel modeling are combined according to the model in section 2.5. The channel modeling parameters are configured for the simulation as follows: Reference distance $d_0 = 1$ m, PL exponent $\gamma = 2$, shadowing variance $\sigma^2_{S(\text{dB})} = 0$ dB and multipath variance $\sigma^2_m = 1$. Assuming normalized PL, i.e. $\mathrm{Z}_{PL} = 1$, all CUs

and PUs are uniformly distributed on a circle around the CR-BS with a radius of $distance = d_0$ and free space loss $Z_0 = 1$. It is assumed that $K = 10$ CUs coexist with $L = 7$ PUs. The elements of the desired channels $\mathbf{H}_{D,k,i}, \mathbf{H}_{U,k,i}$, and $\mathbf{T}_{l,i}$ as well as the interference channels $\mathbf{G}_{D,l,i}, \mathbf{G}_{U,k,l,i}$, and $\mathbf{Z}_{k,i}$ are generated as i.i.d. variables as described in the above channel model. The simulation parameters in the following examples are set-up as follows unless otherwise stated. The antenna configuration is $[N_{CB} \times N_c : N_{PB} \times N_p] = [6 \times 5 : 4 \times 4]$, assuming $M = 64$ for OFDM and SC-FDMA tones. The interference temperature parameter of the lth PU is $\alpha_l = 0.01, \forall l$. The link time weight is set to $\tau = 0.5$. We define the SNR of the CR link as $\text{SNR}_{CR} = P_T/\sigma_n^2$ and the PR link as $\text{SNR}_{PR} = P_{PB}/\sigma_n^2$, with $\sigma_n^2 = 1$. The SNR_{PR} is fixed to 100.

4.5.2 Example 1: Comparison of the Proposed Scheme and Alternative Schemes

We compare the proposed scheme with the following five alternative schemes:

(1) *ZF precoding (ZP)*: In this case, a fixed precoding technique is involved based on driving the interference at all PUs to zero forcibly.

(2) *SVD precoding with transmit power control (SPT)*: A fixed precoding technique based on SVD with transmit interference power control at the PUs is used as in [SMpV11] and the MIMO version in [PWLW07].

(3) *Hybrid precoding with transmit power control (HPT)*: A fixed precoding based on involving some orthonormal bases besides the null-space is employed [ZL08a].

The proposed subcarrier mapping developed in Section 4.3 is employed in the schemes above. We also compare our proposal with the following two alternative schemes:

(4) *Adaptive precoding with the initial (approximate) subcarrier allocation (APA)*: This scheme employs the adaptive precoding, an approximate subcarrier allocation, and WF power allocation [YH14].

(5) *Equal power allocation with adaptive precoding (EPA)*: Equal power allocation combined with both the proposed adaptive precoding and subcarrier mapping is conducted in this scheme.

All the above mentioned schemes are extended to fit the UL depending on ***Proposition 3***. In Figure 4.2 and Figure 4.3 the achievable total CR sum-rate for all the schemes mentioned above is drawn versus the SNR scaled over the range 1 to 1000.

Figure 4.2 illustrates an outstanding performance in favor the proposed approach which

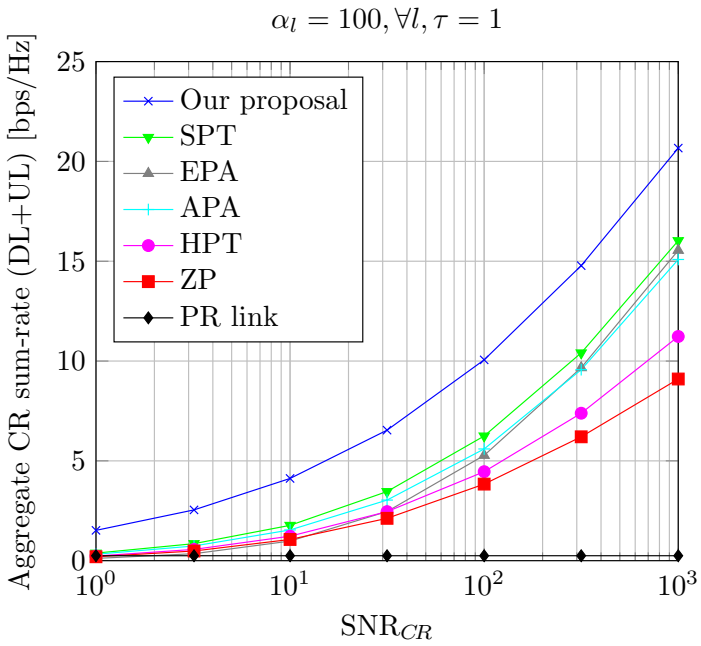

Figure 4.2: Aggregate CR sum-rate as a function of the SNR

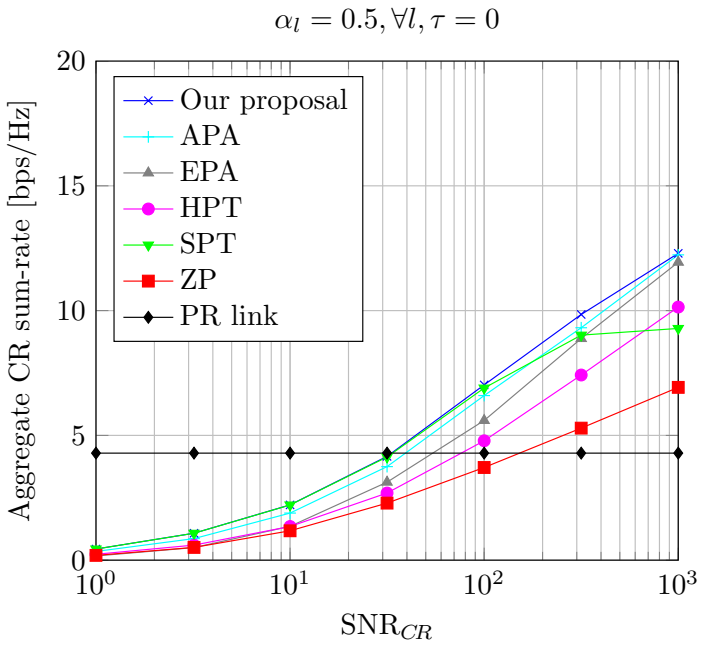

Figure 4.3: Aggregate CR sum-rate as a function of the SNR

is conducted at a relaxed transmission condition, i.e. high PU rate loss that corresponds to $\alpha_l = 100$. Our proposal achieves a remarkable gains: SNR gain of up to 9 dB and spectral gain

of up to 5 bps/Hz for $\tau = 1$, i.e. DL state. However, the gain obtained by our proposal decreases as the transmission conditions get tighter. Figure 4.3 shows an example for the achievable gains at low PU rate loss $\alpha_l = 0.5$ for $\tau = 0$, i.e. UL state. Nevertheless, our proposal still achieves good spectral gain up to 3 bps/Hz and SNR gain up to 5 dB in the high SNR regime, i.e. $\text{SNR}_{CR} > 100$.

4.5.3 Example 2: Effect of the Temperature Parameter on the Primary and CR Sum-Rates

Figure 4.4 shows the aggregate CR sum-rate as well as the sum-rate of the PR link in terms of the temperature parameter α_l. Obviously, little α_l causes minor loss in the PR sum-rate while significantly degrades the CR sum-rate, and vice versa. It is also clear that our proposal outperforms other techniques for the regime $\text{SNR}_{CR} = 15$ dB at both tight and relaxed interference temperatures achieving a spectral gain of up to 5 bps/Hz. Furthermore, it demonstrates robustness against the tight transmission conditions of the CR network.

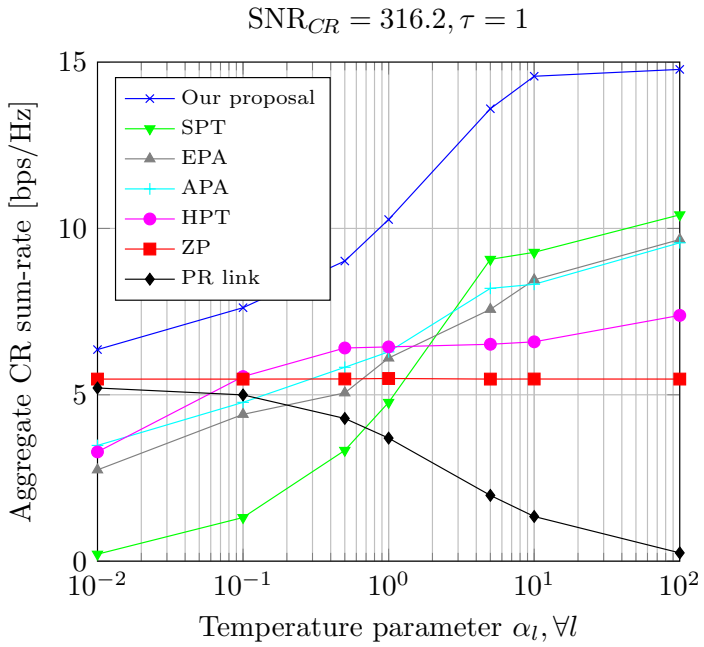

Figure 4.4: Aggregate CR sum-rate as a function of temperature parameter

Another illustration is the sum-rate of the PR link as a function of the aggregate CR sum-rate as in Figure 4.5, which draws the capacity region of both PR and CR systems in the low

regime $\text{SNR}_{CR} = 10$. The proposed scheme achieves higher capacity than other techniques at any transmission conditions, i.e. for α_l in the range 10^{-2} to 10^{2}.

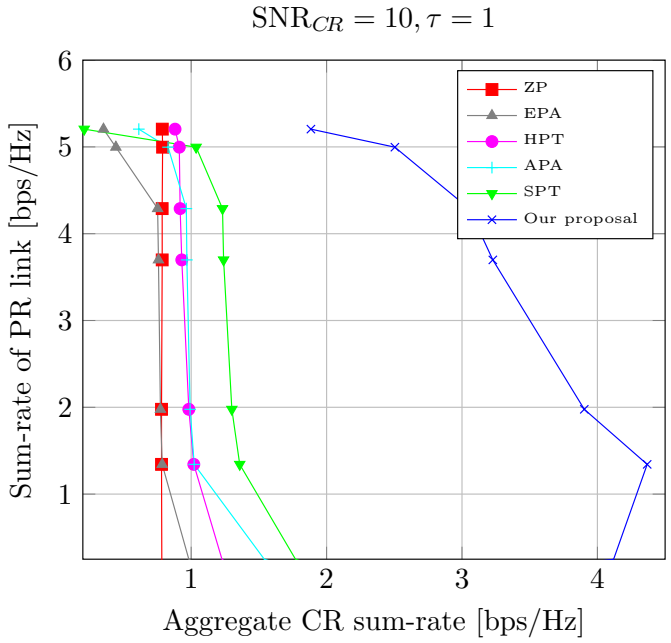

Figure 4.5: Capacity region: PR sum-rate as a function of the aggregate CR sum-rate

4.5.4 Example 3: Effect of the Distributive RA on the CR Sum-Rate

Figure 4.6 and Figure 4.7 compare the central and distributive RA schemes of both DL and UL. The comparisons are conducted by employing the CR sum-rate as an assessment metric in terms of the SNR_{CR} and the temperature parameter α_l. Generally, there is a better performance in favor the distributive scheme in the DL, but in favor the central scheme in the UL. The per-user adaptive precoding provides the CUs with more degrees of freedom in the DoF assignment. Unlike the common DoF assigned to all CUs in the central scheme, the distributive DoF for the CU k is independent of else's CUs, i.e. $\forall j, j \neq k$. That contributes toward little CR sum-rate enhancement. In the UL distributive RA, despite the independence of the DoF assignment, the per-user power constraints degrade the performance compared to the central. In other words, the sum-power constraint, which enables the fast subcarrier mapping in the central RA, provides the strong subcarriers of $\mathcal{S}_k$ with higher power than the per-user power constraint does. The significance of the UL distributive RA is the near-optimal capacity it provides compared to the optimal central scheme.

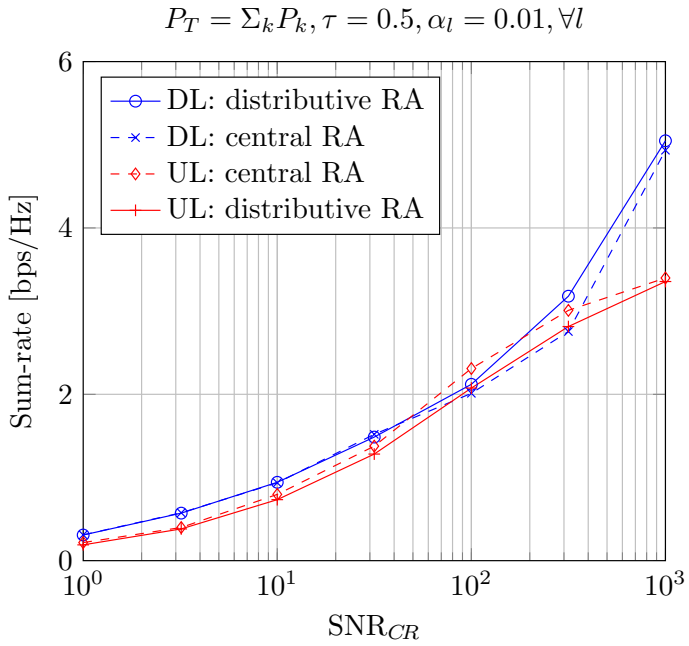

Figure 4.6: CR sum-rate of both DL and UL individually as a function of the SNR

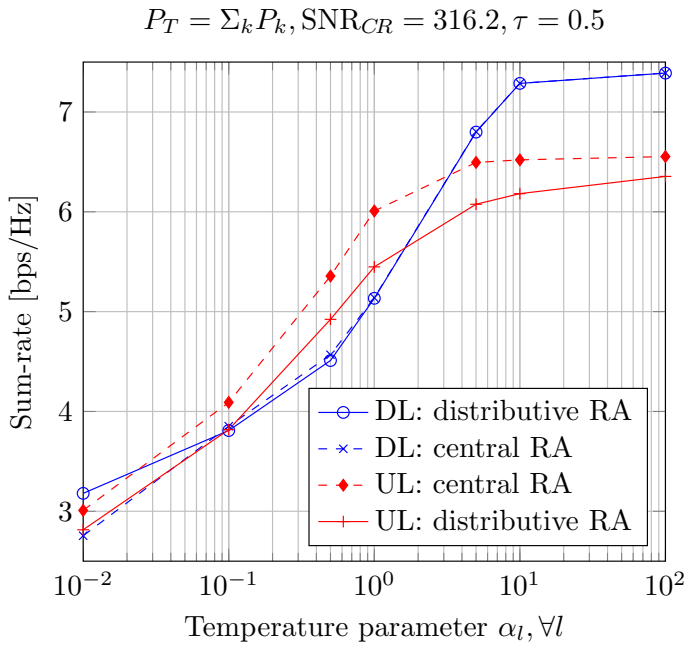

Figure 4.7: CR sum-rate of both DL and UL individually as a function of the temperature parameter

4.5.5 Example 4: Complexity

Figure 4.8 shows the computational cost of our proposal compared with other techniques for $K = 10$ CUs and cardinality of DoFs set equals $|\mathcal{D}| = 5$ for the adaptive precoder. It can be observed that the complexity of our proposal increases slightly with the number of subcarriers unlike the optimal exhaustive search. Although the proposed approach consumes a little more time than other RA schemes, it makes better performance.

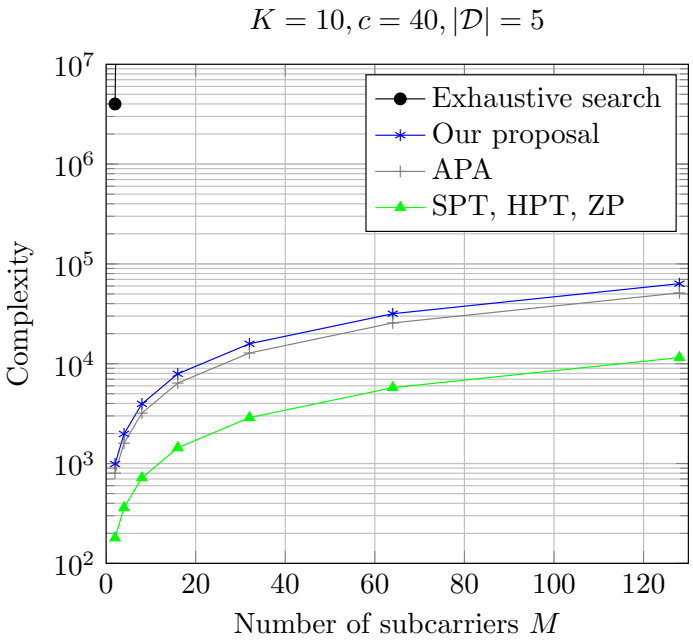

Figure 4.8: Computational cost as a function of the number of subcarriers

4.6 Chapter Summary

In this chapter, we have developed efficient RA scheme for MIMO-OFDM/SC-FDMA CR networks. Since the formulated optimization problem has a combinatorial complexity, we separated it into a two-phase procedure to elaborate computational efficiency: Adaptive precoding (DoF assignment) and subcarrier mapping. From the implementation perspective, the RA of the DL is central based, but the UL is semi-distributed based. The central RA task has been solved to obtain both the central adaptive precoding and the subcarrier mapping for both the DL and UL. The subcarrier mapping is optimal for the DL, but near-optimal for the UL due to the per-user resource constraints. Furthermore, the distributive RA task is necessary to resolve the

power allocation of the UL, but an option for the DL. The semi-distributed scheme in the UL is computationally and spectrally efficient. It also leads to a small data overhead and simplifies the terminal structure. Numerical simulations illustrated remarkable spectral and SNR gains provided by the proposed scheme. Moreover, it demonstrated robustness in tight and relaxed transmission conditions. Therefore, it enables larger communication range for underlay CR networks.

5

MIMO Broadcasting Cognitive Radio Networks

Cognitive radio has versatile applications in the future mobile network as a broadcast channel. In the underlay spectrum sharing strategy, CR transmits concurrently with primary radio (PR), thus CR should constrain its transmit power to manage the interference at PR users (PUs) to be below a predefined threshold [Hay05] aiming to protect the PR performance from degradation. Meanwhile, CR should provide a qualitative service for CUs fulfilling their minimum SNR. With such a challenge in the underlay CR network, CR can hardly provide a good quality of service for CUs. Motivated by this, some methods have been developed to build platforms for multiuser CR downlink systems employing multiple antennas like [ZXL09, LL11]. Typically, since CR systems are unlicensed and have limitations with respect to transmission, they should utilize the data-carrying time slots spectrally and computationally efficient. On one hand, non-linear processing like [ZXL09] performs serial-based computations. Hence, its major drawback is that it cannot handle parallel computing facilities despite its spectral efficiency. On the other hand, although linear precoding techniques developed in [LL11, SSH04, SLL09b, JUN05, ZLC10]

(even in non-CR context) have lower sum-rate, they are highly preferred in real-time CR networks as they require less computations.

In [SSH04, SLL09b, LL11], MMSE based preprocessing has demonstrated better performance versus ZF based preprocessing for multi-antenna multiuser downlink systems since it addresses the transmit power boost issue, which is equivalent to the noise enhancement issue in ZF linear receivers. The MMSE precoder regularizes channel inversion using the entire transmit power and noise variance. Recently, an MMSE CR based block diagonalization (MMSE-BD) scheme [LL11] has been extended the MMSE based channel inversion scheme [SLL09b] to meet CR requirements. However, we claim that the multiple antenna structure of the MIMO channels in the conventional MMSE based precoding approach has not been fully utilized.

In this chapter, we propose two adaptive linear precoders based on ZF and MMSE criteria, respectively, both employing a precoding diversity concept for a multiuser MIMO CR based downlink. Unlike the conventional ZF-BD CR based (ZF-BD) precoder, the proposed scheme utilizes the MIMO channel paths and spaces to create precoding diversity in order to excite a multiuser interference (MUI) diversity. Such a diversity can achieve considerable SINR and spectral efficiency gains in the low SNR region. Although the adaptive ZF-BD precoding (AZB) method improves the SINR, it still suffers from the transmit power boost issue. Therefore, we propose an adaptive MMSE-BD (AMB) scheme for the CR downlink to address it. The proposed AMB employs a non-iterative solution and overcomes the transmit power issue inherent in AZB by means of engaging a regularization factor. We mitigate the interference produced by the PR system at the CUs' receivers by means of a whitening process. Although the proposed adaptive precoding requires relatively higher complexity than the conventional ZF-BD and MMSE-BD precoders, it can be handled by parallel computing facilities unlike the non-linear precoder developed in [ZXL09]. As will be seen in the simulation results, the proposed AMB precoder considerably improves the SINR as well as the spectral efficiency and outperforms the conventional MMSE-BD precoder.

5.1 System Model and Problem Statement

This section presents the system model and states the problem of multiuser MIMO communication systems which is investigated in later sections.

5.1.1 System Model

Consider a CR-BS equipped with N_{CB} antennas that communicates with a set of K CUs denoted as $\mathcal{K} = \{1, \ldots, K\}$ each having N_c antennas on a cognitive based multiuser MIMO broadcast channel as shown in Figure 5.1. Denote the total number of CU receive antennas as $N_r = K\,N_c$. Let the MIMO channel between the CR-BS and the kth CU denoted as $\mathbf{H}_k \in \mathbb{C}^{N_c \times N_{BS}}$. A PR network (a PR-BS having N_{PB} antennas communicates with a single PU that has N_p antennas) coexists with the CR network. Denote the channel between the CR-BS and the PU as $\mathbf{G} \in \mathbb{C}^{N_p \times N_{CB}}$, the channel between the PR-BS and the PU as $\mathbf{T} \in \mathbb{C}^{N_p \times N_{PB}}$, and the channel between the PR-BS and the kth CU as $\mathbf{Z}_k \in \mathbb{C}^{N_c \times N_{PB}}$. The assumption is that all $\{\mathbf{H}_k\}$ and $\mathbf{G}$ are known at the CR-BS, while the kth CU only knows $\mathbf{H}_k$ and $\mathbf{Z}_k$ infers that the MUI should be managed at the transmitter side via preprocessing.

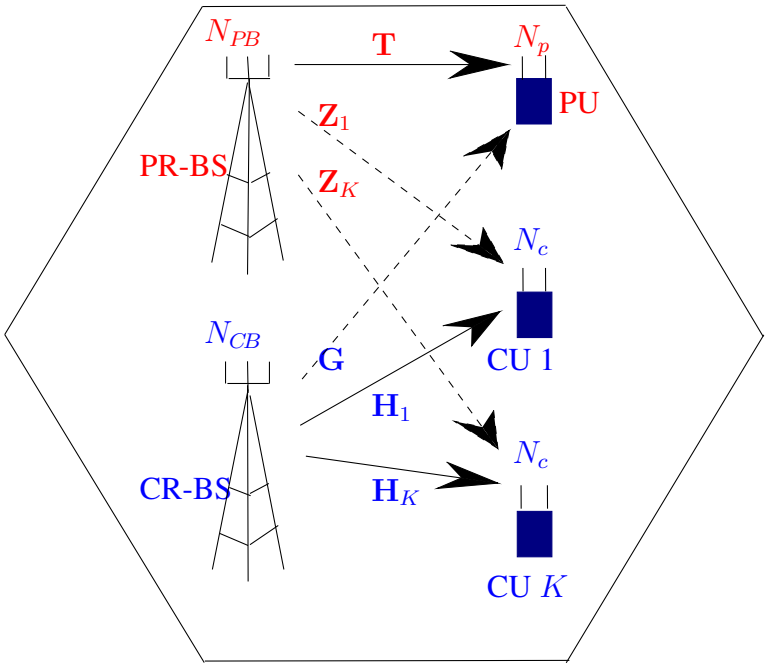

Figure 5.1: Multiuser MIMO CR based broadcast channel model

The kth data vector, noise vector, power matrix, preprocessing matrix, and post-processing matrix are denoted as $\mathbf{s}_k \in \mathbb{C}^{N_c \times 1}$, $\mathbf{n}_k \in \mathbb{C}^{N_c \times 1}$, $\mathbf{P}_k \in \mathbb{C}^{N_c \times N_c}$, $\mathbf{F}_k \in \mathbb{C}^{N_{CB} \times N_c}$, and $\mathbf{W}_k \in \mathbb{C}^{N_c \times N_c}$, respectively. Regarding the PR network, the data vector, noise vector, power matrix, and precoding matrix are denoted as $\mathbf{s}_p \in \mathbb{C}^{N_p \times 1}$, $\mathbf{n}_p \in \mathbb{C}^{N_p \times 1}$, $\mathbf{P}_p \in \mathbb{R}^{N_p \times N_p}$, and $\mathbf{F}_p \in \mathbb{C}^{N_{PB} \times N_p}$, respectively. The entries of noise vectors $\mathbf{n}_k$ and $\mathbf{n}_p$ are i.i.d. Gaussian random variables, i.e., $\mathbf{n}_k \sim \mathcal{CN}(\mathbf{0}, \sigma_n^2 \mathbf{I}_{N_c})$ and $\mathbf{n}_p \sim \mathcal{CN}(\mathbf{0}, \sigma_n^2 \mathbf{I}_{N_p})$. Therefore, the aggregate received

signal of the CR system under investigation can be expressed as

$$\underline{\mathbf{y}} = \underline{\mathbf{H}}\,\underline{\mathbf{F}}\,\underline{\mathbf{s}} + \underline{\mathbf{Z}}\mathbf{F}_p\mathbf{s}_p + \underline{\mathbf{n}} \tag{5.1}$$

where the multiuser vectors and matrices in (5.1), i.e. receive vector $\underline{\mathbf{y}} \in \mathbb{C}^{N_r \times 1}$, data vector $\underline{\mathbf{s}} \in \mathbb{C}^{N_r \times 1}$, channel matrix $\underline{\mathbf{H}} \in \mathbb{C}^{N_r \times N_{CB}}$, precoding matrix $\underline{\mathbf{F}} \in \mathbb{C}^{N_{CB} \times N_r}$, noise vector $\underline{\mathbf{n}} \in \mathbb{C}^{N_r \times 1}$, channel matrix of the PR-BS-to-CUs cross link $\underline{\mathbf{Z}} \in \mathbb{C}^{N_r \times N_{PB}}$, are defined as follows

$$\underline{\mathbf{y}} = [\mathbf{y}_1^T \dots \mathbf{y}_K^T]^T$$

$$\underline{\mathbf{s}} = [\mathbf{s}_1^T \dots \mathbf{s}_K^T]^T$$

$$\underline{\mathbf{H}} = [\mathbf{H}_1^T \dots \mathbf{H}_K^T]^T$$

$$\underline{\mathbf{F}} = [\mathbf{F}_1 \dots \mathbf{F}_K]$$

$$\underline{\mathbf{n}} = [\mathbf{n}_1^T \dots \mathbf{n}_K^T]^T$$

$$\underline{\mathbf{Z}} = [\mathbf{Z}_1^T \dots \mathbf{Z}_K^T]^T$$

It is assumed that each data symbol has unit variance $\mathbb{E}\left\{\underline{\mathbf{s}}\,\underline{\mathbf{s}}^H\right\} = \mathbf{I}_{N_r}$, therefore the CR-BS transmit power fulfills $\mathbb{E}\left\{\|\underline{\mathbf{F}}\,\underline{\mathbf{s}}\|^2\right\} \leq P_T$.

In the PR network, the received signal at the PU, i.e. $\mathbf{y}_p \in \mathbb{C}^{N_p \times 1}$, can be written as

$$\mathbf{y}_p = \mathbf{T}\mathbf{F}_p\mathbf{s}_p + \mathbf{y}_{ni} \tag{5.2}$$

where $\mathbf{F}_p$ is a SVD precoder, $\mathbf{P}_p$ is obtained by distributing the PR-BS power P_{PB} over the data streams (eigenmodes) of $\mathbf{T}$ via waterfilling such that $\text{Tr}(\mathbf{P}_p) = \text{Tr}(\mathbf{F}_p\mathbb{E}\left\{\mathbf{s}_p\mathbf{s}_p^H\right\}\mathbf{F}_p^H) \leq P_{PB}$ assuming that $\mathbb{E}\left\{\mathbf{s}_p\mathbf{s}_p^H\right\} = \mathbf{I}_{N_p}$. On one hand, the second term $\mathbf{y}_{ni} \in \mathbb{C}^{N_p \times 1}$ refers to the CR-BS interference plus noise induced at the PU, which defined as $\mathbf{y}_{ni} = \mathbf{G}\underline{\mathbf{F}}\,\underline{\mathbf{s}} + \mathbf{n}_p$. On the other hand, the PR-BS interference plus the noise covariance matrix at the kth CU can be factorized as

$$(\mathbf{Z}_k\mathbf{P}_p\mathbf{Z}_k^H + \sigma_n^2\mathbf{I}_{N_c})^{-1} = \mathbf{\Gamma}_k\mathbf{\Gamma}_k^H \tag{5.3}$$

$\mathbf{\Gamma}_k \in \mathbb{C}^{N_c \times N_c}$ is defined as a receive whitening filter at the kth CU. The block of whitening filters can be written as $\underline{\tilde{\mathbf{W}}} = \text{blkd}\,(\mathbf{\Gamma}_1 \dots \mathbf{\Gamma}_K)$. Therefore, the whitened version of the entire received vector of all CUs defined in (5.1) can be written as

$$\underline{\tilde{\mathbf{y}}} = \underline{\tilde{\mathbf{H}}}\,\underline{\mathbf{F}}\,\underline{\mathbf{s}} + \underline{\tilde{\mathbf{n}}} \tag{5.4}$$

in the above equation

$$\underline{\tilde{\mathbf{H}}} = [\tilde{\mathbf{H}}_1^T \tilde{\mathbf{H}}_2^T \dots \tilde{\mathbf{H}}_K^T]^T = \underline{\tilde{\mathbf{W}}}\ \underline{\mathbf{H}}$$

and

$$\underline{\tilde{\mathbf{n}}} = [\tilde{\mathbf{n}}_1^T \tilde{\mathbf{n}}_2^T \dots \tilde{\mathbf{n}}_K^T]^T = \underline{\tilde{\mathbf{W}}}(\underline{\mathbf{Z}}\mathbf{F}_p\mathbf{s}_p + \underline{\mathbf{n}})$$

The whitened noise vector $\tilde{\mathbf{n}}$ is characterized as a zero-mean vector with identity covariance matrix. Thus, the whitened received vector of CU k is given by

$$\tilde{\mathbf{y}}_k = \tilde{\mathbf{H}}_k\mathbf{F}_k\mathbf{s}_k + \tilde{\mathbf{H}}_k \sum_{j=1, j\neq k}^{K} \mathbf{F}_j\mathbf{s}_j + \tilde{\mathbf{n}}_k \tag{5.5}$$

where $\tilde{\mathbf{H}}_k = \tilde{\mathbf{W}}_k\mathbf{H}_k$ and $\tilde{\mathbf{n}}_k = \tilde{\mathbf{W}}_k(\mathbf{Z}_k\mathbf{F}_p\mathbf{s}_p + \mathbf{n}_k)$. Thus, the whitened noise vector $\tilde{\mathbf{n}}_k$ is characterized as a zero-mean vector with identity covariance matrix.

5.1.2 Problem Statement

The spectral efficiency and low latency of multiuser MIMO communications are the main concerns in future mobile network. In regard to non-orthogonal access systems, non-linear transmit precoding, i.e. dirty paper coding based, methods are known as computationally expensive techniques despite their high spectral efficiency. On the other hand, linear techniques can offer affordable complexities but at, however, lower spectral efficiencies. Therefore, new designs which have acceptable complexities and relatively high spectral efficiencies are required. Some linear techniques optimize either one of the following common quality measures: Sum-rate maximization and MMSE. The sum-rate maximization problem has the following structure

$$\begin{aligned} \max_{\{\underline{\mathbf{F}}(d), \forall d\in\mathcal{D}\}} \quad & \sum_{k=1}^{K} \log_2 |\mathbf{I}_{N_c} + \text{SINR}_k| \\ \text{subject to} \quad & \mathbb{E}\left\{\|\mathbf{G}\underline{\mathbf{F}}(d)\underline{\mathbf{s}}\|^2\right\} \leq I_{th} \\ & \mathbb{E}\left\{\|\underline{\mathbf{F}}(d)\underline{\mathbf{s}}\|^2\right\} \leq P_T \end{aligned} \tag{5.6}$$

where

$$\text{SINR}_k = \frac{\mathbf{W}_k(d)\mathbf{H}_k\mathbf{F}_k(d)\mathbf{F}_k^H(d)\mathbf{H}_k^H\mathbf{W}_k^H(d)}{\sigma_n^2\mathbf{I}_{N_c} + \mathbf{W}_k(d)\mathbf{H}_k\left(\sum_{j\neq k}^{K}\mathbf{F}_j(d)\mathbf{F}_j^H(d)\right)\mathbf{H}_k^H\mathbf{W}_k^H(d)}$$

The MMSE optimization problem has a different objective function as follows

$$\begin{aligned} \min_{\gamma, \underline{\mathbf{F}}(d), d\in\mathcal{D}} \quad & \mathbb{E}\left\{\|\underline{\mathbf{s}} - \gamma^{-1}\underline{\tilde{\mathbf{y}}}\|^2\right\} \\ \text{subject to} \quad & \mathbb{E}\left\{\|\mathbf{G}\underline{\mathbf{F}}(d)\underline{\mathbf{s}}\|^2\right\} \leq I_{th} \\ & \mathbb{E}\left\{\|\underline{\mathbf{F}}(d)\underline{\mathbf{s}}\|^2\right\} \leq P_T \end{aligned} \tag{5.7}$$

where γ is a scaling factor for the received signal. In general, some prior precoding techniques categorized under ZF criterion include [CM04, LLa11, SSH04, SLL09b] and others incorporating MMSE criterion in precoding contain [JBU04, SH08, SLL09b, SLL09a, JL07]. These preliminaries have not taken into account the CR requirement. However, the scheme in [LL11] has imposed a constraint to restrict PUI effectively extending ZF and MMSE criteria to meet CR requirements as will be detailed in the following section.

5.2 Proposed Adaptive Linear Precoding

Conventional linear preprocessing designs have substantially low complexity, therefore from the complexity perspective it is convenient to develop new linear preprocessing techniques in an adaptive manner utilizing the multiple antenna structure for enhancing spectrum efficiency. Particularly in the proposed adaptive linear precoding schemes, we map the antenna diversity to a precoding diversity with countable independent DoF. The precoding diversity produces a MUI diversity and thus improves the SNR of the CR system under investigation. The network adapts the precoding according to the maximum achievable SNR which fulfills the network constraints. Concerning the complexity, on one hand the comparable conventional precoding schemes, i.e. ZF-BD and MMSE-BD, only have one DoF compared to the proposed adaptive schemes which is an advantage in favor of computations reduction. On the other hand, advances of the parallel computing can handle the calculations of the independent precoding DoFs in the proposed adaptive methods efficiently. In the following, we present the details of the proposed adaptive linear precoders AZB and AMB. Without loss of generality, both MUI and PUI conditions in the adaptive linear preprocessing schemes are formed as: $\tilde{\mathbf{H}}_j\mathbf{F}_k \geq \mathbf{0}_{N_c\times N_c}$ and $\mathbf{G}\mathbf{F}_j \geq \mathbf{0}_{N_p\times N_c}, \forall j, j\neq k$, respectively. Therefore, the mechanism of the proposed approaches works on producing a precoding and a MUI diversity while satisfying the PUI condition $\sum_{k=1}^{K}\mathbb{E}\left\{\|\mathbf{G}\mathbf{F}_k\mathbf{s}_k\|^2\right\} \leq I_{th}$, and dissipating the entire transmit power P_T spectrally efficiently. Specifically, the key idea beyond the adaptive based preprocessing considers a part of complementary MIMO channel's paths (or subspaces) when computing a corresponding precoding DoF as will be described below. In other words, the design of the dth

precoding DoF counts on one combination of complementary MIMO channel's paths (rows) or subspaces. Through scanning the entire combinations of paths (or subspaces), we can create a precoding set indexed for the kth CU as $\mathcal{D}_k = \{1, 2, \ldots, |\mathcal{D}_k|\}$. As we consider equal number of antennas per CU N_c, all CUs will have similar size precoding set, i.e. $|\mathcal{D}| = |\mathcal{D}_k|, \forall k$. From CUs' precoding sets, we combine the overall DoF set of network as K-tuples. To establish a low complexity solution, we combine the similar indices of the K precoding sets of the K CUs together, i.e. the K-tuple $\underline{\mathbf{F}}(d) \in \{\underline{\mathbf{F}}(1), \ldots, \underline{\mathbf{F}}(|\mathcal{D}|)\}$, where for instance the first K-tuple in the DoF set is defined as $\underline{\mathbf{F}}(1) = [\mathbf{F}_1(1)\mathbf{F}_2(1)\ldots\mathbf{F}_K(1)]$.

5.2.1 Adaptive Zero Forcing Block Diagonalization

In this approach, we address the sum-rate maximization (5.6) which considered non-convex problem as the MUI occurs in the denominator of each CU's SINR. To solve it in the context of the proposed AZB method, we should find the best K-tuple precoding $\underline{\mathbf{F}}(\hat{d})$ which maximizes the sum-rate.

To exploit the antenna diversity of CUs, we generate precoding diversity by two means: Subspace (orthogonal basis) combining and channel path combining. Note that the cardinality of $\mathcal{D}$ is a function of the number of rows of the complementary MIMO channel for the kth CU

$$\bar{\mathbf{H}}_k = [\mathbf{G}^T\tilde{\mathbf{H}}_1^T \ldots \tilde{\mathbf{H}}_{k-1}^T\tilde{\mathbf{H}}_{k+1}^T \ldots \tilde{\mathbf{H}}_K^T]^T$$

i.e. $|\mathcal{D}| = f(\mathcal{R}_k)$, where $\mathcal{R}_k = N_p + N_r - N_c$. To this end, we consider the MUI seen by other $K-1$ CUs but not the intra-user interference seen by the kth CU itself. Note that the conventional ZF-BD approach can be seen as one candidate DoF within the proposed AZB scheme and is the only case causing convexity. We will consider the waterfilling solution of this convex case $\mathbf{P}^{\text{ZB}}$ as a power allocation solution for the proposed AZB precoder. The details of both subspace and channel path combining methods follow.

1. *Subspace Combining (AZB-SC):*

   In this approach, all paths of the complementary MIMO channel are considered in the preprocessing (rows of MIMO channel), however, the subspaces of the complementary MIMO channel are combined. Precisely, not only the null space of $\bar{\mathbf{H}}_k$ is taken into account, but also the spaces of the non-zero singular values. For the CU k, the cardinality of the precoding set in this method is $|\mathcal{D}| = \mathcal{R}_k + 1$ and the DoF set is indexed as $\mathcal{D} = \{0, 1, 2, \ldots, \mathcal{R}_k\}$. For instance, let the singular values of $\bar{\mathbf{H}}_k$ be ordered as $\bar{\lambda}_1 \geq \bar{\lambda}_2 \geq \cdots \geq \bar{\lambda}_{\mathcal{R}_k}$ and the null space is indexed as $d = 0$, therefore the index $d = 3$

refers to the spaces of the null as well as the smallest three non-zero singular values. For the CU k and the precoding index d, denote $\bar{\mathbf{H}}_k^{(d)} \in \mathbb{C}^{N_{CB}\times(N_c+d)}$ as the space of the null as well as the smallest d non-zero singular values in $\bar{\mathbf{H}}_k$. Then, apply the SVD as $\tilde{\mathbf{H}}_k\bar{\mathbf{H}}_k^{(d)} = \check{\mathbf{U}}_k^{(d)}\check{\mathbf{\Lambda}}_k^{(d)}\check{\mathbf{V}}_k^{(d)H}$ to diagonalize the effective channel before applying power solution $\mathbf{P}_k^{\text{ZB}}$. The precoder and receive filter can be written as

$$\mathbf{F}_k^{\text{AZB1}}(d)=\bar{\mathbf{H}}_k^{(d)}\check{\mathbf{V}}_k^{(d)}(\mathbf{P}_k^{\text{ZB}})^{\frac{1}{2}} \text{ and } \mathbf{W}_k^{\text{AZB1}}(d)=\check{\mathbf{U}}_k^{(d)H}\mathbf{\Gamma}_k \tag{5.8}$$

Remark 1: For zero PUI constraint $I_{th} = 0$, we use the null space of $\mathbf{G}$ denoted as $\mathbf{G}^{\perp}$ which is defined as

$$\mathbf{G}^{\perp} = \mathbf{I}_{N_{CB}} - \mathbf{G}^H(\mathbf{G}\mathbf{G}^H)^{-1}\mathbf{G} \tag{5.9}$$

such that the effective channel of the kth CU is projected onto $\mathbf{G}^{\perp}$ before applying the SVD operation as $\tilde{\mathbf{H}}_k\mathbf{G}^{\perp}\bar{\mathbf{H}}_k^{(d)} = \check{\mathbf{U}}_k^{(d)}\check{\mathbf{\Lambda}}_k^{(d)}\check{\mathbf{V}}_k^{(d)H}$ for the diagonalization and power allocation steps. The precoder becomes $\mathbf{F}_k^{\text{AZB1}}(d)=\mathbf{G}^{\perp}\bar{\mathbf{H}}_k^{(d)}\check{\mathbf{V}}_k^{(d)}(\mathbf{P}_k^{\text{ZB}})^{\frac{1}{2}}$.

2. *Channel Path Combining (AZB-CPC):*

In this method, we define the complementary channel model of the CU k, excluding the kth CU's channel model $\tilde{\mathbf{y}}_k = \tilde{\mathbf{H}}_k\mathbf{s}_k + \tilde{\mathbf{n}}_k$ as

$$\underline{\tilde{\mathbf{y}}}_k^{\text{AZB2}}(d) = \underline{\tilde{\mathbf{H}}}_k(d)\ \underline{\mathbf{F}}_k(d)\ \underline{\mathbf{s}}_k + \underline{\tilde{\mathbf{n}}}_k(d) \tag{5.10}$$

where $\underline{\tilde{\mathbf{y}}}_k(d)$, $\underline{\mathbf{F}}_k(d)$, $\underline{\mathbf{s}}_k$, $\underline{\tilde{\mathbf{n}}}_k(d)$, and $\underline{\tilde{\mathbf{H}}}_k(d)$ are given, respectively, as

$$\begin{aligned}
\underline{\tilde{\mathbf{y}}}_k(d) &= [\mathbf{y}_{ni}^T\tilde{\mathbf{y}}_1^T\ldots\tilde{\mathbf{y}}_{k-1}^T\tilde{\mathbf{y}}_{k+1}^T\ldots\tilde{\mathbf{y}}_K^T]^T && (5.11)\\
\underline{\mathbf{F}}_k(d) &= [\mathbf{F}_1(d)\ldots\mathbf{F}_{k-1}(d)\mathbf{F}_{k+1}(d)\ldots\mathbf{F}_K(d)] && (5.12)\\
\underline{\mathbf{s}}_k &= [\mathbf{s}_1^T\ldots\mathbf{s}_{k-1}^T\mathbf{s}_{k+1}^T\ldots\mathbf{s}_K^T]^T && (5.13)\\
\underline{\tilde{\mathbf{n}}}_k(d) &= [\mathbf{n}_p^T\tilde{\mathbf{n}}_1^T\ldots\tilde{\mathbf{n}}_{k-1}^T\tilde{\mathbf{n}}_{k+1}^T\ldots\tilde{\mathbf{n}}_K^T]^T && (5.14)\\
\underline{\tilde{\mathbf{H}}}_k(d) &= \mathbf{M}_k^{(d)}\odot\bar{\mathbf{H}}_k\\
&= \mathbf{M}_k^{(d)}\odot[\mathbf{G}^T\tilde{\mathbf{H}}_1^T\ldots\tilde{\mathbf{H}}_{k-1}^T\tilde{\mathbf{H}}_{k+1}^T\ldots\tilde{\mathbf{H}}_K^T]^T && (5.15)
\end{aligned}$$

given that $\odot$ is the Hadamard "element wise product" operator and $\mathbf{M}_k^{(d)} \in \mathbb{R}^{\mathcal{R}_k\times N_{CB}}$ is the so-called inclusion matrix which corresponds to the precoding index d of the CU k. The cardinality of the precoding set is $|\mathcal{D}| = \sum_{j=1}^{\mathcal{R}_k} {}^{\mathcal{R}_k}C_j = 2^{\mathcal{R}_k} - 1$ per CU, where ${}^mC_n$ refers to the number of possible n-tuples combined from m entities. The entries of each column in $\mathbf{M}_k^{(d)}$ are expressed as the binary conversion of the decimal index d as shown in

Table 5.1: Entries of $\mathbf{M}_k^{(d)}, \forall d \in \mathcal{D}$ of AZB-CPC

Row index of $\mathbf{M}_k^{(d)} \downarrow$ $\mathbf{M}_k^{(d)} \rightarrow$	$\mathbf{M}_k^{(1)}$	$\mathbf{M}_k^{(2)}$	$\mathbf{M}_k^{(3)}$	...	$\mathbf{M}_k^{(\lvert\mathcal{D}\rvert)}$
1	$\mathbf{0}^T$	$\mathbf{0}^T$	$\mathbf{0}^T$		$\mathbf{1}^T$
$\vdots$	$\vdots$	$\vdots$	$\mathbf{0}^T$	...	$\vdots$
	$\mathbf{0}^T$	$\mathbf{1}^T$	$\mathbf{1}^T$		
$\mathcal{R}_k$	$\mathbf{1}^T$	$\mathbf{0}^T$	$\mathbf{1}^T$		$\mathbf{1}^T$

Table 5.1 in which $\mathbf{0}^T$ and $\mathbf{1}^T$ are $1 \times N_{CB}$ all-zero and all-one row vectors, respectively. For instance, for $\mathcal{R}_k = 8$ and precoding index $d = 3$, the inclusion matrix $\mathbf{M}_k^{(3)}$ has N_{CB} equal column vectors each written as $[0\,0\,0\,0\,0\,0\,1\,1]^T$, where $\mathcal{R}_k$ determines the number of binary digits of the vector and d represents the decimal value of the binary column vector. For the CU k and index d, denote $\underline{\tilde{\mathbf{H}}}_k^{(0)}(d)$ as the null space of $\underline{\tilde{\mathbf{H}}}_k(d)$, then apply the SVD to the effective channel as $\tilde{\mathbf{H}}_k \underline{\tilde{\mathbf{H}}}_k^{(0)}(d) = \check{\mathbf{U}}_k^{(d)} \check{\mathbf{\Lambda}}_k^{(d)} \check{\mathbf{V}}_k^{(d)H}$ for the diagonalization purpose before the waterfilling power allocation solution $\mathbf{P}_k^{\text{ZB}}$. Thus, the ultimate form of the precoder and receive filter of the kth CU can be written as

$$\mathbf{F}_k^{\text{AZB2}}(d) = \underline{\tilde{\mathbf{H}}}_k^{(0)}(d) \check{\mathbf{V}}_k^{(d)} (\mathbf{P}_k^{\text{ZB}})^{\frac{1}{2}} \text{ and } \mathbf{W}_k^{\text{AZB2}}(d) = \check{\mathbf{U}}_k^{(d)H} \mathbf{\Gamma}_k \tag{5.16}$$

Remark 2: For zero PUI $I_{th} = 0$, similar to *Remark 1* the effective channel of the kth CU should be projected on $\mathbf{G}^{\perp}$ defined in (5.9) before applying the SVD operation as $\tilde{\mathbf{H}}_k \mathbf{G}^{\perp} \underline{\tilde{\mathbf{H}}}_k^{(0)}(d) = \check{\mathbf{U}}_k^{(d)} \check{\mathbf{\Lambda}}_k^{(d)} \check{\mathbf{V}}_k^{(d)H}$. The precoder becomes $\mathbf{F}_k^{\text{AZB2}}(d) = \mathbf{G}^{\perp} \underline{\tilde{\mathbf{H}}}_k^{(0)}(d) \check{\mathbf{V}}_k^{(d)} (\mathbf{P}_k^{\text{ZB}})^{\frac{1}{2}}$.

Therefore, the optimal K-tuple $\left\{ \underline{\mathbf{F}}^{\text{AZB}}(\hat{d}), \underline{\mathbf{W}}^{\text{AZB}}(\hat{d}) \right\}, \hat{d} \in \mathcal{D}$, should achieve the maximum sum-rate while satisfying the PUI condition.

5.2.2 Power Allocation of the Adaptive Zero Forcing Block Diagonalization

In this section, we illustrate the derivation of the waterfilling power $\mathbf{P}_k^{\text{ZB}}, \forall k$ employed in the proposed AZB precoder. Note that the objective function to be optimized is the sum-rate subjected to a single constraint: The power budget. First, the Lagrangian can be written as

$$\mathcal{L}_{\text{ZB}}(\{\mathbf{P}_k\}, \mu) = \sum_{k=1}^{K} \log_2 \left| \mathbf{I}_{N_c} + \check{\mathbf{\Lambda}}_k^2 \mathbf{P}_k \right| - \mu \left(\sum_{k=1}^{K} \text{Tr}\left(\mathbf{P}_k\right) - P_T \right) \tag{5.17}$$

where μ is a Lagrange multiplier associated with the power constraint and both $\hat{\mathbf{\Lambda}}_k$ as well as $\mathbf{P}_k$ are diagonal matrices. Note that the MUI vanishes in the ZF-BD technique.

Then we obtain the optimal power by applying the Karush-Kuhn-Tucker (KKT) conditions [BV04]. The gradient $\frac{\partial \mathcal{L}_{\text{ZB}}}{\partial \mathbf{P}_k} = 0$ can be easily derived from which the optimal power is written as

$$\mathbf{P}_k^{\text{ZB}} = \left[\{\ln 2\,(\mu \mathbf{I}_{N_c})\}^{-1} - \check{\mathbf{\Lambda}}_k^{-2}\right]^+, \forall k \tag{5.18}$$

The power is obtained after n iterations for the dual variable μ using a numerical method like the bisection method [BV04].

5.2.3 Adaptive Minimum Mean Square Error Block Diagonalization

In this section, we develop the conventional MMSE based precoding scheme into the proposed AMB precoding. As mentioned earlier, the precoding diversity enhances the network performance as it causes a notable improvement of the downlink SNR. Based on the MMSE criterion, the MMSE based precoder regularizes the channel inversion via a regularization factor containing the transmit power and noise covariance. We address the MMSE optimization problem in (5.7).

In the proposed AMB approach, we develop a precoder to suppress the MUI and to fulfill both transmit power as well as PUI constraints. To exploit the multiple antenna structure of CUs, a DoF set with a cardinality $|\mathcal{D}|$ collecting all path combinations is computed as mentioned. Then, we find the optimal precoding K-tuple according to the following criterion:

$$\underline{\mathbf{F}}(\hat{d}) = \arg\max_{d \in \mathcal{D}} \sum_{k=1}^{K} r_k\left(\underline{\mathbf{F}}(d)\right) \tag{5.19}$$

where $r_k\left(\underline{\mathbf{F}}(d)\right)$ is the data rate of the kth CU given as a function of the dth K-tuple $\underline{\mathbf{F}}(d)$, $d \in \mathcal{D}$. Therefore, we first solve (5.7) for all DoFs, i.e. $\forall d \in \mathcal{D}$, then apply (5.19) to find the optimal network precoding $\underline{\mathbf{F}}(\hat{d})$. Toward this goal, we define the network channel model of the dth DoF as

$$\underline{\tilde{\mathbf{y}}}^{\text{AMB}}(d) = \underline{\tilde{\mathbf{H}}}(d)\,\underline{\mathbf{F}}(d)\,\underline{\mathbf{s}} + \underline{\tilde{\mathbf{n}}} \tag{5.20}$$

where $\underline{\tilde{\mathbf{y}}}^{\text{AMB}}(d)$, $\underline{\mathbf{F}}(d)$ and $\underline{\tilde{\mathbf{H}}}(d)$ are defined, respectively, as

$$\underline{\tilde{\mathbf{y}}}^{\text{AMB}}(d) = [\tilde{\mathbf{y}}_1(d)^T\, \tilde{\mathbf{y}}_2(d)^T \ldots \tilde{\mathbf{y}}_K(d)^T]^T \tag{5.21}$$

$$\underline{\mathbf{F}}(d) = [\mathbf{F}_1(d)\, \mathbf{F}_2(d) \ldots \mathbf{F}_K(d)] \tag{5.22}$$

$$\underline{\tilde{\mathbf{H}}}(d) = \mathbf{M}^{(d)} \odot \underline{\tilde{\mathbf{H}}} \tag{5.23}$$

where $\mathbf{M}^{(d)} \in \mathbb{R}^{N_r \times N_{CB}}$ is the inclusion matrix of the dth DoF for which the entries are tabulated in Table 5.2. Here, we point out that the precoding set has a cardinality of $|\mathcal{D}| = \sum_{j=1}^{N_r} {}^{N_r}C_j = 2^{N_r} - 1$ DoFs. Each j-tuple corresponds to one path combination produced by (5.21). To this

Table 5.2: Entries of $\mathbf{M}_k^{(d)}$ of AMB, $\forall d \in \mathcal{D}$

Row index of $\mathbf{M}^{(d)} \downarrow$ $\mathbf{M}^{(d)} \rightarrow$	$\mathbf{M}^{(1)}$	$\mathbf{M}^{(2)}$	$\mathbf{M}^{(3)}$	$\ldots$	$\mathbf{M}^{(\lvert\mathcal{D}\rvert)}$
1	$\mathbf{0}^T$	$\mathbf{0}^T$	$\mathbf{0}^T$		$\mathbf{1}^T$
$\vdots$	$\vdots$	$\vdots$	$\mathbf{0}^T$	$\ldots$	$\vdots$
	$\mathbf{0}^T$	$\mathbf{1}^T$	$\mathbf{1}^T$		
N_r	$\mathbf{1}^T$	$\mathbf{0}^T$	$\mathbf{1}^T$		$\mathbf{1}^T$

end, we apply the channel model defined in (5.21) to the MMSE network precoding resulted from solving (5.7) as described in [LL11]. The MMSE based precoding is given by

$$\begin{aligned}\underline{\hat{\mathbf{F}}}(d) &= \gamma\, \underline{\bar{\mathbf{F}}}(\mu, d) \\ &= \gamma \left(\underline{\tilde{\mathbf{H}}}(d)^H \underline{\tilde{\mathbf{H}}}(d) + \mu \mathbf{G}^H \mathbf{G} + \frac{N_r - \mu I_{th}}{P_T} \mathbf{I}_{N_{CB}} \right)^{-1} \underline{\tilde{\mathbf{H}}}(d)^H \end{aligned} \tag{5.24}$$

where $\gamma = \sqrt{P_T / \mathrm{Tr}\left(\underline{\bar{\mathbf{F}}}(\mu, d) \underline{\bar{\mathbf{F}}}(\mu, d)^H\right)}$ and μ is a positive parameter that lies in the interval $0 \leq \mu \leq N_r / I_{th}$ in order to regularize the precoding matrix such that the entire transmit power P_T is dissipated while fulfilling the PUI constraint. μ can be found numerically by the bisection method [BV04].

Remark 3: For zero PUI constraint $I_{th} = 0$, the regularized channel inversion in (5.24) takes another form considering the null space of $\mathbf{G}$ defined in (5.9) as

$$\underline{\hat{\mathbf{F}}}(d) = \gamma\, \mathbf{G}^{\perp} \underline{\tilde{\mathbf{H}}}(d)^H \left(\underline{\tilde{\mathbf{H}}}(d) \mathbf{G}^{\perp} \underline{\tilde{\mathbf{H}}}(d)^H + \frac{N_r}{P_T} \mathbf{I}_{N_r} \right)^{-1} \tag{5.25}$$

Then, the space of the orthonormal bases of the kth CU which are spanned by the column vectors of the corresponding projection matrix $\hat{\mathbf{F}}_k(d)$ can be obtained by the QR decomposition as follows:

$$\hat{\mathbf{F}}_k(d) = \mathbf{Q}_k(d) \mathbf{R}_k(d), \forall k \tag{5.26}$$

where $\mathbf{Q}_k(d) \in \mathbb{C}^{N_{CB} \times N_c}$ contains N_c-dimensional columns of orthonormal bases. Then, we apply the power allocation counting on the MMSE combining matrix $\mathbf{P}_k^{\text{AMB}}$ for the kth CU which

minimizes the sum MSE subject to a transmit power constraint as shown in [SLL09b]. Mathematically, $\mathbf{P}_k^{\text{AMB}}(d)$ is computed for the dth DoF as described in (3.9) as $\mathbf{P}_k^{\text{AMB}}(d) = \beta(d)\bar{\mathbf{P}}_k^{\text{AMB}}(d)$, where

$$\bar{\mathbf{P}}_k^{\text{AMB}}(d) = \left(\mathbf{Q}_k(d)^H \Sigma_{j=1}^K \tilde{\mathbf{H}}_j^H \tilde{\mathbf{H}}_j \mathbf{Q}_k(d) + \frac{N_r}{P_T}\mathbf{I}_{N_c}\right)^{-1} \mathbf{Q}_k(d)^H \tilde{\mathbf{H}}_k^H \tilde{\mathbf{H}}_k \mathbf{Q}_k(d) \tag{5.27}$$

and $\beta(d)$ is computed as $\beta(d) = \sqrt{P_T / \Sigma_{k=1}^K \text{Tr}\left(\bar{\mathbf{P}}_k^{\text{AMB}}(d)^H \bar{\mathbf{P}}_k^{\text{AMB}}(d)\right)}$.

To this end, applying the SVD decouples the effective channel into parallel subchannels for carrying parallel data streams as $\tilde{\mathbf{H}}_k \mathbf{Q}_k(d)\mathbf{P}_k^{\text{AMB}}(d) = \check{\mathbf{U}}_k(d)\check{\mathbf{\Lambda}}_k(d)\check{\mathbf{V}}_k(d)^H$. Ultimately, the precoder and receive filter of the proposed AMB technique are expressed as

$$\mathbf{F}_k^{\text{AMB}} = \mathbf{Q}_k(d)\mathbf{P}_k^{\text{AMB}}(d)\check{\mathbf{V}}_k(d) \text{ and } \mathbf{W}_k^{\text{AMB}} = \check{\mathbf{U}}_k(d)^H \mathbf{\Gamma}_k \tag{5.28}$$

5.3 Performance Evaluation

In this section, we carry out an analysis of the performance of the proposed adaptive precoding approaches. We consider an analysis in terms of the sum-rate and computational complexity.

5.3.1 Achievable Sum-Rate Analysis

Note that the AMB precoding regularizes the inversion by a regularization factor, which is inversely proportional to the SNR operating point of the downlink. Therefore, in the high SNR regime the regularization factor approaches zero, and consequently the MMSE based precoding method converges to the ZF based precoding and therefore exhibits a similar sum-rate [LL11, SLL09b]. However, in the low SNR regime, we expect an achievable sum-rate in favor of AMB precoding outperforming the AZB solution due to the fact that the regularization factor mitigates the degradation caused by the noise term. Unlike fixed precoding based conventional methods, i.e. ZF-BD and MMSE-BD, the proposed adaptive MMSE based precoding scheme calculates a set of precoding matrices (precoding diversity) for the kth CU and therefore exhibits a MUI diversity at each CU. Intuitively speaking, precoding diversity likely improves the SNR and the spectral efficiency gains of the CUs. Furthermore, we emphasize that those gains grow proportionally in terms of the number of antennas per CU because of the antenna coordination at the receiver. To calculate the maximum SNR and achievable sum-rate of the proposed schemes, we count on the output signal of the kth CU receive filter considering the optimal pair

$\mathbf{F}_k(\hat{d}), \mathbf{W}_k(\hat{d})$ obtained from (5.19) as

$$\tilde{\mathbf{y}}_k = \mathbf{W}_k(\hat{d})\mathbf{H}_k\mathbf{F}_k(\hat{d})\mathbf{s}_k + \mathbf{W}_k(d)\mathbf{H}_k\sum_{j=1,j\neq k}^{K}\mathbf{F}_j(\hat{d})\mathbf{s}_j + \mathbf{W}_k(\hat{d})\mathbf{n}_k \tag{5.29}$$

By substituting (5.8), (5.16), and (5.28) in (5.29), we get

$$\tilde{\mathbf{y}}_k^{\text{AZB}} = \check{\mathbf{\Lambda}}_k(\hat{d})\left(\mathbf{P}_k^{\text{ZB}}\right)^{\frac{1}{2}}\mathbf{s}_k + \check{\mathbf{U}}_k(\hat{d})^H\tilde{\mathbf{H}}_k\sum_{j=1,j\neq k}^{K}\mathbf{F}_j(\hat{d})\mathbf{s}_j + \check{\mathbf{U}}_k(\hat{d})^H\tilde{\mathbf{n}}_k \tag{5.30}$$

$$\tilde{\mathbf{y}}_k^{\text{AMB}} = \check{\mathbf{\Lambda}}_k(\hat{d})\mathbf{s}_k + \check{\mathbf{U}}_k(\hat{d})^H\tilde{\mathbf{H}}_k\sum_{j=1,j\neq k}^{K}\mathbf{F}_j(\hat{d})\mathbf{s}_j + \check{\mathbf{U}}_k(\hat{d})^H\tilde{\mathbf{n}}_k \tag{5.31}$$

It is worth noting that the statistical characteristics of $\tilde{\mathbf{n}}_k$ do not change when multiplied by a unitary matrix $\mathbf{U}_k^H$. Therefore, the maximum achievable sum-rate of the proposed AZB and AMB precoding schemes can be expressed, respectively, as follows:

$$R_{\text{AZB}} = \sum_{k=1}^{K}\sum_{i=1}^{N_c}\log_2\left(1+\frac{\check{\Lambda}_{k,i}(\hat{d})^2P_{k,i}^{\text{ZB}}}{1+\sum\limits_{j=1,j\neq k}^{K}\left\|\mathbf{w}_{k,i}(\hat{d})\mathbf{H}_k\mathbf{F}_j(\hat{d})\right\|^2}\right) \tag{5.32}$$

$$R_{\text{AMB}} = \sum_{k=1}^{K}\sum_{i=1}^{N_c}\log_2\left(1+\frac{\check{\Lambda}_{k,i}^2(\hat{d})}{1+\sum\limits_{j=1,j\neq k}^{K}\left\|\mathbf{w}_{k,i}(\hat{d})\mathbf{H}_k\mathbf{F}_j(\hat{d})\right\|^2}\right) \tag{5.33}$$

where $\check{\Lambda}_{k,i}(\hat{d})$ and $P_{k,i}^{\text{ZB}}$ refer to the ith diagonal element of $\check{\mathbf{\Lambda}}_k(\hat{d})$ and $\mathbf{P}_k^{\text{ZB}}$, respectively. $\mathbf{w}_{k,i}(\hat{d})$ is the ith row vector of $\mathbf{W}_k(\hat{d})$.

5.3.2 Computational Complexity Analysis

In this section, we present an analysis of the computational complexity of the proposed method. Relying on the floating point operations (FLOPS) stated in [GL96, SLL09b, ZdLH13], the FLOPS of the required matrix operations are described as follows:

- Multiplication of $m \times n$ by $n \times p$ complex matrices: $8mnp - 2mp$
- QR decomposition of an $m \times n (m \leq n)$ complex matrix: $16(n^2m - nm^2 + \frac{1}{3}m^3)$

- SVD of an $m \times n (m \leq n)$ complex matrix where only $\mathbf{\Lambda}$ and $\mathbf{V}$ are obtained: $32(nm^2 + 2m^3)$
- SVD of an $m \times n (m \leq n)$ complex matrix where $\mathbf{U}, \mathbf{\Lambda}$, and $\mathbf{V}$ are obtained: $8(4n^2m + 8nm^2 + 9m^3)$
- Inversion of an $m \times m$ matrix using Gauss-Jordan elimination: $\frac{4}{3}m^3$
- Hadamard product of $m \times n$ real and $m \times n$ complex matrices: mn

We illustrate the required FLOPS for the proposed adaptive linear precoding techniques AZB-SC, AZB-CPC, and AMB in Tables 5.3, 5.4, 5.5, respectively.

Table 5.3: Computational complexity of AZB-SC

Steps	Operations	FLOPS $\times(\lvert\mathcal{D}\rvert = \mathcal{R}_k + 1)$
1	SVD of $\bar{\mathbf{H}}_k$	$32K(N_{CB}\mathcal{R}_k^2 + 2\mathcal{R}_k^3)/\lvert\mathcal{D}\rvert$
2	$\tilde{\mathbf{H}}_k \bar{\mathbf{H}}_k^{(d)}$	$K(8N_c^2 N_{CB} + 8N_c N_{CB} d - 2N_c^2 - 2N_c d)$
3	SVD of $\tilde{\mathbf{H}}_k \bar{\mathbf{H}}_k^{(d)}$	$8K(18N_c^3 + 10N_c^2 d + N_c d^2)$
4	Calculation of $\mathbf{P}_k^{\text{ZB}}$	$6KnN_c/\lvert\mathcal{D}\rvert$

Table 5.4: Computational complexity of AZB-CPC

Steps	Operations	FLOPS $\times(\lvert\mathcal{D}\rvert = 2^{\mathcal{R}_k} - 1)$
1	$\mathbf{M}_k^{(d)} \odot \bar{\mathbf{H}}_k$	$K\mathcal{R}_k N_{CB}$
2	SVD of $\tilde{\mathbf{H}}_k(d)$	$32K(N_{CB}\mathcal{R}_k^2 + 2\mathcal{R}_k^3)$
3	$\tilde{\mathbf{H}}_k \tilde{\mathbf{H}}_k^{(0)}(d)$	$K(8N_c^2 N_{CB} - 2N_c^2)$
4	SVD of $\tilde{\mathbf{H}}_k \tilde{\mathbf{H}}_k^{(0)}(d)$	$8K(21N_c^3)$
5	Calculation of $\mathbf{P}_k^{\text{ZB}}$	$6KnN_c/\lvert\mathcal{D}\rvert$

Note that the computational complexity primarily counts on the system antenna configuration. For instance the CR configurations $8 \times (3,3)$ and $8 \times (2,2,2)$ for a given PR configuration

Table 5.5: Computational complexity of AMB

Steps	Operations	FLOPS $\times(\lvert\mathcal{D}\rvert = 2^{N_r} - 1)$
1	$\mathbf{M}^{(d)} \odot \underline{\tilde{\mathbf{H}}}$	$N_r N_{CB}$
2	$\underline{\hat{\mathbf{F}}}(d)$	$\frac{4}{3}N_{CB}^3 + N_{CB}(2-2N_r) + N_{CB}^2(24N_r + 8N_p - 6)$
3	QR of $\hat{\mathbf{F}}_k(d)$	$16K(N_{CB}^2 N_c - N_c^2 N_{CB} + \frac{1}{3}N_c^3)$
4	Calculation of $\mathbf{P}_k^{\text{AMB}}(d)$	$K\{N_c^3(\frac{28}{3}+8) + N_c^2(16N_{CB}-7) + N_c(16N_{CB}^2 - 4N_{CB} + 1$ $+8N_{CB}^2/\lvert\mathcal{D}\rvert) - 2N_{CB}^2/\lvert\mathcal{D}\rvert\}$
5	$\tilde{\mathbf{H}}_k \mathbf{Q}_k(d) \mathbf{P}_k^{\text{AMB}}(d)$	$8KN_c^3 + KN_c^2(8N_{CB} - 4)$
6	SVD of $\tilde{\mathbf{H}}_k \mathbf{Q}_k(d) \mathbf{P}_k^{\text{AMB}}(d)$	$8K(21N_c^3)$

2×2, although they have a similar N_r, present different complexity and performance due to the contrast in K and $\mathcal{R}_k$. The best selection of antenna configuration can be a capacity-complexity trade-off as will be demonstrated in the simulation results.

5.4 Simulation Results

5.4.1 Channel Model and System Configuration

In the simulations, we conduct experiments for a multiuser MIMO CR based broadcast channel model suffering from Rayleigh flat fading. The elements of the channels of the cognitive links $\mathbf{H}_k, \forall k$ and the interference link $\mathbf{G}$ are generated as i.i.d random variables as described in the statistical channel model described in section 2.5 in which the path loss, shadowing, and Rayleigh-distributed multipath fading are combined. The channel parameters are configured as follows. We assume a normalized free space loss, i.e. $\mathrm{Z}_0 = 1$, $\gamma = 2$, shadowing variance $\sigma^2_{S(dB)} = 0$, and Rayleigh multipath fading variance $\sigma_m^2 = 1$.

The SNR of the PU link is defined as $\text{SNR}_{PR} = P_{PB}/\sigma_n^2$, and the CUs link as $\text{SNR}_{CR} = P_T/\sigma_n^2$ with noise variance $\sigma_n^2 = 1$.

The CR link is configured as $14\times(4,4,4)$, i.e. three CUs with $N_c = 4$, and the PR link as 2×2 unless otherwise stated.

5.4.2 Example 1: Comparison of the Achievable Sum-Rates

In this section, simulations are conducted for six different precoders including the proposed techniques as illustrated in Figure 5.2. The comparable precoder successive MMSE (SMMSE) described in [LLHL08] is modified to fit CR requirement. Generally speaking, Figure 5.2 demonstrates that the proposed adaptive precoders outperform the conventional precoders in the low and moderate SNR regions which are of practical importance. Also, it exhibits the superiority of the AMB precoder with achievable spectral efficiency gain of 5 bps/Hz at $\text{SNR}_{CR} = 5$ dB and a SNR gain about 3 dB at a spectral efficiency of 10 bps/Hz. Furthermore, it shows that employing a larger number of antenna per CU improves the sum-rate as a consequence for the antenna coordination at the receiver. From another perspective, setting more antennas per CU causes a bigger capacity gap between the proposed AMB precoder and the conventional schemes and, however, smaller gap toward the AZB precoder curves.

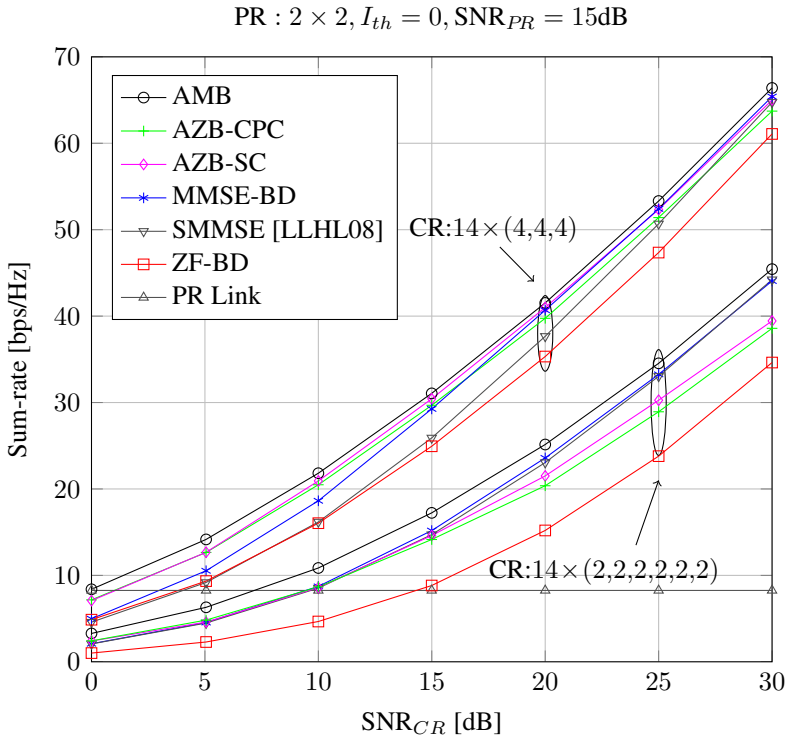

Figure 5.2: Sum-rate versus SNR_{CR} for two antenna configurations

5.4.3 Example 2: Effect of the Whitening Process and Primary SNR on the CR Sum-Rate

In this example, an illustration is presented about the effect of the whitening process on the sum-rate of a CR link configured as $14\times(2,2,2,2,2,2)$ at the operating point $\text{SNR}_{PR} = 5$ dB. As mentioned in the system model, the whitening process reduces the effect of the interference produced by the PR-BS and received by the CUs enhancing the CR sum-rate. Figure 5.3 verifies this fact for which the whitening process takes the advantage of the PR-BS interference to improve the SNR. Note that a small SNR_{PR} produces small PR sum-rate and little PR-BS interference causing little improvement for the whitened CR sum-rate over the non-whitened. Non-whitening can be implemented by setting $\mathbf{\Gamma}_k, \forall k$ as identity matrix. Moreover, it is worth to note that the proposed AMB precoder can achieve a spectral efficiency gain up to 3 bps/Hz in the high SNR region when the number of the antennas per CU decreases whether with or without whitening process.

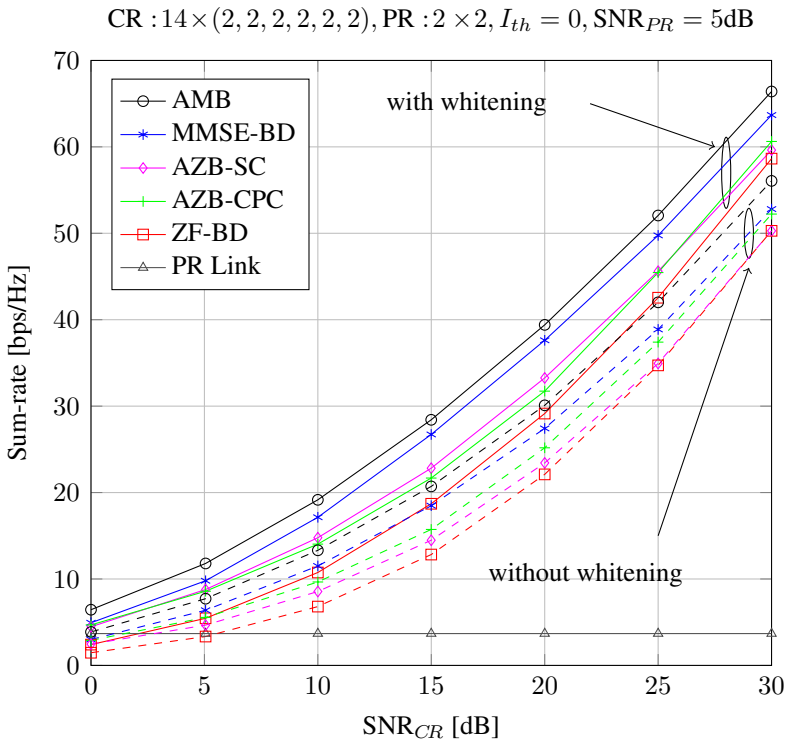

Figure 5.3: Effect of the whitening process on sum-rate

5.4.4 Degree of Freedom and Complexity Analysis

In this example, we present an illustration on the precoding DoF diversity and its influence on the capacity and complexity of the proposed AMB precoder. Concerning the capacity aspect, Figure 5.4 exhibits an instantaneous CR sum-rate conducted at $\text{SNR}_{CR} = 25$ dB in terms for the dth index of DoF, $\forall d \in \mathcal{D}$. It illustrates that the DoF diversity causes MUI and PUI diversities. Furthermore, it demonstrates that the optimal DoF selected for the AMB precoder meets the PUI constraint while achieving a spectral efficiency gain.

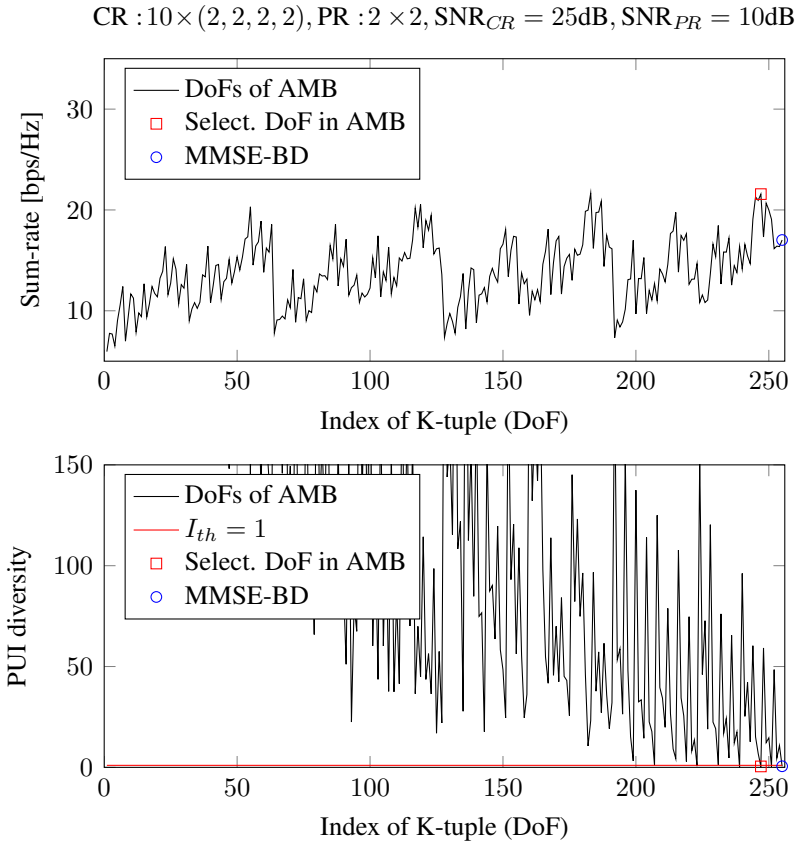

Figure 5.4: Effect of the DoF diversity on the sum-rate

Regarding to the complexity aspect, the antenna configuration and number of CUs K to be served both affect the number of the required FLOPS. Figure 5.5 and Figure 5.6 exhibits the number of FLOPS as a function of K and N_c, respectively. It shows that the proposed AZB-SC scheme is the least complex as it has linear complexity, but both AMB and AZB-CPC schemes are expensive computationally as they have exponential complexities. It is also obvious that the growth of N_c increases the complexities more than the growth of K.

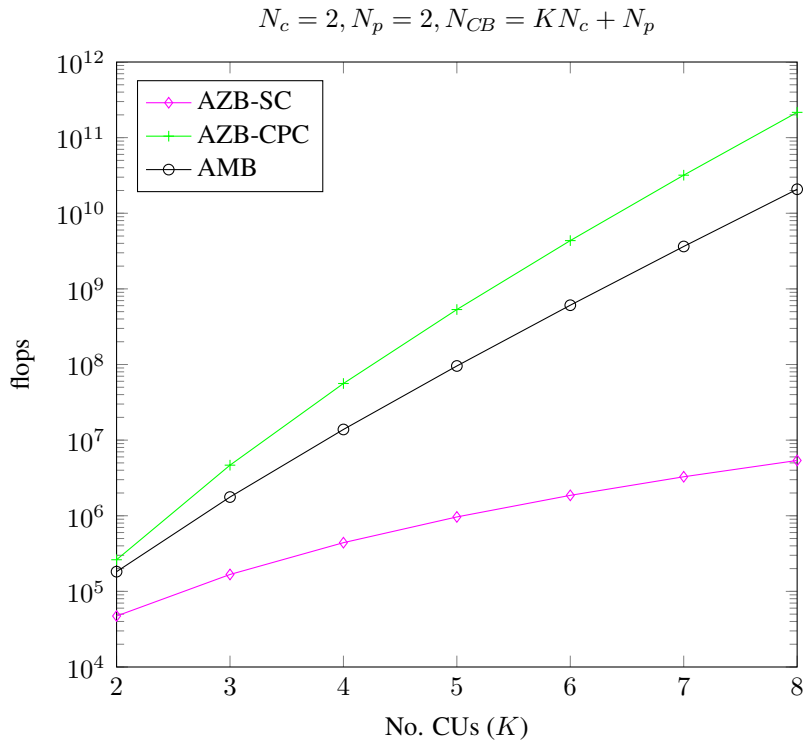

Figure 5.5: Effect of the DoF diversity on the complexity for fixed N_c

5.5 Chapter Summary

In this chapter, we have developed a non-iterative linear adaptive MMSE based precoder dubbed "AMB" suitable for multiuser MIMO CR based broadcasting. The proposed AMB precoder employs our developed conception so-called precoding diversity in which the multiple antenna structure is better utilized compared to conventional precoders. We have also extended the conventional ZF based precoding approach into an adaptive precoding dubbed "AZB" exploiting precoding diversity. Roughly speaking, the proposed AMB precoder resolves notable spectral and SNR gains over the state-of-the-art and the AZB precoder in the SNR region of interest: The low SNR region. In the high SNR region, the AMB precoder is characterized by an increment of spectral efficiency gain when the number of antennas per CU decreases. Unlike non-linear iterative precoders, the proposed precoders are linear non-iterative and therefore provide less complexity along with a spectral efficiency achievement. The degrees of freedom of the proposed AMB precoder can be handled independently by parallel computing. The characteristics of our proposed precoder make it a candidate for future mobile CR networks.

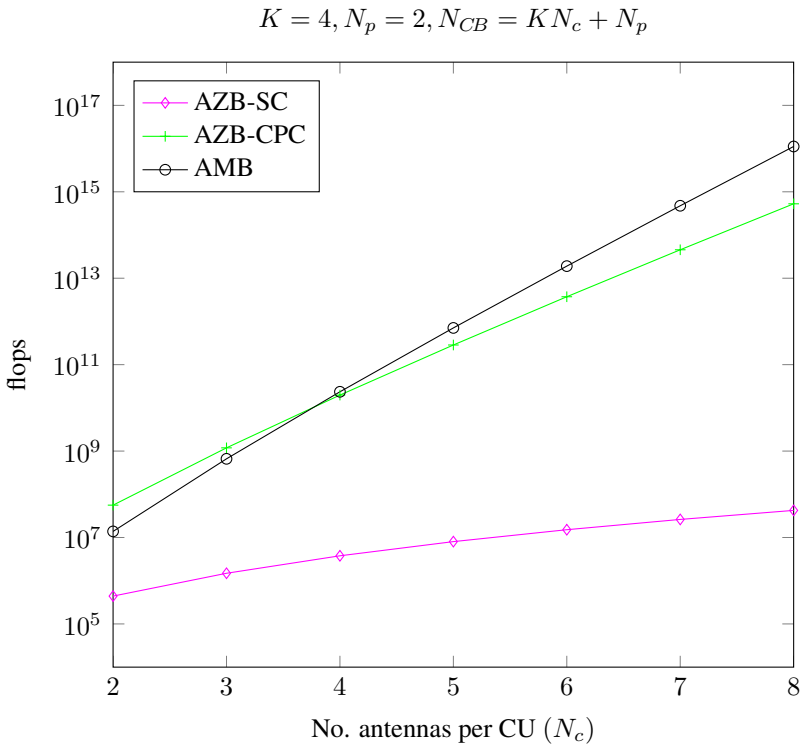

Figure 5.6: Effect of the DoF diversity on the complexity for fixed K

6

Conclusions and Outlook

6.1 Conclusions

In this thesis, we have developed efficient RA and precoding schemes for both multiuser MIMO-OFDM and multiuser MIMO based CR networks. In the context of the multiuser MIMO-OFDM CR network, we have developed RA and adaptive precoding schemes for both the DL and UL. The proposed schemes are characterized by both computational and spectral efficiencies. The adaptive precoder operates based on generating countable degrees of freedom by combining the spaces of the block interference channel. The RA has been formulated as a sum-rate maximization problem subject to total power and PUI constraints. The variables of the problem were matrix of the precoding and integer indicator of the subcarrier mapping. Since the formulated optimization problem is a mixed integer having a combinatorial complexity which is hard to solve, we separated it into a two-phase procedure to elaborate computational efficiency: Adaptive precoding (DoF assignment) and subcarrier mapping.

From the implementation perspective, the RA of the DL is central based processing, but the UL is semi-distributed based. Central RA task has been solved to maintain central adaptive

precoding and subcarrier mapping for both the DL and UL. The subcarrier mapping has been performed by optimal and efficient method for the DL as the problem is modeled as convex. But, it is characterized by near-optimality for the UL despite the convexity due to the per-user resource constraints of the UL problem. The DL problem has been solved by using the Lagrangian multiplier theory which is regarded as an efficient alternative methodology compared to the convex optimization theory. The solution is not only characterized by low-complexity, but also by optimality. Concerning the UL, the distributive RA task is necessary to resolve the power allocation of the UL. However, the distributive RA processing can be an option for the DL to provide more degrees of freedom in the adaptive precoding on the user level design. The prominent advantages of the semi-distributed scheme in the UL are the provided computational and spectral efficiencies. Moreover, such scheme also leads to a small data overhead and helps simplify the terminal structure. Numerical simulations illustrated remarkable spectral and SNR gains provided by the proposed scheme. In addition, it demonstrated robustness against the tight and relaxed transmission conditions, i.e. interference constraints. Therefore, the proposed schemes enable larger communication range for underlay CR networks.

We have also developed a non-iterative linear adaptive MMSE block diagonalization based precoder "AMB" for multiuser MIMO CR based broadcasting. The proposed AMB precoder employs the proposed DoF concept which we call it here *precoding diversity*. In this context, DoFs of the proposed precoder are generated by space combining and channel path combining methods. We have also extended the conventional ZF block diagonalization based precoding approach into an adaptive precoding "AZB" using our precoding diversity concept. Roughly speaking, the proposed AMB precoder illustrated a notable spectral and SNR gains over the conventional and the AZB precoders in the SNR region of interest: The low SNR region. Unlike non-linear iterative precoders, the proposed precoders are linear non-iterative and therefore provide low-complexity along with a spectral efficiency achievement. The extra complexity provided by the proposed precoders is an indispensable price for the gained spectral efficiency compared to the state-of-the-art linear precoders. More specifically, the antenna configuration affects the complexity of both AMB and AZB precoders, which is designed according to the capacity-complexity trade-off. The growth in complexity of the proposed AMB and AZB precoders is exponential with order $\mathcal{O}(2^{\mathcal{R}_k})$. Since the high complexity is a major limiting factor w.r.t tractability, we address it by the following reduction aspects

- Parallel Computing: Since the DoFs of the precoders AMB and AZB-CPC can be computed independently, the parallel computing is an option for complexity reduction with investment in the hardware part. This aspect is not applicable in non-linear DPC based

schemes as they are serial based precoders despite the high spectral efficiency they can provide.

- Exponential complexity breaking: Another practical solution for reducing the complexity is to break the exponential complexity. Intuitively, the multiuser MIMO broadcasting scenario produces higher spectral efficiency than the single-user MIMO scenario. From this observation, the size of DoF set can be reduced and confined to those DoFs that take all CUs into account. In other words, at least one channel path from each CU should be considered in each DoF of the AMB precoder. The DoFs that skip some CUs harm the spectral efficiency as those excluded CUs have no interference control mechanism, and thus it is likely they introduce severe MUI at other users. Expectations of complexity reduction can be up to 80% based on the number of antenna per CU. Hence, that improves the practicality of the proposed adaptive precoders.

- SVD Replacement: Concerning the AZB-CPC, replacing the SVDs by QR decompositions, as in [ZdLH13], is another aspect for complexity reduction.

Taking complexity reduction aspects into considerations, the characteristics of our proposed precoder make it a candidate for future mobile CR networks.

6.2 Outlook

In the work of this thesis, the inter-cell interference was not considered in the proposed adaptive precoding and resource allocation schemes. This assumption does not make sense in realistic cellular systems due to the fact that cell-edge users experience strong path loss and inter-cell interference. Therefore, the proposed precoding and power allocation solutions in this thesis are not sufficient to address the poor performance of the cell-edge user, however they can be seen as a step toward that goal. Extension of this work by considering smart cooperation, heterogeneous networking, and inter-node coordination scenario(s) is an advantage to address the poor conditions experienced by cell-edge users and to further improve the capacity. In particular, relaying not only improves the coverage range of the cell, but additionally reduces the interference at cell edges by reducing the transmit power over a smaller range. In inter-node coordinations, neighbor base stations are grouped into clusters such that each cluster coordinate the transmission directed to the cell-edge user in order to avoid the inter-cell interference. Despite the benefits of the inter-node coordination, the inter-cluster interference is still problematic. State-of-the-art precoders such as those proposed in this thesis along with wise relaying

and scheduled coordination schemes can play a role to have a strategic solution for the problem.

One interesting application for our proposed precoding is the simultaneous transmission reception which is proposed for the upcoming 5G networks according to [4G 14]. In this scheme, both UL and DL transmissions are performed simultaneously on the same physical radio resource such that they interfere each other. Interference cancellation is a candidate technique to address it, but it brings no performance when the received signals are weak compared to the strong transmitted signals. In this context, such kind of self-interference can be managed by engaging the spatial division multiplexing and interference management which have been used in the proposed precoding schemes in this thesis.

The proposed adaptive precoding in this work has been established upon the concept of precoding diversity which is based on DoFs. In fact, using such kind of processing may not be computationally efficient in case of being developed into massive MIMO with tens or hundreds of antennas. Toward the compatibility with massive MIMO, it is better to design an efficient paradigm for the adaptive precoding without DoFs. Such design is possible in the context of multiuser MIMO-OFDM CR scenario by finding the optimal precoding via direct derivation from the cost function of the problem. That implies using Lagrange multiplier and convex optimization theories for solving the problem away from the ZF and MMSE criteria.

A

Abbreviations and Acronyms

1G	First Generation
1xEV-DO	1x Evolution Data-Optimized
2G	Second Generation
2.5G	2.5 Generation
2.75G	2.75 Generation
3G	Third Generation
3.5G	3.5 Generation
3GPP	3rd Generation Partnership Project
4G	Fourth Generation
5G	Fifth Generation
AMB	Adaptive MMSE Block Diagonalization
AMPS	Advanced Mobile Phone System
APA	Adaptive Precoding with an initial (Approximate) subcarrier allocation
AWGN	Additive White Gaussian Noise
AZB	Adaptive ZF Block Diagonalization

AZB-CPC	AZB with Channel Path Combining
AZB-SC	AZB with Subspace Combining
BC	Broadcast Channel
CDMA	Code Division Multiple Access
CR	Cognitive Radio
CR-BS	CR Base Station
CSCG	Circular Symmetric Complex Gaussian
CSI	Channel State Information
CU	CR User
DFT	Discrete Fourier Transform
DL	Downlink
DoF	Degree of Freedom
DPC	Dirty paper coding
EDGE	Enhanced Data Rates for GSM Evolution
EPA	Equal Power allocation with Adaptive precoding
ETSI	European Telecommunication Standards Institute
FCC	Federal Communication Commission
FDMA	Frequency Division Multiple Access
FOMA	Freedom of Mobile Multimedia Access
GPRS	General Packet Radio Service
GSM	Global System for Mobile Communications
HEW	High-Efficiency WLAN
HPT	Hybrid Precoding with Transmit power control
HSD/UPA	High Speed Downlink/Uplink Packet Access
IEEE	Institute of Electrical and Electronics Engineers
i.i.d.	Independent and identically distributed
IMT-2000	International Mobile Telecommunications-2000
IS-95	Interim Standard 95
IS-136	Interim Standard 136
ISI	Inter-Symbol Interference
ITU	International Telecommunication Union
KKT	Karush-Kuhn-Tucker
LTE	Long Term Evolution
LTE-A	LTE-Advanced

MAC	Multiple Access Channel
MIMO	Multiple-Input Multiple-Output
MMSE	Minimum Mean Square Error
MMSE-BD	MMSE Block Diagonalization
MSE	Mean Square Error
MRT	Maximum Ratio Transmission
MUI	Multiuser Interference
NGMN	Next Generation Mobile Networks
NMT	Nordic Mobile Telephones
NNT	Nippon Telephone and Telegraph
OFDM	Orthogonal Frequency Division Multiplexing
OFDMA	Orthogonal Frequency Division Multiple Access
PL	Path Loss
PR	Primary Radio
PR-BS	PR Base Station
PU	PR User
PUI	PU Interference
PRL	PU Rate Loss
QoS	Quality-of-Service
RA	Resource Allocation
RRM	Radio Resource Management
SC-FDMA	Single Carrier FDMA
SDMA	Spatial Division Multiple Access
SDR	Software-Defined Radio
SINR	Signal-to-Interference-plus-Noise Ratio
SMMSE	Successive MMSE
SNR	Signal-to-Noise Ratio
SPT	SVD Precoding with Transmit Power control
SVD	Singular Value Decomposition
TACS	Total Access Communication Systems
TDD	Time-Division Duplexing
TDMA	Time Division Multiple Access
UL	Uplink
UMTS	Universal Mobile Telecommunication System

WCDMA	Wideband CDMA
WF	Waterfilling
WiMAX	Worldwide Interoperability for Microwave Access
WLAN	Wireless Local Area Network
WRAN	Wireless Regional Area Networks
ZF	Zero-Forcing
ZF-BD	ZF Block Diagonalization
ZP	Zero-Forcing Precoding

B

Notation

Conventions

Matrices and vectors are denoted by boldface capital and small letters, respectively. Determinant, rank, and trace of a matrix are written as $|.|$, Rank(.), and Tr(.), respectively. $(.)^T$ and $(.)^H$ are the transpose and conjugate transpose, respectively. Inverse of a square matrix is written as $(.)^{-1}$. blkd$(\mathbf{A}_1 \dots \mathbf{A}_M)$ represents the block diagonal matrix with diagonal matrices given by the set $\{\mathbf{A}_1, \dots, \mathbf{A}_M\}$ and zero off-diagonal elements. diag$(\mathbf{x})$ denotes a diagonal matrix with diagonal elements given by the vector $\mathbf{x}$.

Unless otherwise stated, whitened parameters, projected entities, complementary elements, and hard/optimized decisions are marked by $\tilde{(.)}$, $\bar{(.)}$, $\check{(.)}$, and $\hat{(.)}$. Block parameters are marked by $\underline{(.)}$.

Specific Sets

$\mathbb{C}$	Complex numbers
$\mathbb{C}^n$	Complex n-vectors

$\mathbb{C}^{m\times n}$	Complex $m \times n$ matrices
$\mathbb{R}$	Real numbers
$\mathbb{R}^n$	Real n-vectors
$\mathbb{R}^{m\times n}$	Real $m \times n$ matrices
$\mathbb{R}_{++}$	Positive real numbers
$\mathbb{S}^n_{++}$	Symmetric positive definite $n \times n$ matrices

Operations on Scalars, Vectors, and Matrices

$\odot$	Hadamard product of two matrices
${}^mC_n$	Binomial coefficient $\left(= \frac{m!}{(m-n)!n!}\right)$
$[x]^+$	Semi-definite operator $(= \max(x, 0))$
$(.)^T$	Transposed of a vector or a matrix
$(.)^H$	Conjugate transposed of a vector or matrix $(.)^H = ((.)^*)^T = \left((.)^T\right)^*$
diag($\mathbf{x}$)	Diagonal matrix with diagonal elements given by the vector $\mathbf{x}$
$\mathbf{X}^{-1}$	Inverse of a square matrix $\mathbf{X}$
$\mathbb{E}\{.\}$	Expectation operator
$\|.\|$	Euclidean norm
blkd($\mathbf{A}_1 \dots \mathbf{A}_M$)	Block diagonal matrix with diagonal matrices given by the set $\{\mathbf{A}_1, \dots, \mathbf{A}_M\}$
$\mathcal{CN}(\mathbf{x}, N_o\mathbf{I})$	Complex Gaussian circular symmetric distribution with mean vector $\mathbf{x}$ and covariance matrix $N_o\mathbf{I}$

List of Variables

Variables Used for Channel Modeling (Chapter 2)

d_0	Reference distance
$distance$	Destination distance
γ	Path loss exponent
λ	Wavelength
P_r	Receive power
P_t	Transmit power
$\psi_{\text{S(dB)}}$	Log mean of shadowing component
Z_0	Free space path loss

Z_{m}	Multipath component
$Z_{m,I}$	In-phase component of multipath
$Z_{m,Q}$	Quadrature component of multipath
Z_{PL}	Path loss component
$Z_{S(dB)}$	Shadowing component

General Variables (Chapter 3)

$\mathbf{0}_{m\times n}$	All-zero matrix of $m \times n$ dimensions
β	Power normalization parameter
$\mathbf{F}_k$	Precoding matrix of the kth CU
$\underline{\hat{\mathbf{F}}}$	Block that stacks the pre-precoding matrices of all CUs
$\mathbf{G}$	MIMO channel coefficients of the link CR base station-to-PU
$\mathbf{G}^{\perp}$	Null space of $\mathbf{G}$
γ	Scaling factor for the received vector in the MMSE precoding scheme
$\mathbf{H}_k$	MIMO channel coefficients of the kth CU
$\bar{\mathbf{H}}_k$	Complementary interference channel of the kth CU
$\bar{\mathbf{H}}_k^{(0)}$	Null space of $\bar{\mathbf{H}}_k$
$\underline{\hat{\mathbf{H}}}$	Channel block that stacks MIMO channels of all CUs
I_{th}	Interference threshold at PU
$\mathbf{I}_n$	$n \times n$ identity matrix
K	Count of served CUs
$\mathbf{\Lambda}_k$	Diagonal matrix containing eigenvalues of the kth CU channel $\mathbf{H}_k$
μ	Positive number connected to Lagrange multipliers of the MMSE optimization constraints
N_c	Number of antennas at each CU
N_{CB}	Number of antennas at CR base station
N_p	Number of antennas at PU
$\mathbf{P}_k$	Diagonal power matrix of the kth CU
$\mathbf{P}_k^{\text{MB}}$	MMSE transmit combining matrix of CU k (i.e. voltage matrix but the power matrix is $\mathbf{P}_k^{\text{MB}}(\mathbf{P}_k^{\text{MB}})^H$)
P_T	Total transmit power of CR base station
$\mathbf{Q}_k$	Unitary matrix resulted from QR decomposition for the kth CU pre-precoding matrix

$\mathbf{R}_k$	Upper triangular matrix resulted from QR decomposition for the kth CU pre-precoding matrix
$\mathbf{S}_k$	Covariance matrix of the kth CU
$\mathbf{U}_k$	Left unitary matrix for the kth CU resulted from SVD
$\mathbf{V}_k$	Right unitary matrix for the kth CU resulted from SVD

Variables Used for MIMO-OFDM System Modeling (Chapter 4)

α_l	Temperature parameter of PU l
C_D^{opt}	Optimal channel capacity of the DL
C_U^{opt}	Optimal channel capacity of the UL
d	Index of the dth DoF in the adaptive precoding
$\mathcal{D}$	DoF index set
$\boldsymbol{\delta}_D$	Lagrangian multipliers for PUI constraint (*C2*) of the DL
$\mathcal{F}_D$	The overall DoF set of the DL
$\mathbf{F}_{D,k,i}^{(d)}$	The dth DoF of the adaptive precoder at the CR-BS transmitter toward CU k on subcarrier i
$\mathbf{F}_{l,i}$	SVD precoder at PR-BS transmitter toward PU l on subcarrier i
$\mathbf{F}_{U,k,i}^{(d)}$	The dth DoF of the adaptive precoder at terminal transmitter of CU k on subcarrier i
$\mathbf{G}_{D,l,i}$	Channel matrix of the cross downlink (CR-BS-to-PU) toward PU l on subcarrier i
$\mathbf{G}_{U,l,k,i}$	Channel matrix of the cross uplink from CU k toward PU l on subcarrier i
$\mathbf{\Gamma}_{D,k,i}$	Coefficients of whitening filter at the terminal receiver of CU k on subcarrier i
$\mathbf{\Gamma}_{U,k,i}$	Coefficients of whitening filter at the CR-BS receiver for CU k on subcarrier i
$\mathcal{G}_D$	Lagrangian dual function of the DL
$\mathbf{H}_{D,k,i}$	Channel matrix of the cognitive downlink (CR-BS-to-CU) for CU k on subcarrier i
$\mathbf{H}_{U,k,i}$	Channel matrix of the cognitive uplink (CU-to-CR-BS) for CU k on subcarrier i
I_l^{th}	PUI threshold at the lth PU
$\mathbf{I}_{l,i}^{th}$	PUI diagonal matrix

K	Count of served CUs
$\mathcal{K}$	Set containing all CUs
$\mathcal{L}_D$	Lagrangian function of the DL
L	Count of served PUs
λ_j	The jth singular value of $\mathbf{G}_{D,l,i}$
$\Lambda_{j,l}$	The jth singular value of $\mathbf{T}_{l,i}$
M	Number of OFDM tones
$\mathcal{M}$	Set containing all OFDM tones
μ_D	Lagrangian multiplier for transmit power constraint (*C1*) of the DL
$\mathbf{n}_{k,i}$	noise vector for CU k at terminal/CR-BS receiver on subcarrier i
N_c	Number of antennas of each CU
N_{CB}	Number of antennas of the CR-BS
N_p	Number of antennas of each PU
N_{PB}	Number of antennas of PR-BS
$\mathbf{\Omega}_{D,k,i}^{(d)}$	Effective interfering channel power CR-BS-to-PU for DoF d on subcarrier i allocated to CU k
$P_{D,th}^{(d,d-1)}$	Precoding-threshold between the DoFs d and $d-1$ for the DL
P_k	Power budget of the kth CU
P_T	Transmit power of the CR-BS
$\mathbf{P}_{D,k,i}$	Diagonal transmit power matrix of the cognitive downlink toward CU k on subcarrier i
$\mathbf{P}_{l,i}$	Diagonal transmit power matrix on the PR link towards PU l on subcarrier i
$\mathbf{P}_{U,k,i}$	Diagonal transmit power matrix of the cognitive uplink between CU k on subcarrier i
PRL_l	The lth PU rate loss
$\mathbf{\Psi}_D$	Lagrangian multipliers for the semi-definite power constraint (*C5*) of the DL
r_k	Data rate of the kth CU
$\mathcal{R}$	Rank of the matrix $\mathbf{G}_{D,l,i}$
ρ	Multiplexing indicator of binary value
$\mathbf{s}_{D,k,i}$	Transmit data vector on the cognitive downlink toward CU k on subcarrier i
$\mathbf{s}_{l,i}$	Transmit data vector on the PR link towards PU l on subcarrier i

$\mathbf{s}_{U,k,i}$	Transmit data vector on the cognitive uplink from CU k on subcarrier i
$\mathcal{S}_k$	Subcarrier set allocated to the kth CU
$\mathcal{S}_l$	Subcarrier set occupied by the lth PU
$\mathbf{T}_{l,i}$	Channel matrix of the PR-BS-to-PU link towards PU l on subcarrier i
τ_D	Time sharing weight of CR downlink
τ_U	Time sharing weight of CR uplink
$\theta_{k,i}^{(d)}$	Subcarrier mapping indicator of binary value
$\mathbf{V}_{D,l,i}^{(d)}$	The spaces of the dth DoF obtained from $\mathbf{G}_{D,l,i}$
$\mathbf{W}_{D,k,i}$	Post-coding filter at the terminal receiver of CU k on subcarrier i
$\mathbf{W}_{U,k,i}$	Post-coding filter at the CR-BS receiver for CU k on subcarrier i
$\mathbf{y}_{D,k,i}$	Received vector at kth CU terminal on subcarrier i for the DL
$\mathbf{y}_{PR}$	Received vector at the PR users
$\mathbf{Z}_{k,i}$	Channel matrix of the PR-BS-to-CU link towards CU k on subcarrier i
$\boldsymbol{\zeta}_D$	Lagrangian multipliers for OFDMA constraint (*C4*) of the DL

Variables Used for System Modeling (Chapter 5)

$\mathbf{0}$	Column vector of all-zero elements
$\mathbf{1}$	Column vector of all-one elements
β	Power normalization parameter
$\mathcal{D}$	DoF index set of the adaptive precoding scheme
$\mathbf{F}_k$	Precoding matrix of the kth CU
$\mathbf{F}_p$	SVD precoder of the PR link
$\mathbf{G}$	Coefficients of the channel between the CR-BS and the PU
$\mathbf{G}^{\perp}$	Null space of $\mathbf{G}$
γ	Scaling factor for the received signal in the MMSE precoding scheme
$\mathbf{\Gamma}_k$	Coefficients of the whitening filter of the kth CU receiver
$\mathbf{H}_k$	Coefficients of the channel between the CR-BS and CU k
$\bar{\mathbf{H}}_k^{(d)}$	The space of the dth DoF in the AZB-SC scheme
$\underline{\hat{\mathbf{H}}}_k^{(0)}$	Null space of the complementary channel $\underline{\hat{\mathbf{H}}}_k$ in the AZB-CPC scheme
I_{th}	Interference threshold at the PU
K	Number of served CUs
$\mathcal{K}$	Set containing all CUs
$\mathbf{\Lambda}_k$	Diagonal matrix containing eigenvalues of the kth CU channel
$\mathbf{M}_k^{(d)}$	Inclusion matrix of the dth DoF for the kth CU

μ	Positive number connected to Lagrange multipliers of the MMSE optimization constraints
N_c	Number of antennas of each CUs
N_{CB}	Number of antenna elements of the CR-BS
N_p	Number of antenna elements of the PU
$\mathbf{n}_k$	Noise vector of the kth CU
$\mathbf{n}_p$	Noise vector of the PU
P_T	Transmit power of the CR-BS
$\mathbf{P}_k$	Power matrix of the kth CU
$\mathbf{P}_p$	Power matrix of the PU
$\mathbf{Q}_k$	Unitary matrix resulted from QR decomposition for the kth CU pre-precoding matrix
$\mathcal{R}_k$	Rank of the complementary channel $\bar{\mathbf{H}}_k$
$\mathbf{R}_k$	Upper triangular matrix resulted from QR decomposition for the kth CU pre-precoding matrix
$\mathbf{s}_k$	Data vector of the kth CU
$\mathbf{s}_p$	Data vector of the PU
$\mathbf{T}$	Coefficients of the channel between the PR-BS and PU
$\mathbf{U}_k$	Left unitary matrix for the kth CU resulted from SVD
$\mathbf{V}_k$	Right unitary matrix for the kth CU resulted from SVD
$\mathbf{W}_k$	Post-coding filter at the kth CU receiver
$\mathbf{Z}_k$	Coefficients of the channel between the PR-BS and the kth CU

C

Matrix Calculus

C.1 Hadamard Product

The *Hadamard product* of two $(m \times n)$ matrices $\mathbf{A}$ and $\mathbf{B}$ is the element-wise multiplication which is defined as follows

$$\mathbf{A} \odot \mathbf{B} = \begin{bmatrix} a_{11}b_{11} & \dots & a_{1n}b_{1n} \\ \vdots & \ddots & \vdots \\ a_{m1}b_{m1} & \dots & a_{mn}b_{mn} \end{bmatrix} \tag{C.1}$$

C.2 Cholesky and Singular Value Decompositions

Cholesky Decomposition

If $\mathbf{A} \in \mathbb{C}^{n \times n}$ is Hermitian and positive definite, then it can be decomposed as

$$\mathbf{A} = \mathbf{\Gamma}\mathbf{\Gamma}^H \tag{C.2}$$

where $\mathbf{\Gamma}$ is nonsingular and lower triangular matrix with positive diagonal elements. It is called the *Cholesky decomposition* of $\mathbf{A}$.

Singular Value Decomposition

Assuming $\mathbf{B} \in \mathbb{C}^{m \times n}$ with rank$(\mathbf{B}) = \mathcal{R}$. $\mathbf{B}$ can be factored as [BV04, GL96]

$$\mathbf{B} = \mathbf{U}\mathbf{\Lambda}\mathbf{V}^H \tag{C.3}$$

where $\mathbf{U}$ is a $m \times m$ unitary matrix containing the eigenvectors of $\mathbf{B}\mathbf{B}^H$ and satisfying $\mathbf{U}\mathbf{U}^H = \mathbf{I}_m$. $\mathbf{V}$ is a $n \times n$ unitary matrix containing the eigenvectors of $\mathbf{B}^H\mathbf{B}$ and fulfilling $\mathbf{V}\mathbf{V}^H = \mathbf{I}_n$. $\mathbf{\Lambda}$ is a $m \times n$ diagonal matrix containing the non-negative singular values such that $\mathbf{\Lambda} = \text{diag}(\lambda_1, \ldots, \lambda_{\mathcal{R}})$ with $\lambda_1 \geq \lambda_2 \geq \cdots \geq \lambda_{\mathcal{R}} \geq 0$. The *singular value decomposition* can be written as

$$\mathbf{B} = \sum_{i=1}^{\mathcal{R}} \mathbf{u}_i \boldsymbol{\lambda}_i \mathbf{v}_i^H \tag{C.4}$$

where $\mathbf{u}_i \in \mathbb{C}^m$ are the left singular vectors and $\mathbf{v}_i \in \mathbb{C}^n$ are the right singular vectors.

C.3 Useful Rules and Properties

Some useful rules and properties concerning trace, determinant, inverse, and derivatives follow [PP12]

Trace

$$\begin{aligned}
\text{Tr}(\mathbf{A}) &= \sum_i A_{ii} = \sum_i \lambda_i, \quad \lambda_i = \text{eig}(\mathbf{A}) && \text{(C.5)} \\
\text{Tr}(\mathbf{AXB}) &= \text{Tr}(\mathbf{BAX}) = \text{Tr}(\mathbf{XBA}) && \text{(C.6)} \\
\text{Tr}(\mathbf{A} + \mathbf{B}) &= \text{Tr}(\mathbf{A}) + \text{Tr}(\mathbf{B}) && \text{(C.7)} \\
& && \text{(C.8)}
\end{aligned}$$

Determinant

Assuming $\mathbf{A}$ is an $n \times n$ matrix

$$|\mathbf{A}| = \prod_i \lambda_i, \quad \lambda_i = \text{eig}(\mathbf{A}) \tag{C.9}$$

$$|\mathbf{A}^T| = |\mathbf{A}| \tag{C.10}$$

$$|\mathbf{A}^{-1}| = 1/|\mathbf{A}| \tag{C.11}$$

$$|\mathbf{AB}| = |\mathbf{A}|\,|\mathbf{B}| \tag{C.12}$$

Inverse

$$(\mathbf{AB})^{-1} = \mathbf{B}^{-1}\mathbf{A}^{-1} \tag{C.13}$$

$$\text{If} \quad (\mathbf{A}+\mathbf{B})^{-1} = \mathbf{A}^{-1}+\mathbf{B}^{-1} \quad \text{then} \quad \mathbf{AB}^{-1}\mathbf{A} = \mathbf{BA}^{-1}\mathbf{B} \tag{C.14}$$

Properties

$$\partial\mathbf{A} = 0 \qquad \mathbf{A}\text{is a constant} \tag{C.15}$$

$$\partial(a\mathbf{X}) = a\partial\mathbf{X} \tag{C.16}$$

$$\partial(\mathbf{X}+\mathbf{Y}) = \partial\mathbf{X}+\partial\mathbf{Y} \tag{C.17}$$

$$\partial(\text{Tr}(\mathbf{X})) = \text{Tr}(\partial\mathbf{X}) \tag{C.18}$$

$$\partial\mathbf{X}^H = (\partial\mathbf{X})^H \tag{C.19}$$

$$\partial(\ln|\mathbf{X}|) = \text{Tr}(\mathbf{X}^{-1}\partial(\mathbf{X})) \tag{C.20}$$

Derivative

$$\frac{\partial}{\partial\mathbf{X}}\text{Tr}(\mathbf{X}) = \mathbf{I} \tag{C.21}$$

$$\frac{\partial}{\partial\mathbf{X}}\text{Tr}(\mathbf{AX}^T) = \mathbf{A} \tag{C.22}$$

$$\frac{\partial}{\partial\mathbf{X}}\text{Tr}(\mathbf{AX}^T\mathbf{B}) = \mathbf{BA} \tag{C.23}$$

(C.24)

D

Convex Optimization Theory

The general form of optimization problem is defined as follows

$$\begin{aligned} \min_{\mathbf{x}} \quad & f_0(\mathbf{x}) \\ \text{subject to} \quad & f_i(\mathbf{x}) \leq b_i, \qquad i = 1, \ldots, m \end{aligned} \tag{D.1}$$

where the functions $f_0, \ldots, f_m : \mathbb{R}^n \to \mathbb{R}$. The problem (D.1) is called

- *linear* if $f_0, \ldots, f_m$ are linear (affine) functions such that for all $\mathbf{x}_1, \mathbf{x}_2 \in \mathbb{R}^n$ and $\eta \in [0, 1]$ fulfill $f_i(\eta\mathbf{x}_1 + (1-\eta)\mathbf{x}_2) = \eta f_i(\mathbf{x}_1) + (1-\eta) f_i(\mathbf{x}_2)$.
- *convex* if $f_0, \ldots, f_m$ are convex functions such that for all $\mathbf{x}_1, \mathbf{x}_2 \in \mathbb{R}^n$ and $\eta \in [0, 1]$ fulfill $f_i(\eta\mathbf{x}_1 + (1-\eta)\mathbf{x}_2) \leq \eta f_i(\mathbf{x}_1) + (1-\eta) f_i(\mathbf{x}_2)$.
- *quasi-convex* if $f_0, \ldots, f_m$ are quasi-convex functions such that for all $\mathbf{x}_1, \mathbf{x}_2 \in \mathbb{R}^n$ and $\eta \in [0, 1]$ fulfill $f_i(\eta\mathbf{x}_1 + (1-\eta)\mathbf{x}_2) \leq \max(f_i(\mathbf{x}_1), f_i(\mathbf{x}_2))$.
- *monotonic* if $f_0, \ldots, f_m$ are monotonic functions (any combination of decreasing and increasing functions).

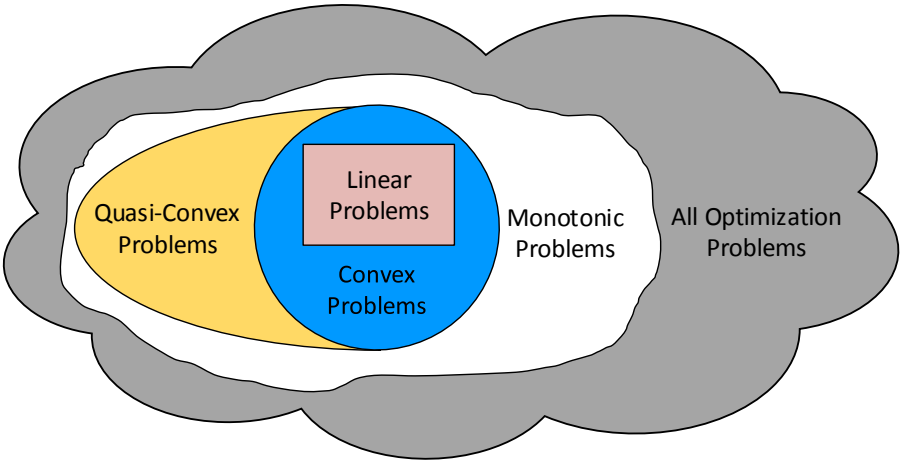

Figure D.1: Classes of optimization problems.

The above mentioned classes are ordered according to conditions: every linear problem is counted convex, every convex problem is considered quasi-convex, and every quasi-convex problem is classified monotonic. Figure D.1 illustrates such a relationship between optimization classes.

Generally speaking, most optimization problems can be solved numerically since they have no analytical solutions. Appropriate algorithms are used for solving optimization problems based on their class. For instance, *simplex method* is an efficient algorithm to solve linear problems [KB95]. It costs polynomial complexity growth with the problem dimensions and number of constraints n and m, respectively.

D.1 Solving and Using Convex Optimization

There is no close-form solution for convex optimization problems, however there are efficient numerical approaches such as Interior-point method. For solving the problem (D.1, the number of iterations is almost between 10 and 100 such that each iteration requires the order $\max(n^3, n^2m, Q)$ operations, where Q is the evaluation cost of the first and second derivatives for the objective and constraints functions $f_0, \ldots, f_m$. Solving general convex optimization problems cannot be claimed as a mature technology yet as research on interior-point methods for general non-linear convex problems is still a hot research topic. However, it is fair to confirm that interior-point methods are close to be a technology for some subclasses of convex problems such as second-order cone programming and geometric programming [BV04]. The

use of convex optimization is alike to the use of least-squares or linear programming. Once a practical problem is modeled as a convex optimization problem, it is solved efficiently, but it is difficult to recognize or formulate a convex function. However, once the skill of formulating or recognizing convex problems is acquired, many problems can be solved via convex optimization theory. This means the challenge in convex optimization is the formulation and recognition. Interior-point methods solve both linear and convex optimization problems under polynomial complexity [BV04]. General purpose interior-point methods based solvers include SeDuMi [Stu99], SDPT3 [TTT03], CVX [GS11], and YALMIP [LÖ4].

D.2 Convex Sets

The convex set can be either one of the following [BV04]

Affine Sets

A $C \subseteq \mathbb{R}^n$ is *affine* if the line connecting any two points in C lies in C. This refers to all possible linear combinations of any two points in C given that the sum of the coefficients is one. As a generalization, the point $\eta_1\mathbf{x}_1 + \cdots + \eta_k\mathbf{x}_k$, where $\eta_1 + \cdots + \eta_k = 1$, is seen as an *affine combination* of the points $\mathbf{x}_1, \ldots, \mathbf{x}_k$.

Convex Sets

A set C is *convex* if the line joining any two points in C lies in C, i.e. for any $\mathbf{x}_1, \mathbf{x}_2$ with $\eta \in [0, 1]$ satisfy

$$\eta\mathbf{x}_1 + (1 - \eta)\mathbf{x}_2 \in C.$$

Figure D.2 shows illustration for some convex and non-convex sets in $\mathbb{R}^2$. As a generalization, the point $\eta_1\mathbf{x}_1 + \cdots + \eta_k\mathbf{x}_k$, with $\eta_1 + \cdots + \eta_k = 1$ for $\eta_i \geq 0, i = 1, \ldots, k$, is seen as an *convex combination* of the points $\mathbf{x}_1, \ldots, \mathbf{x}_k$. The *convex hull* is a always convex and defined for a set C as all convex combinations of points in C:

$$\mathbf{conv}C = \{\eta_1\mathbf{x}_1 + \cdots + \eta_k\mathbf{x}_k | \mathbf{x}_i \in C, \eta_i \geq 0, i = 1, \ldots, k, \sum_{i=1}^{k} \eta_i = 1\}.$$

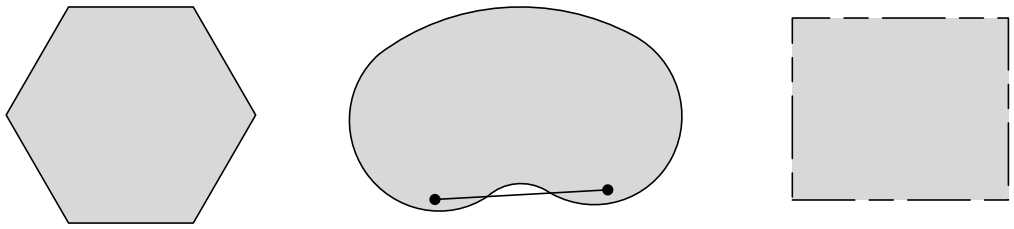

(a) (b) (c)

Figure D.2: Examples for some sets in $\mathbb{R}^2$. (a) Hexagon is convex. (b) Kidney shape is non-convex. (c) Square with excluded boundaries is non-convex.

Examples

Some important convex sets are listed as follows [BV04]

- The empty set $\emptyset$ is convex.
- Any line is affine, hence convex.
- A line segment is convex.
- Any subspace is affine, hence convex.
- Hyperplanes, ellipsoids, polyhedra, positive semidefinite cones, and many other sets are convex. Interested readers can refer to [BV04] for more details.

D.3 Convex Functions and Operations Preserving Convexity

This section is cited from [BV04] and covers the definition of convex function with illustration and examples. Then, operations that preserve convexity are briefly introduced.

Convex Functions

A function $f : \mathbb{R}^n \to \mathbb{R}$ is *convex* if **dom** f is a convex and for any $\mathbf{x}_1, \mathbf{x}_2 \in$ **dom** f and $\eta \in [0, 1]$ satisfies

$$f(\eta\mathbf{x}_1 + (1-\eta)\mathbf{x}_2) \leq \eta f(\mathbf{x}_1) + (1-\eta)f(\mathbf{x}_2) \tag{D.2}$$

The geometrical interpretation is that the line segment between the pairs $(\mathbf{x}_1, f(\mathbf{x}_1))$ and $(\mathbf{x}_2, f(\mathbf{x}_2))$ lies above the curvature of f as depicted in Figure D.3. f is described strictly convex if the inequality in (D.2) strictly holds. The function f is *concave* if $-f$ is convex and strictly concave if $-f$ strictly convex.

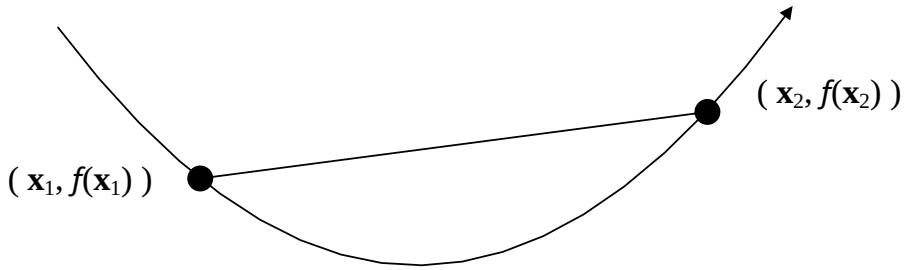

Figure D.3: Graph of a convex function.

Examples

Some examples for convex and concave functions on $\mathbb{R}$ follow

- Logarithm. $\log x$ is concave on $\mathbb{R}_{++}$.
- Exponential. e^{ax} is convex for any $a \in \mathbb{R}$.
- Powers. x^a is convex on $\mathbb{R}_{++}$ for $a \geq 1$ or $a \leq 0$, and concave for $0 \leq a \leq 1$.
- Powers of absolute values. $|x|^a$ is convex on $\mathbb{R}$ for $a \geq 1$.
- Negative entropy. $x \log x$ is convex on $\mathbb{R}_{++}$.

Other examples on $\mathbb{R}^n$ follow

- Log-determinant. The function defined as $f(\mathbf{X}) = \log |\mathbf{X}|$ is concave on $\mathbf{dom} f = \mathbb{S}^n_{++}$.
- Norms. Every norm on $\mathbb{R}^n$ is convex.
- Max function. The function defined as $f(\mathbf{x}) = \max\{\mathbf{x}_1, \ldots, \mathbf{x}_n\}$ is convex on $\mathbb{R}^n$.
- Log-sum-exp. The function defined as $f(\mathbf{x}) = \log(e^{\mathbf{x}_1} + \cdots + e^{\mathbf{x}_n})$ is convex on $\mathbb{R}^n$.
- Geometric mean. The function $f(\mathbf{x}) = (\Pi_{i=1}^n \mathbf{x}_i)^{1/n}$ is concave on $\mathbf{dom} f = \mathbb{R}^n_{++}$.

Operations Preserving Convexity

The operations that preserve convexity of functions and allow constructing other convex functions are described as follows

- Non-negative weighted sums.
- Composition with affine mapping.
- Point-wise maximum and supremum.
- Composition.
- Minimization.
- Perspective of functions. The perspective functions normalize vectors such that the last component becomes one in order to skip it afterwords.

E

Lagrange Multiplier Theory

By means of Lagrange multiplier theory, useful tools for solving, bounding, and analyzing optimization problems are provided. Particularly, it reveals optimality conditions for obtaining solutions to constrained optimization problems. The objective function and conditions generalize an unconstrained optimization which has global minimum $\mathbf{x}^*$ of $f_0(\mathbf{x})$ fulfilling $\nabla f_0(\mathbf{x}^*) = \mathbf{0}$. Let's first define general form for optimization problems as follows

$$\begin{aligned} \min_{\mathbf{x}} \quad & f_0(\mathbf{x}) \\ \text{subject to} \quad & f_i(\mathbf{x}) \leq 0, \qquad i = 1, \ldots, m \end{aligned} \tag{E.1}$$

with $\mathbf{x} \in \mathbb{R}^n$ assuming its domain $D_x = \bigcap_{i=0}^{m} \mathbf{dom} f_i$ is nonempty. The functions $f_i : \mathbb{R}^n \to \mathbb{R}$ are the constraint functions.

E.1 The Lagrangian

The Lagrangian is formed taking the constraints into account by augmenting the objective function with a weighted sum of the constraint functions. The Lagrangian function $\mathcal{L} : \mathbb{R}^n \times \mathbb{R}^m \rightarrow \mathbb{R}$ associated with the problem (E.1) is defined as

$$\mathcal{L}(\mathbf{x}, \boldsymbol{\mu}) = f_0(\mathbf{x}) + \sum_{i=1}^{m} \mu_i f_i(\mathbf{x}) \tag{E.2}$$

with **dom** $\mathcal{L} = D_x \times \mathbb{R}^m$. μ_i refers to the *Lagrange multiplier* associated with the ith constraint $f_i(\mathbf{x}) \leq 0$. The vector $\boldsymbol{\mu} = [\mu_1 \dots \mu_m]$ is called the *dual variables* or *Lagrange multiplier vector* associated with the problem (E.1). The *Lagrange dual function* (or just *dual function*) $\mathcal{G} : \mathbb{R}^m \rightarrow \mathbb{R}$ is the minimum value of the Lagrangian over $\mathbf{x}$

$$\mathcal{G}(\boldsymbol{\mu}) = \inf_{\mathbf{x} \in D_x} \mathcal{L}(\mathbf{x}, \boldsymbol{\mu}) \tag{E.3}$$

The concept of the Lagrangian function is the augmentation of the cost function $f_0(\mathbf{x})$ with the constraints. That means the cost is increased as a penalty due the constraint violations. Since the dual function is the point wise infimum of a family of affine functions of $(\boldsymbol{\mu})$, it is concave even if the optimization problem (E.1) is not convex. The computation of the infimum may be difficult in some cases, thus the dual function provides lower bounds on the optimal value $\mathbf{x}^*$. For any $\boldsymbol{\mu} \geq \mathbf{0}$, we have

$$\mathcal{G}(\boldsymbol{\mu}) \leq f_0(\mathbf{x}^*) \tag{E.4}$$

Based on the fact in (E.4), a maximization for the lower bound is necessary to get close to the optimal solution.

E.2 The Lagrange Dual Problem, Optimality Conditions, and Strong Duality

The Lagrange dual problem associated with (E.1) is given as

$$\max_{\boldsymbol{\mu} \geq \mathbf{0}} \mathcal{G}(\boldsymbol{\mu}) \tag{E.5}$$

The Lagrange dual problem is considered a convex optimization as the objective and the constraint are concave and convex, respectively. It does not matter whether the original problem in (E.1) is convex or not. On the other hand, the convexity of the original problem ensures global optimal solution for the dual problem, i.e. denoted as $\boldsymbol{\mu}^*$. The optimal solution of the original

problem $\mathbf{x}^*$ is connected with the Lagrange multiplier vector $\boldsymbol{\mu}$ via the *Karush-Kuhn-Tucker (KKT) conditions*. The KKT conditions imply that an optimal Lagrange multiplier vector $\boldsymbol{\mu}^*$ exists such that

$$\nabla f_0(\mathbf{x}^*) + \sum_{i=1}^{m} \mu_i^* \nabla f_i(\mathbf{x}^*) = \mathbf{0}, \tag{E.6}$$

$$f_i(\mathbf{x}^*) \leq 0, \quad i = 1, \ldots, m \tag{E.7}$$

$$\mu_i^* \geq 0, \quad i = 1, \ldots, m \tag{E.8}$$

$$\mu_i^* f_i(\mathbf{x}^*) = 0 \quad i = 1, \ldots, m \tag{E.9}$$

The above conditions are called as *stationary, original feasibility, dual feasibility,* and *complementary slackness*, respectively. They are generally insufficient and unnecessary for the optimal solution. However, they become necessary for optimality if the optimization problem is convex. The optimal value of original problem (E.1) is related to the optimal value of the dual problem (E.5) as

$$f_0(\mathbf{x}^*) \geq \mathcal{G}(\boldsymbol{\mu}^*) \tag{E.10}$$

It is observed that the optimal solution of the original problem is always greater than or equal to that of the dual problem. The difference $f_0(\mathbf{x}^*) - \mathcal{G}(\boldsymbol{\mu}^*)$ is positive and known as the *duality gap*. Strong duality implies zero duality gap which is held when the original problem is convex. This means the solution of the dual problem can be an exact solution for the original problem. Moreover, the strong duality refers to the necessity and sufficiency of the KKT conditions. From another perspective, a saddle point existence in the Lagrangian function interprets strong duality as follows

$$\sup_{\boldsymbol{\mu} \geq \mathbf{0}} \inf_{\mathbf{x} \in D_x} \mathcal{L}(\mathbf{x}, \boldsymbol{\mu}) = \inf_{\mathbf{x} \in D_x} \sup_{\boldsymbol{\mu} \geq \mathbf{0}} \mathcal{L}(\mathbf{x}, \boldsymbol{\mu}) \tag{E.11}$$

In words, if $\mathbf{x}^*$ and $\boldsymbol{\mu}^*$ are original and dual optimal points for a convex problem, they form a saddle point for the Lagrangian. The opposite is true: if $(\mathbf{x}, \boldsymbol{\mu})$ is a saddle point of the Lagrangian, then $\mathbf{x}$ is original optimal, $\boldsymbol{\mu}$ is dual optimal, and the optimal duality gap is zero.

In this context, it is really interesting to have an alternative and relatively efficient method to solve the convex problems. As a conclusion, the convexity of the optimization problem facilitates involving Lagrange multiplier theory as efficient alternative to convex optimization theory.

F

Proofs

F.1 Proof of Proposition 1

Assuming N_p eigenmodes for the PU l, the PU achievable rate equals the superposition of the rates of whose eigenmodes. Thus, it make sense to prove the PRL_l for the jth eigenmode as follows

$$\begin{aligned}\frac{C_{SINR}}{C_{SNR}} &= \frac{\log_2\left(1+\frac{p_{j,l}\Lambda_{j,l}^2}{\sigma_l^2+\alpha_l\sigma_l^2}\right)}{\log_2\left(1+\frac{p_{j,l}\Lambda_{j,l}^2}{\sigma_l^2}\right)} \\ &= \lim_{\text{SNR}_{PR}\to B}\frac{\log_2\left(1+\frac{\text{SNR}_{PR}}{1+\alpha_l}\right)}{\log_2\left(1+\text{SNR}_{PR}\right)} \\ &= \begin{cases}\frac{0}{0}, & \text{for } B=0 \\ \frac{\infty}{\infty}, & \text{for } B\to\infty\end{cases}\end{aligned} \tag{F.1}$$

Applying L'Hospital's rule and reforming gives

$$\frac{C_{SINR}}{C_{SNR}} = \lim_{\text{SNR}_{PR}\to B} \frac{\frac{1}{1+\alpha_l}\left(1+\text{SNR}_{PR}\right)}{1+\frac{\text{SNR}_{PR}}{1+\alpha_l}} \tag{F.2}$$

For the low SNR_{PR} regime ($B = 0$),

$$\frac{C_{SINR}}{C_{SNR}} = \frac{1}{1+\alpha_l} \tag{F.3}$$

For the high SNR_{PR} regime ($B \to \infty$),

$$\frac{C_{SINR}}{C_{SNR}} = \lim_{\text{SNR}_{PR}\to\infty} \frac{\frac{1}{1+\alpha_l}\left(1+\frac{1}{\text{SNR}_{PR}}\right)}{\frac{1}{1+\alpha_l}+\frac{1}{\text{SNR}_{PR}}} = 1 \tag{F.4}$$

Substituting (F.3) and (F.4) in the PRL_l defined in (4.9) gives

$$\text{PRL}_l = \begin{cases} \frac{\alpha_l}{1+\alpha_l} & \text{for } \text{SNR}_{PR} \to 0 \\ 0 & \text{for } \text{SNR}_{PR} \to \infty \end{cases} \tag{F.5}$$

Hence, for $\text{SNR}_{PR} \to 0, \alpha_l = \frac{\text{PRL}_l}{1-\text{PRL}_l}$.

F.2 Proof of Proposition 2

To compute the precoding-thresholds, we should assume an interference-limited CR system, i.e. $P_T \to \infty$. Then, it is clear that the PUI threshold matrix $\mathbf{I}_{l,i}^{th}$ set an upper bound of the maximum transmission power of the subcarrier i based on *C2* in (4.14). Hence, *C2* is a rule of thumb to calculate the maximum transmission power for each DoF of the adaptive precoder (i.e. $\forall d \in \mathcal{D}$) as

$$\text{Tr}\left(\mathbf{P}_{D,k,i}^{(d),max}\right) = \max_l \text{Tr}\left(\mathbf{\Omega}_{D,k,i}^{(d)\ -1}\mathbf{I}_{l,i}^{th}\right), \forall d \in \mathcal{D}, \forall k, i \tag{F.6}$$

Toward calculating the precoding-threshold between the dth and $(d-1)$th DoFs, we sum up of the maximum power of all OFDM tones for the dth or $(d-1)$th DoF (as they provide similar sum-rate $C_D^{(d)} = C_D^{(d-1)}$ based on **Corollary 1**) as

$$\left\{P_{D,th}^{(d,d-1)} = \sum_{i=1}^{M} \text{Tr}(\mathbf{P}_{D,\bar{k},i}^{(d),max}) = \sum_{i=1}^{M} \max_l \text{Tr}\left(\mathbf{\Omega}_{D,\bar{k},i}^{(d)\ -1}\mathbf{I}_{l,i}^{th}\right)\right\}_{d=1}^{\mathcal{R}} \tag{F.7}$$

However, each OFDM tone must be allocated to one CU to enable the computation of the precoding-threshold set defined in (F.7). Therefore, we need an *initial* subcarrier mapping (best user per subcarrier policy) for each DoF given by

$$\bar{k} = \textit{arg}\max_k r_{D,k,i}^{(d),max} \tag{F.8}$$

where $r_{D,k,i}^{(d),max} = \log_2 \left| \mathbf{I}_{N_c} + \check{\mathbf{\Lambda}}_{D,k,i}^{(d)2} \mathbf{P}_{D,k,i}^{(d),max} \right|$ is the maximum achievable rate. Note that this initial mapping is necessary for each DoF since the effective precoded channel power $\bar{\mathbf{\Lambda}}_{D,k,i}^{(d)2}$ depends on the dth DoF. For instance, to calculate the threshold $P_{D,th}^{(2,1)}$ use the 2nd DoF ($d = 2$) to compute $\mathbf{\Omega}_{D,k,i}^{(2)}, \check{\mathbf{\Lambda}}_{D,k,i}^{(2)2}$, and $\mathbf{P}_{D,k,i}^{(2),max}, \forall k, i$, then assign the best CU $\bar{k}$ to the subcarrier i according to (F.8). Next, apply (F.7) to get $P_{D,th}^{(2,1)}$. It is worth to note that the initial subcarrier mapping depends on the assumption of interference-limited CR in which *C2* of (4.14) is tighter than *C1*. Thus, once the CR system is power-limited (i.e. *C1* is tighter than *C2*), the initial subcarrier mapping is no longer accurate.

F.3 Proof of Theorem 2

The KKT conditions are sufficient for optimality [BV04] since our problem is convex. The main KKT condition holds zero gradient equality as

$$\frac{\partial \mathcal{L}_D}{\partial \mathbf{P}_{D,k,i}} = 0 \tag{F.9}$$

We can solve (F.9) by using the following rules and properties [PP12]

$$\begin{aligned} \partial(\ln |\mathbf{X}|) &= \text{Tr}(\mathbf{X}^{-1}\partial(\mathbf{X})) \\ \frac{\partial \text{Tr}(\mathbf{A}\mathbf{X}^T)}{\partial \mathbf{X}} &= \mathbf{A} \\ \text{Tr}(\mathbf{AXB}) &= \text{Tr}(\mathbf{BAX}) \\ (\mathbf{AB})^{-1} &= \mathbf{B}^{-1}\mathbf{A}^{-1} \end{aligned}$$

The gradient (F.9) can be derived as follows

$$\begin{aligned} \frac{\partial \mathcal{L}_D}{\partial \mathbf{P}_{D,k,i}} &= \frac{\partial}{\partial \mathbf{P}_{D,k,i}} \Bigg[\frac{\tau_D}{M} \sum_{k=1}^{K} \sum_{i=1}^{M} \theta_{k,i} \log_2 \left| \mathbf{I}_{N_c} + \check{\mathbf{\Lambda}}_{D,k,i}^2 \mathbf{P}_{D,k,i} \right| \\ &\quad - \mu_D \left(\sum_{i=1}^{M} \sum_{k=1}^{K} \theta_{k,i} \text{Tr}(\hat{\mathbf{F}}_{D,k,i}^H \hat{\mathbf{F}}_{D,k,i} \mathbf{P}_{D,k,i}) - P_T \right) \\ &\quad - \sum_{i=1}^{M} \delta_{D,i} \left(\sum_{k=1}^{K} \theta_{k,i} \text{Tr}\left(\mathbf{\Omega}_{D,k,i} \mathbf{P}_{D,k,i}\right) - \text{Tr}(\mathbf{I}_{l,i}^{th}) \right) \Bigg] \\ &= \frac{\tau_D}{M \ln 2} \frac{\text{Tr}\left[\left(\mathbf{I}_{N_c} + \check{\mathbf{\Lambda}}_{D,k,i}^2 \mathbf{P}_{D,k,i} \right)^{-1} \partial \left(\check{\mathbf{\Lambda}}_{D,k,i}^2 \mathbf{P}_{D,k,i} \right) \right]}{\partial \mathbf{P}_{D,k,i}} \\ &\quad - \mu_D \hat{\mathbf{F}}_{D,k,i}^H \hat{\mathbf{F}}_{D,k,i} - \delta_{D,i} \mathbf{\Omega}_{D,k,i} \\ &= \frac{\tau_D}{M \ln 2} \left(\mathbf{I}_{N_c} + \check{\mathbf{\Lambda}}_{D,k,i}^2 \mathbf{P}_{D,k,i} \right)^{-1} \bar{\mathbf{\Lambda}}_{D,k,i}^2 - \mu_D \hat{\mathbf{F}}_{D,k,i}^H \hat{\mathbf{F}}_{D,k,i} - \delta_{D,i} \mathbf{\Omega}_{D,k,i} \\ &= 0 \end{aligned} \tag{F.10}$$

Then, reforming (F.10) and separating the power matrix gives (4.22).

G

Publications

- A. Yaqot and P. A. Hoeher, "Efficient resource allocation for MIMO-OFDM cognitive networks with adaptive precoding," in *Proc. 18th International OFDM Workshop (InOWo'14)*, Essen, Germany, Aug. 2014, pp. 85-91.

- A. Yaqot and P. A. Hoeher, "Adaptive MMSE-based precoding in multiuser MIMO broadcasting with application to cognitive radio," in *Proc. 20th International ITG Workshop on Smart Antennas (WSA2016)*, Munich, Germany, Mar. 2016, pp. 340-347.

- A. Yaqot and P. A. Hoeher, "On precoding diversity in cognitive networks," in *Proc. 23rd International Conference on Telecommunications (ICT2016)*, Thessaloniki, Greece, May 2016, pp. 48-52.

- A. Yaqot and P. A. Hoeher, "Efficient resource allocation for cognitive radio networks," *IEEE Transaction on Vehicular Technology*, accepted for publication, 2017.

Bibliography

[3GP] 3GPP. [Online]. Available: http://www.3gpp.org/technologies/keywords-acronyms/98-lte

[3GP06] ——, "Technical specification group radio access network: Requirements for Evolved UTRA (E-UTRA) and Evolved UTRAN (E-UTRAN) (Release 7)," 3GPP, Technical Report 25.913, March 2006.

[4G 14] 4G Americas, "4G Americas recommendations on 5G requirements and solutions," Technical Report, October 2014.

[5G 15] 5G Initiative Team, "NGMN 5G white paper," NGMN Alliance, Technical Report, February 2015.

[AA14] M. Adian and H. Aghaeinia, "Low complexity resource allocation in MIMO-OFDM-based cooperative cognitive radio networks," *Transactions on Emerging Telecommunications Technologies*, vol. 27, no. 1, pp. 92–100, 2014.

[AAN14] M. Adian, H. Aghaeinia, and Y. Norouzi, "Optimal resource allocation for opportunistic spectrum access in heterogeneous MIMO cognitive radio networks," *Transactions on Emerging Telecommunications Technologies*, vol. 27, no. 1, pp. 74–83, 2014.

[ALVM08] I. F. Akyildiz, W.-Y. Lee, M. C. Vuran, and S. Mohanty, "A survey on spectrum management in cognitive radio networks," *IEEE Commun. Mag.*, vol. 46, no. 4, pp. 40–48, April 2008.

[AY12] M. Abdullah and A. Yonis, "Performance of LTE release 8 and release 10 in wireless communications," in *Proc. International Conference on Cyber Security, Cyber Warfare and Digital Forensic (CyberSec)*, 2012, pp. 236–241.

[BBL92] J.-E. Berg, R. Bownds, and F. Lotse, "Path loss and fading models for microcells at 900 MHz," in *Proc. Veh. Technol. Conf.*, May 1992, pp. 666–671.

[BGG+13] E. Biglieri, A. Goldsmith, L. J. Greenstein, N. Mandayam, and H. V. Poor, *Principles of Cognitive Radio*. Cambridge University Press, 2013.

[BHB11] G. Bansal, M. Hossain, and V. Bhargava, "Adaptive power loading for OFDM-based cognitive radio systems with statistical interference constraint," *IEEE Trans. Wireless Commun.*, vol. 10, no. 9, pp. 2786–2791, Sep. 2011.

[BJ13] E. Björnson and E. Jorswieck, "Optimal resource allocation in coordinated multi-cell systems," *Foundations and Trends in Communications and Information Theory*, vol. 9, no. 2-3, pp. 113–381, 2013.

[BV04] S. Boyd and L. Vandenberghe, *Convex Optimization*. Cambridge, UK: Cambridge Univ. Press, 2004.

[Cha66] R. Chang, "Synthesis of band-limited orthogonal signals for multichannel data transmission," *Bell Syst. Tech. J.*, vol. 45, no. 10, pp. 1775–1796, December 1966.

[Che03] Y. Chen, "Soft handover issues in radio resource management for 3G WCDMA networks," Ph.D. dissertation, Queen Mary, University of London, UK, 2003.

[Cim85] L. Cimini, "Analysis and simulation of a digital mobile channel using orthogonal frequency division multiplexing," *IEEE Trans. Commun.*, vol. 33, no. 7, pp. 665–675, July 1985.

[CM04] L. Choi and R. D. Murch, "A transmit preprocessing technique for multiuser MIMO systems using a decomposition approach," *IEEE Trans. Wireless Commun.*, vol. 3, no. 1, pp. 20–24, January 2004.

[DMA03] M. Dillinger, K. Madai, and N. Alonistioti, *Software Defined Radio: Architectures, Systems, and Functions*. New York: Wiley, 2003.

[DMW95] D. M. Devasirvathan, R. R. Murray, and D. R. Woiter, "Time delay spread measurements in a wireless local loop test bed," in *Proc. IEEE VTC*, May 1995, pp. 241–245.

[DRX98] G. Durgin, T. S. Rappaport, and H. Xu, "Partition-based path loss analysis for in-home and residential areas at 5.85 GHz," in *Proc. IEEE GLOBECOM*, November 1998, pp. 904–909.

[EGT+99] V. Erceg, L. J. Greenstein, S. Y. Tjandra, S. R. Parkoff, A. Gupta, B. Kulic, A. A. Julius, and R. Bianchi, "An empirically based path loss model for wireless channels in suburban environments," *IEEE J. Selected Areas Commun.*, vol. 17, no. 7, pp. 1205–1211, July 1999.

[Eri05] Ericsson, "Some aspects of single-carrier transmission for E-UTRA," 3GPP Technical Report, TSG-RAN-42 R1-050765, Sep. 2005.

[Eri13] ——, "Ericsson mobility report," Sep 2013. [Online]. Available: http://www.ericsson.com/ericsson-mobility-report

[FABSE02] D. Falconer, S. Ariyavisitakul, A. Benyamin-Seeyar, and B. Eidson, "Frequency domain equalization for single-carrier broadband wireless systems," *IEEE Commun. Mag.*, vol. 40, pp. 58–66, April 2002.

[FCC02a] FCC, "Broadcast ownership rules, report and order," Federal Communication Commission, MM Docket 02-235, November 2002.

[FCC02b] ——, "Report of the spectrum efficiency working group," Spectrum Policy Task Force, Tech. Rep. 02-135, November 2002.

[FCC03a] ——, "Facilitating opportunities for flexible, efficient, and reliable spectrum use employing cognitive radio technologies," Federal Communication Commission, ET Docket 03-108, December 2003.

[FCC03b] ——, "Notice of proposed rule making and order," Federal Communication Commission, ET Docket 03-322, December 2003.

[FG98] G. J. Foschini and M. J. Gans, "On limits of wireless communications in a fading environment when using multiple antennas," *Wireless Personal Communication*, vol. 6, no. 3, pp. 311–335, March 1998.

[GC08] L. Gao and S. Cui, "Efficient subcarrier, power, and rate allocation with fairness consideration for OFDMA uplink," *IEEE Trans. Wireless Commun.*, vol. 7, no. 5, pp. 1507–1511, 2008.

[GG93] A. J. Goldsmith and L. J. Greenstein, "A measurement-based model for predicting coverage areas of urban microcells," *IEEE J. Selected Areas Commun.*, vol. 11, no. 7, pp. 1013–1023, September 1993.

[GGK+03] S. S. Ghassemzadeh, L. J. Greenstein, A. Kavcic, T. Sveinsson, and V. Tarokh, "UWB indoor path loss model for residential and commercial buildings," in *Proc. IEEE VTC*, October 2003, pp. 3115–3119.

[GJMS09] A. Goldsmith, S. A. Jafar, I. Maric, and S. Srinivasa, "Breaking spectrum gridlock with cognitive radios: An information theoretic perspective," *Proceedings of the IEEE*, vol. 97, no. 5, pp. 894–914, May 2009.

[GKHJ+07] D. Gesbert, M. Kountouris, R. Heath Jr., C.-B. Chae, and T. Sälzer, "Shifting the MIMO paradigm," *IEEE Signal Processing Magazine*, vol. 24, no. 5, pp. 36–46, 2007.

[GL96] G. Golub and C. Loan, *Matrix Computations*, 3rd ed. The Johns Hopkins Univ. Press, 1996.

[Gol05] A. Goldsmith, *Wireless Communication*. Cambridge, UK: Cambridge Univ. Press, 2005.

[GS11] M. Grant and B. S., "CVX: Matlab software for disciplined convex programming," April 2011. [Online]. Available: http://cvx.com/cvx/

[Gud91] M. Gudmundson, "Correlation model for shadow fading in mobile radio systems," *Electronics Letters*, vol. 7, pp. 2145–2146, November 1991.

[Hay05] S. Haykin, "Cognitive radio: Brain-empowered wireless communications," *IEEE J. Sel. Areas Commun.*, vol. 23, no. 2, pp. 201–220, February 2005.

[HHI+12] L. Hanzo, H. Haas, S. Imre, D. O. Brien, M. Rupp, and L. Gyongyosi, "Wireless myths, realities, and futures: From 3G/4G to optical and quantum wireless," *Proc. IEEE*, vol. 100, pp. 1853–1888, May 2012.

[HL05] S. Han and J. Lee, "An overview of peak-to-average power ratio reduction techniques for multicarrier transmission," *IEEE Trans. Wireless Commun.*, vol. 12, no. 2, pp. 56–65, Apr. 2005.

[HM72] H. Harashima and H. Miyakawa, "Matched-transmission technique for channels with intersymbol interference," *IEEE Trans. Commun.*, vol. 20, no. 4, pp. 7740–780, August 1972.

[HSAB09] J. Huang, V. Subramanian, R. Agrawal, and R. Berry, "Joint scheduling and resource allocation in uplink OFDM systems for broadband wireless access networks," *IEEE Journal on Selected Areas in Communications*, vol. 27, no. 2, pp. 226–234, 2009.

[HW11] P. Hoeher and T. Wo, "Superposition modulation: Myths and facts," *IEEE Communications Magazine*, vol. 49, no. 12, pp. 110–116, 2011.

[HZL07] K. Hamdi, W. Zhang, and K. B. Letaief, "Joint beamforming and scheduling in cognitive radio networks," in *Proc. IEEE Global Telecommun. Conf.*, November 2007, pp. 2977–2981.

[IEE08] IEEE 802.22/WDv0.4.7, "Draft standard for wireless regional area networks part 22: Cognitive wireless RAN medium access control (MAC) and physical layer (PHY) specifications: Policies and procedures for operation in the TV bands," International Telecommunication Union, Tech. Rep., March 2008, (Available only to working group members.).

[IEE15] IEEE 802.11 Task Group, "Status of project IEEE 802.11ax," International Telecommunication Union, Tech. Rep., 2015, Available at http://www.ieee802.org/11/Reports/tgax_update.htm.

[ITU09] ITU, "Definitions of software defined radio (SDR) and cognitive radio system (CRS)," International Telecommunication Union, ITU-R SM.2152, 2009.

[Jak74] W. Jakes, *Microwave Mobile Communications*. New York: Wiley, 1974, reprinted by IEEE Press.

[JBU04] M. Joham, J. Brehmer, and W. Utschick, "MMSE approaches to multiuser spatio-temporal Tomlinson-Harashima precoding," in *Proc. 5th International ITG Conf. on Source and Channel Coding (ITGSCC'04)*, January 2004, pp. 387–394.

[JH07] M. Jiang and L. Hanzo, "Multiuser MIMO-OFDM for next-generation wireless systems," *Proceeding of the IEEE*, vol. 95, no. 7, pp. 1430–1469, 2007.

[JL07] J. Joung and Y. H. Lee, "Regularized channel diagonalization for multiuser MIMO downlink using a modified MMSE criterion," *IEEE Trans. Signal Process.*, vol. 55, no. 4, pp. 1573–1579, April 2007.

[JUN05] M. Joham, W. Utschick, and J. A. Nossek, "Linear transmit processing in MIMO communications systems," *IEEE Trans. Signal Process.*, vol. 53, no. 8, pp. 2700–2712, Aug. 2005.

[KB95] B. Kolman and R. Beck, *Elementary Linear Programming with Applications*. Academic Press, 1995.

[KHK07] K. Kown, Y. Han, and S. Kim, "Efficient subcarrier and power allocation algorithm in OFDMA uplink system," *IEICE Trans. Commun.*, vol. 90, no. 2, pp. 368–371, 2007.

[KLSD10] A. Kumar, Y. Liu, J. Sengupta, and Divya, "Evolution of mobile wireless communication networks: 1G to 4G," *International Journal of Electronics and Communication Technology*, vol. 1, no. 1, Dec. 2010.

[Kol05] P. J. Kolodzy, *Cognitive Radio Fundamentals*. Singapore: SDR Forum, 2005.

[LÖ4] J. Löfberg, "YALMIP: A toolbox for modeling and optimization in MATLAB," in *Proc. IEEE International Symposium on Computer Aided Control System Design*, 2004, pp. 284–289.

[Law99] E. Lawrey, "Multiuser OFDM," in *Proc. Int. Symp. on Signal Processing and its Applications (ISSPA)*, Brisbane, Australia, August 1999, pp. 761–764.

[LHCT11] W. Liu, Y. Hu, S. Ci, and H. Tang, "Adaptive resource allocation and scheduling for cognitive radio MIMO-OFDMA systems," in *Proc. 73rd IEEE Veh. Techn. Conf.*, May 2011, pp. 1–6.

[LL11] K.-J. Lee and I. Lee, "MMSE based block diagonalization for cognitive radio MIMO broadcast channels," *IEEE Trans. Wireless Commun.*, vol. 10, no. 10, pp. 3139–3144, Oct. 2011.

[LLa11] W. Li and M. Latva-aho, "An efficient channel block diagonalization method for generalized zero forcing assisted MIMO broadcasting systems," *IEEE Trans. Wireless Commun.*, vol. 10, no. 3, pp. 739–744, March 2011.

[LLHL08] H. Lee, K. Lee, B. Hochwald, and I. Lee, "Regularized channel inversion for multiple-antenna users in multiuser MIMO downlink," in *Proc. IEEE ICC*, 2008, pp. 351–355.

[Lo99] T. Lo, "Maximum ratio transmission," *IEEE Trans. Communi.*, vol. 47, no. 10, pp. 1458–1461, 1999.

[MBR05] R. Menon, R. M. Buehrer, and J. H. Reed, "Outage probability based comparison of underlay and overlay spectrum sharing techniques," in *Proc. IEEE DySPAN*, November 2005, pp. 101–109.

[MF70] R. Mueller and G. Foschini, "The capacity of linear channels with additive Gaussian noise," *The Bell System Technical Journal*, pp. 81–94, 1970.

[Mis04] A. K. Mishra, *Fundamentals of Cellular Network Planning and Optimization, 2G/2.5G/3G ... Evolution of 4G*. John Wiley and Sons, 2004.

[Mit00] J. Mitola, "Cognitive radio: An integrated agent architecture for software defined radio," Ph.D. dissertation, KTH Royal Institute of Technology, Stockholm, Sweden, Dec. 2000.

[MM99] J. Mitola and G. Q. Maguire, "Cognitive radio: Making software radios more personal," *IEEE Pers. Commun.*, vol. 6, no. 4, pp. 13–18, August 1999.

[Nek06] M. Nekovee, "Dynamic spectrum access concepts and future architectures," *IEEE Spectrum*, vol. 24, no. 2, pp. 111–116, April 2006.

[NS08] C. Ng and C. Sung, "Low complexity subcarrier and power allocation for utility maximization in uplink OFDMA systems," *IEEE Trans. Wireless Commun.*, vol. 7, no. 5, pp. 1667–1675, 2008.

[PP02] A. Papoulis and S. U. Pillai, *Probability, Random Variables and Stochastic Processes*, 4th ed. McGraw-Hill, 2002.

[PP12] K. Petersen and M. Pedersen, *The Matrix Cookbook*, 2012. [Online]. Available: http://matrixcookbook.com

[PWLW07] T. Peng, W. Wang, Q. Lu, and W. Wang, "Subcarrier allocation based on water-filling level in OFDMA-based cognitive radio networks," in *Proc. Int. Conf. Wireless Commun., Networking and Mobile Computing*, Sep. 2007, pp. 196–199.

[RCL10] Y. Rahulamathavan, K. Cumanan, and S. Lambotharan, "Optimal resource allocation techniques for MIMO-OFDMA based cognitive radio networks using integer

linear programming," in *Proc. 11th IEEE Int. Workshop on Signal Process. Advances in Wireless Commun.*, Jun. 2010, pp. 1–5.

[RO91] R. Roy and B. Ottersten, "Spatial division multiple access wireless communication systems," US Patent 5515378, 1991.

[SAR09] S. Sadr, A. Anpalagan, and K. Raahemifar, "Radio resource allocation algorithms for the downlink of multiuser OFDM communication systems," *IEEE Commun. Surv. & Tutor.*, vol. 11, no. 3, pp. 92–106, Sep. 2009.

[SB05] M. Schubert and H. Boche, "QoS-based resource allocation and transceiver optimization," *Foundations and Trends in Communications and Information Theory*, vol. 2, no. 6, pp. 383–529, 2005.

[SH08] V. Stankovic and M. Haardt, "Generalized design of multi-user MIMO precoding matrices," *IEEE Trans. Wireless Commun.*, vol. 7, no. 3, pp. 953–961, March 2008.

[Sha48] C. Shannon, "A mathematical theory of communication," *Bell System Technical Journal*, vol. 27, pp. 379–423, 1948.

[Skl97] B. Sklar, "Rayleigh fading channels in mobile digital communication systems part I: Characterization," *IEEE Commun. Mag.*, vol. 35, no. 7, pp. 90–100, 1997.

[SLL09a] H. Sung, K.-J. Lee, and I. Lee, "An MMSE based block diagonalization for multiuser MIMO downlink channels with other cell interference," in *Proc. IEEE VTC Fall*, September 2009, pp. 1–5.

[SLL09b] H. Sung, S. Lee, and I. Lee, "Generalized channel inversion methods for multiuser MIMO systems," *IEEE Trans. Commun.*, vol. 57, no. 11, pp. 3489–3499, November 2009.

[SMpV11] H. Shahraki, K. Mohamed-pour, and L. Vangelista, "Efficient resource allocation for MIMO-OFDMA based cognitive radio networks," in *Proc. Wireless Telecommun. Symposium*, Apr. 2011, pp. 1–6.

[Spe95] "Special issue on software radio," *IEEE Commun. Mag.*, vol. 33, no. 5, May 1995.

[SSH04] Q. H. Spencer, A. L. Swindelhurst, and M. Haardt, "Zero-forcing methods for downlink spatial multiplexing in multiuser MIMO channels," *IEEE Trans. Signal Process.*, vol. 52, no. 2, pp. 461–471, February 2004.

[Stu99] J. Sturm, "Using SeDuMi 1.02, a MATLAB toolbox for optimization over symmetric cones," *Optimization Methods and Software*, vol. 11-12, pp. 625–653, 1999.

[Stu01] G. Stuber, *Principles of Mobile Communications*, 2nd ed. Boston: Kluwer Academic Press, 2001.

[SW04] G. Staple and K. Werbach, "The end of spectrum scarcity," *IEEE Spectrum*, vol. 41, no. 3, pp. 48–52, March 2004.

[Tel99] I. E. Telatar, "Capacity of multi-antenna Gaussian channels," *European Trans. on Telecommun. (ETT)*, vol. 10, no. 6, pp. 1–28, 1999.

[Toh02] C. K. Toh, *Ad Hoc Mobile Wireless Networks: Protocols and Systems*. USA: Prentice Hall, New Jersey, 2002.

[Tom71] M. Tomlinson, "New automatic equalizer employing modulo arithmetic," *Electron. Lett.*, vol. 7, no. 5, pp. 138–139, March 1971.

[TRV01] N. D. Tripathi, J. H. Reed, and H. F. Vanlandingham, *Radio Resource Management in Cellular Systems*. Springer, 2001.

[TT92] A. F. Toledo and A. M. Turkmani, "Propagation into and within buildings at 900, 1800, and 2300 MHz," in *Proc. IEEE Veh. Technol. Conf.*, May 1992, pp. 633–636.

[TTP98] A. F. Toledo, A. M. Turkmani, and J. D. Parsons, "Estimating coverage of radio transmission into and within buildings at 900, 1800, and 2300 MHz," *IEEE Personal Communications Magazine*, vol. 5, no. 2, pp. 40–47, April 1998.

[TTT03] R. Tütüncü, K. Toh, and M. Todd, "Solving semidefinite-quadratic-linear programs using SDPT3," *Optimization Methods and Software*, vol. 95, no. 2, pp. 189–217, 2003.

[Tut02] W. Tuttlebee, *Software Defined Radio: Origins, Drivers, and International Perspectives*. New York: Wiley, 2002.

[UB12] W. Utschick and J. Brehmer, "Monotonic optimization framework for coordinated beamforming in multicell networks," *IEEE Transactions on Signal Processing*, vol. 60, no. 4, pp. 1899–1909, 2012.

[Wan09] W. Wang, *Cognitive Radio Systems*. InTech, November 2009, Available at http://www.intechopen.com/books/cognitive-radio-systems.

[Wan10] S. Wang, "Efficient resource allocation algorithm for cognitive OFDM systems," *IEEE Commun. Letters*, vol. 14, no. 8, pp. 725–727, Aug. 2010.

[WE71] S. Weinstein and P. Ebert, "Data transmission by frequency-division multiplexing using the discrete Fourier transform," *IEEE Trans. Commun. Tech.*, vol. 19, no. 5, pp. 628–634, October 1971.

[WH08a] H. Wu and T. Haustein, "Radio resource management for the multi-user uplink using DFT-precoded OFDM," in *Proc. IEEE International Conference on Communications (ICC)*, Beijing, China, May 2008, pp. 4724–4728.

[WH08b] ——, "Sum rate optimization by spatial precoding for a multiuser MIMO DFT-precoded OFDM uplink," *EURASIP Journal on Advances in Signal Processing*, vol. 2011, pp. 927–936, May 2008.

[WN07] Z. Wu and B. Natarajan, "Interference tolerant agile cognitive radio: Maximize channel capacity of cognitive radio," in *Proc. Consumer Communications and Networking Conference*, January 2007, pp. 1027–1031.

[WSS04] H. Weingarten, Y. Steinberg, and S. Shamai, "The capacity region of the Gaussian MIMO broadcast channel," in *Proc. IEEE Int. Symp. Inform. Theory (ISIT)*, Chicago, 2004, p. 174.

[WSS06] ——, "The capacity region of the Gaussian multiple-input multiple-output broadcast channel," *IEEE Trans. Inf. Theory*, vol. 52, no. 9, pp. 3936–3964, 2006.

[Wu10] H. Wu, "Adaptive multi-user MIMO resource allocation for uplink DFT-precoded OFDMA," Ph.D. dissertation, Chair of Information and Coding Theory, University of Kiel, Germany, Sep 2010.

[WZGW12] S. Wang, Z.-H. Zhou, M. Ge, and C. Wang, "Resource allocation for heterogeneous multiuser OFDM-based cognitive radio networks with imperfect spectrum sensing," in *Proc. IEEE Infocom.*, 2012, pp. 2264–2274.

[XL14] D. Xu and Q. Li, "Resource allocation for outage probability minimisation in cognitive radio multicast networks," *Transactions on Emerging Telecommunications Technologies*, vol. 27, no. 1, pp. 51–63, 2014.

[YEHD14] E. Yaacoub, A. El-Hajj, and Z. Dawy, "Uplink OFDMA resource allocation with discrete rates: Optimal solution and suboptimal implementation," *Transactions on Emerging Telecommunications Technologies*, vol. 23, no. 2, pp. 148–162, 2014.

[YH14] A. Yaqot and P. A. Hoeher, "Efficient resource allocation for MIMO-OFDM cognitive networks with adaptive precoding," in *Proc. 18th International OFDM Workshop (InOWo'14)*, Essen, Germany, August 2014, pp. 85–91.

[YH16a] ——, "Adaptive MMSE-based precoding in multiuser MIMO broadcasting with application to cognitive radio," in *Proc. 20th International ITG Workshop on Smart Antennas (WSA2016)*, Munich, Germany, March 2016, pp. 340–347.

[YH16b] ——, "On precoding diversity in cognitive networks," in *Proc. 23rd International Conference on Telecommunications (ICT2016)*, Thessaloniki, Greece, May 2016, pp. 48–52.

[YH17] ——, "Efficient resource allocation for cognitive radio networks," *IEEE Trans. Vehicular Technology*, accepted for publication, 2017.

[ZC05] H. Zheng and L. Cao, "Device-centric spectrum management," in *Proc. IEEE DySPAN*, November 2005, pp. 56–65.

[ZdLH13] K. Zu, R. C. de Lamare, and M. Haardt, "Generalized design of low-complexity block diagonalization type precoding algorithms for multiuser MIMO systems," *IEEE Trans. Commun.*, vol. 61, no. 10, pp. 4232–4242, October 2013.

[ZJL16] A. Zappone, E. Jorswieck, and A. Leshem, "Distributed assignment and resource allocation for energy efficiency in MIMO wireless networks," in *Proc. WSA2016*, Munich, Germany, March 2016, pp. 165–169.

[ZL05] Y. J. Zhang and K. B. Letaief, "An efficient resource-allocation scheme for spatial multiuser access in MIMO/OFDM systems," *IEEE Trans. Commun.*, vol. 53, no. 1, pp. 107–116, Jan. 2005.

[ZL08a] R. Zhang and Y.-C. Liang, "Exploiting multi-antennas for opportunistic spectrum sharing in cognitive radio networks," *IEEE J. Sel. Topics Signal Process.*, vol. 2, no. 2, pp. 88–102, Feb. 2008.

[ZL08b] Y. Zhang and C. Leung, "Subcarrier, bit and power allocation for multiuser OFDM-based multi-cell cognitive radio systems," in *Proc. 68th IEEE VTC*, Sep. 2008, pp. 1–5.

[ZLC10] R. Zhang, Y.-C. Liang, and S. Cui, "Dynamic resource allocation in cognitive radio networks," *IEEE Signal Process. Magazine*, vol. 27, no. 3, pp. 102–114, May 2010.

[ZTSC07] Q. Zhao, L. Tong, A. Swami, and Y. Chen, "Decentralized cognitive MAC for opportunistic spectrum access in ad hoc networks: A POMDP framework," *IEEE JSAC*, vol. 25, no. 3, pp. 589–600, April 2007.

[ZW95] W. Zou and Y. Wu, "COFDM: An overview," *IEEE Transactions on Broadcasting*, vol. 41, no. 1, pp. 1–8, 1995.

[ZXL09] L. Zhang, Y. Xin, and Y.-C. Liang, "Weighted sum rate optimization for cognitive radio MIMO broadcast channels," *IEEE Trans. Wireless Commun.*, vol. 8, no. 6, pp. 2950–2959, June 2009.